NTNU – Trondheim
Norwegian University of
Science and Technology

Revised simulation model for a Very Large Crude Carrier (VLCC)

Jørgen Mathiesen Kvale

Marine Technology
Submission date: June 2014
Supervisor: Tor Einar Berg, IMT

Norwegian University of Science and Technology
Department of Marine Technology

Scope

MASTER THESIS IN MARINE TECHNOLOGY
SPRING 2014
Revised simulation model for a Very Large Crude Carrier (VLCC)

Simulators are widely used by the shipping community in feasibility studies, engineering, operational planning and training. The need for quality of the simulation model depends on the actual application and varies from a representative representation of a class of vessels to specific models for single ships. This MSc thesis will be linked to a Research Council of Norway project studying methods to validate simulation models through use of model tests and sea trials for case specific vessels. The student will work with improvements of a simulation model for a specific Very Large Crude Carrier (KVLCC2) being used as one of the case vessels in the SIMMAN 2008 and the planned SIMMAN 2014 workshops.

The main objective for this thesis is to improve, test and validate a deep and calm water simulation model for the case vessel KVLCC2. The MSc thesis will be a based on the results from the student's project thesis, available model test data for this vessel published in connection with the SIMMAN 2008 workshop and any recently presented empirical or model test data for the case vessel. The final simulation model should be based on simulation tools developed and applied by MARINTEK such as the manoeuvring plug-in SIMAN in the ShipX tool box or the simulation tool VeSim. In addition to IMO's standard manoeuvres ship specific low speed manoeuvres shall be used for validation of the simulation model.

Secondary objectives of this MSc thesis are to:

- Understand the process of verification and validation of simulation models
- Calculate and/or estimate manoeuvring forces/moments in applied simulation tools
- Define case specific low speed manoeuvres that shall be used for model validation
- Investigate shallow water effects and compare with full-scale test results from ESSO Osaka
- Compare calculation results with manoeuvring characteristic specified in IMO MSC Res. 137(76) and vessel specific low speed manoeuvres
- Compare simulated manoeuvres with available data from free-sailing model tests with KVLCC2
- Discuss needs for improvement of input parameters and physical models used in MARINTEK's simulation tools for studies of ship manoeuvring performance

In the thesis the candidate shall present his personal contribution to the resolution of problem within the scope of the thesis work.

Theories and conclusions should be based on mathematical derivations and/or logic reasoning identifying the various steps in the deduction.

The candidate should utilize the existing possibilities for obtaining relevant literature.

The thesis should be organized in a rational manner to give a clear exposition of results, assessments, and conclusions. The text should be brief and to the point, with a clear language. Telegraphic language should be avoided.

The thesis shall contain the following elements: A text defining the scope, preface, list of contents, summary, main body of thesis, conclusions with recommendations for further work, list of symbols and acronyms, reference and (optional) appendices. All figures, tables and equations shall be enumerated.

The original contribution of the candidate and material taken from other sources shall be clearly defined. Work from other sources shall be properly referenced using an acknowledged referencing system.

The thesis shall be submitted in two copies:

- Signed by the candidate
- The text defining the scope included
- In bound volume(s)
- Drawings and/or computer prints that cannot be bound should be organized in a separate folder
- The bound volume shall be accompanied by a CD or DVD containing the written thesis in Word or PDF format. In the case computer programs have been made as part of the thesis work, the source code shall be included. In case of experimental work, the experimental results shall be included in a suitable electronic format.

Supervisor: Professor II Tor Einar Berg
Start: 14.01.2014
Deadline: 10.06.2014

Trondheim, 10.01.2014

Tor Einar Berg
Supervisor

Summary

In this thesis a simulation model for a Very Large Crude Carrier is revised. MARINTEK's software ShipX is used to develop, improve, test and validate a model for the case vessel KVLCC2. The Manoeuvring Plug-In (SIMAN, 3-DOF) and the Vessel Simulator Plug-In (VeSim, 6-DOF) are utilized for this purpose. The underlying field of study has been ship manoeuvrability.

KVLCC2's hull lines, propeller and rudder data are available at SIMMAN 2014 websites [4]. Captive and free model tests conducted in connection to the workshop on verification and validation of ship manoeuvring simulation methods SIMMAN 2008 are available. The methodology for improving the simulation model is to use the model to simulate the IMO standard manoeuvres. Turning circles, zig-zag and stopping tests in deep water is simulated. Turning circles(35°), zig-zag(10°/2.5°, 20°/5°) and spiral tests are simulated in shallow water. The simulation results are compared to results from SIMMAN in 2008. The 26th ITTC has suggested benchmark data from average values of the free sailing model tests from the workshop that are used for model validation. The simulation results are also evaluated and compared to the results from MARINTEK's contribution in SIMMAN 2008 using SIMAN. A sensitivity analysis is performed to find which parameters are of high importance in the model. The parameters of high importance are investigated further. The linear velocity coefficients are compared with empirical methods and PMM tests. Shallow water effects and low speed manoeuvring are assessed. The shallow water simulations at low speed are compared with the shallow water effect trends from full-scale trials with Esso Osaka. Validation and verification of simulation models are assessed and understood.

The simulation model does fulfil all the IMO criteria of turning, initial turning/course-changing, yaw-checking abilities in both VeSim and SIMAN. The model in VeSim fulfil the IMO criteria of stopping ability, while the model in SIMAN does not. The differences in the results of VeSim and SIMAN and small. The simulation results do not correspond well with the benchmark data based on free model tests from SIMMAN 2008, and the model can not be validated. MARINTEK's contribution using SIMAN in 2008 was more consistent with the benchmark data, and indicates that the changes made in the plug-in does not give better results for KVLCC2. Changes has been observed in the calculation of the hydrodynamic coefficients and resistance polynomial. Especially the calculation methods of Y_r and N_r have been altered. When using the same input parameters as well as the same hydrodynamic coefficients and resistance polynomial as in 2008 the manoeuvring simulations deviates substantially. These deviations must be because of changes in either non-linear cross-flow drag, rudder module or the propeller module (or all). These subroutines are hard to assess because of lack of updated documentation. The linear damping coefficients proved to be of high importance in the sensitivity analysis, especially N_v and N_r. Wake fraction and thrust deduction are also of some importance. ShipX tends to overestimate N_v and underestimate N_r and can not be validated against results from PMM tests. An input value of 0.150 [-] for the wake fraction of the hull has been observed to be too low compared to literature and other wake fractions used in SIMMAN 2008. The same shallow water trends for KVLCC2 are observed as for Esso Osaka for the turning circle test. The same trends are not found for checking and counter turning ability for KVLCC2. From the 23rd ITTC committee's review of shallow water ratios as well as using methods of Clarke,

Ankudinov and Kijima it seems like SIMAN's shallow water formulae underestimates the linear velocity coefficient ratios.

There has been made several changes in the different subroutines and modules of the plug-in during the last six years. These changes are easily noticed by looking at results when using exactly the same inputs and coefficients. It is impossible to assess and suggest improvements to the cross-flow drag, rudder module and propeller module when the documentation is not updated. N_v is overestimated and N_r is underestimated compared to empirical methods and PMM tests. Due to the high importance of these a review of the current calculation methods of these should be looked into. SIMAN and VeSim is tuned for offshore vessels, which could have an impact of the results since KVLCC2 is a VLCC. An assessment of SIMAN's shallow water formulae is hard to do as well due to lack of documentation, but this should be looked into after SIMMAN 2014.

Sammendrag

En simuleringsmodell av en VLCC er revidert i oppgaven. MARINTEK's programvare ShipX er brukt til å utvikle, forbedre og validere en model for caseskipet KVLCC2. Manøvreringsmodulen SIMAN (3 frihetsgrader) og simulatormodulen VeSim (6 frihetsgrader) er brukt til dette formålet. Det underliggende fagfeltet er skipsmanøvrering.

Skipslinjer, propell og rordata for KVLCC2 er tilgjengelige på SIMMAN 2014 hjemmesider [4]. Captive og frittseilende tester i forbindelse med konferansen om verifikasjon og validering av simuleringsmetoder for skipsmanøvrering SIMMAN 2008 ligger også tilgjengelig. Metoden brukt for å forbedre simuleringsmodellen er å bruke modellen til å simulere IMO's standardmanøvre. Svingesirkler, sikk-sakk tester og stoppe tester i dypt vann er simulert. Svinge sirkler(35°), sikk-sakk(10°/2.5°, 20°/5°) og spiral tester er simulert på grunt vann. Resultatene er sammenlignet med resultatene fra SIMMAN 2008. Den 26. ITTC manøvreringskomitéen har foreslått referansedata fra gjennomsnittlige mål fra de frittseilende modelltestene fra SIMMAN som skal brukes til modellvalidering. Simuleringsresultatene er også evaluert og sammenlignet med MARINTEK's resultater fra SIMAN i SIMMAN 2008. En sensitivitetsanalyse er utført for å finne hvilke parametere som er viktige i modellen. De viktigste parameterne er sett nærmere på. De lineære dempningskoeffisientene sammenlignes med empiriske metoder og PMM tester. Grunt vann simuleringene med lav hastighet er sammenlignet med trender fra full-skala tester med Esso Osaka. Validering og verifisering av simuleringsmodeller er forstått og beskrevet.

Simuleringsmodellen av KVLCC2 oppfyller alle IMO kriterier om svingning, initiell svinging/kursforandring, gir-kontroll evner. Modellen i VeSim oppfyller kriteriet om stopp evne, mens modellen i SIMAN ikke gjør det. Forskjellene i resultatene i VeSim og SIMAN er små. Simuleringsresultatene samsvarer dårlig med referansedataene basert på frittseilende tester fra SIMMAN 2008 og modellen kan ikke bli validert. MARINTEK's bidrag med SIMAN i 2008 samsvarer mer med referansedataene, og indikerer at forandringene som er gjort i manøvreringsmodulen gir dårligere resultater for KVLCC2. Forandringer er gjort i utregningen av de hydrodynamiske koeffisientene og motstand polynomet. Spesielt er kalkulasjonsmetoden av Y_r og N_r blitt endret. Resultatene avviker selvom samme input parametere, hydrodynamiske koeffisienter og motstand polynom som i 2008 blir brukt. Disse avvikene må komme av forandringer i enten ikke-lineær tverr-strøm, rormodulen eller propellmodulen (eller alle). Subrutinene er vanskelige å vurdere grunnet manglende oppdatert dokumentasjon. De lineære dempningskoeffisientene viste seg å være meget viktige i sensitivitetsanalysen, spesielt N_v og N_r. Wakefraksjon og trustfradrag er også av betydning. ShipX har en tendens til å overestimere N_v og underestimere N_r og kan ikke valideres mot resultater fra PMM tester. Verdien 0.150 [-] for skrogets wakefraksjon har blitt observert til å være for lav i forhold til litteratur og andre wakefraksjoner som er brukt i SIMMAN 2008. De samme gruntvannstrendene for KVLCC2 er observert som for Esso Osaka for svingesirkel testen. De samme trendene er ikke funnet for kontroll og kontra-svinging evne for KVLCC2. Ut i fra den 23. ITTC manøvreringskomitéens vurdering av gruntvannsforhold, samt bruk av metoder fra Clarke, Ankudinov og Kijima virker det som SIMANs gruntvannsformler underestimerer de lineære hastighetskoeffisientforholdene.

Det har blitt gjort mange endringer i de forskjellige subrutinene og modulene av manøvreringsmod-

ulen de siste seks årene. Disse forandringene er lett å merke ved å sammenligne resultatene ved bruk av samme input og koeffisienter. Det er umulig å vurdere og foreslå forbedringer til tverrstrøm, ror og propellmodulene når dokumentasjonen ikke er oppdatert. N_v er overestimert og N_r er underestimert sammenlignet med empiriske metoder og PMM tester. På grunn av viktighetsgraden av disse bør kalkulasjonsmetodene for disse gjennomgås. SIMAN og VeSim er tunet for offshore fartøy, hvilket kan ha betydning for resultatene siden KVLCC2 er en VLCC. En vurdering av SIMAN's gruntvannsformler bør sees på etter SIMMAN 2014.

Preface

This master thesis is submitted to fulfil the requirement to the degree of Master of Science in Marin Technology at the Norwegian University of Master and Technology (NTNU). The work is done independently and is partially based on the work done in my project thesis from fall 2013.

The main objective was to improve, test and validate a deep and calm water simulation vessel for the case vessel KVLCC2. Simulation tools in ShipX are used for simulations, both ShipX's Manoeuvring Plug-In (SIMAN)and ShipX's Vessel Simulator Plug-In (VeSim). The work has been challenging at times, regarding both program troubleshooting and lack of plug-in documentation. A lot of time has been spent on the literature review.

I would like to thank my supervisor Tor Einar Berg for guidance and academic support throughout the semester. I would also like to thank Edvard Ringen for help and troubleshooting in ShipX's Manoeuvring Plug-In (SIMAN). As well as help with geometric model of KVLCC2 and input data. Also, I would like to thank Dariusz Fathi for guidance and troubleshooting in ShipX's Vessel Simulator Plug-In (VeSim).

Jørgen Mathiesen Kvale
Trondheim, June 2014

Contents

List of Tables

List of Figures

Abbreviations

ADV	Advance
CFD	Computational Fluid Dynamics
CMT	Circular motion mechanism
DIW	Dead in Water
DOF	Degree of Freedoms
GM	Geometric Metacentre
HAHD	Half Ahead
IMO	International Maritime Organization
ITT	Initial turning time
ITTC	International Towing Tank Conference
ISO	International Organization for Standarization
MER	Minimum effective rudder
PMM	Planar Motion Mechanism
PT	Port
RANS	Reynolds-averaged Navies-Stokes
RAT	Rotating arm test
SAHD	Slow Ahead
SB	Starboard
SNAME	Society of Naval Architects and Marine Engineers
TD	Tactical diameter
UKC	Under keel clearance
VLCC	Very Large Crude Carrier

Nomenclature

B	Ship's breadth
C_D	Drag coefficient
C_H	Zero frequency horizontal added mass coefficient
C_{pa}	Prismatic coefficient of aft hull
C_{wa}	Water plane area coefficient of aft hull
F_n	Froude number
C_D	Drag coefficient
K	Roll moment
L	Ships length (Lpp)
M	Pitch moment
N	Yaw moment
N_r	Coefficient for yaw damping
N_v	Coefficient for yaw damping due to sway velocity
S	Wet surface
T	Ship's draft
X	Longitudinal force component
Y	Lateral force component
Y_r	Coefficient for sway damping due to yaw velocity
Y_v	Coefficient for sway damping
$\vec{V}$	Ship velocity
Z	Vertical force component
β	Drift angle
δ	Rudder angle
ϕ	Roll angle
ψ	Heading angle
e_a	Fullness of aft run
σ_a	Aft sections fullness metric
ρ	Fluid density
k	Effective aspect ratio of the hull
n	Propeller rate
p	Roll rate of turning
q	Pitch rate of turning
r	Yaw rate of turning
u	Longitudinal velocity component
v	Lateral velocity component
w	Vertical velocity component, wake fraction
x_G	Distance between midship and center of gravity

Chapter 1

Introduction

Ship-handling simulators are widely used for training and demonstrating competence of maritime skills and objectives, as well as in the design of ports and fairways. The quality of the simulation model depends on the application of the simulation, as well as the representation of a ship type or a specific ship. The simplest models are used for initial shiphandling training and the more complex models are used in simulation of complex marine operations where accuracy is highly important. Shiphandling simulators can vary from a simple simulator one can install on a PC or a full replication of the bridge of a ship with 360°vision. Some simulators even simulate the motions that are felt on the bridge. An increased quality of simulator models will improve transfer from training to real life, as well as remove uncertainties related to investigation of maritime accidents. The shiphandling simulators uses all areas within ship controllability, but the manoeuvring field is of main interest in this thesis. There are also models that are mainly for prediction of ship manoeuvrability. These are used at design stage of a ship to check that the ship has the desired manoeuvring capabilities. The knowledge of the manoeuvring characteristics of a ship allows time simulations of its path as a function of its control settings. Adequate manoeuvring capability is important for safety and protection of the marine environment. However, the prediction of manoeuvrability of ships are amongst the most challenging problems in ship hydrodynamics. The main difficulties is the evaluation of hydrodynamic forces and moments that characterize the dynamic response of the ship and its motions.

The validation of shiphandling simulators today is not of desired quality [15]. For the SIMMAN 2008 workshop the ITTC suggested four hull characteristics of certain ship types to compare different prediction methods. The results from the different institutes varied significantly, which concludes that the validation of manoeuvring prediction and shiphandling simulators are not good enough.

The scientific research on ship manoeuvring started with Eulers work on equations of motion of a ship in 1749 [30]. However, ship manoeuvring was not systematically focused on before World War II. Before that the research focus had been on resistance and propulsion. The International Symposium on Ship Manoeuvrability was held in 1960 for the first time, where amongst others, Norrbin presented his work on manoeuvrability of ships. Since the 1960's the research and development of ship manoeuvring have increased. Later, organizations such as IMO, ITTC and SNAME became a driving force for further research on ship manoeuvrability. Increasing size of ships, shallow water problems and increasing ship speed has stimulated

research on the topic.

1.1 Controllability

Controllability includes all parts of regulating a vessel's trajectory, speed and orientation at sea. It includes starting, turning, steering a steady course, slowing, stopping and backing. When studying controllability it is convenient to divide controllability into three areas [34]:

- Course-keeping - The maintenance of steady mean course or heading.
- Manoeuvring - The controlled change in the direction of motion.
- Speed-changing - The controlled change in speed.

These performances varies with water, depth, restricted waterways and hydrodynamic interference from nearby vessels or obstacles. The trim of the ship affects the course-keeping and manoeuvring ability. For surface ships the controllability involves forces, moments and motions acting in all directions in the horizontal plane (surge, sway and yaw). Roll can also be of significance for certain ship types. The primary sources to these forces and moments are the hydrodynamic interactions acting on the ship's hull and rudder from the environment. The shiphandling simulators uses all areas within controllability, but the manoeuvring area are of main interest in this thesis. Speed changing is also assessed briefly in low speed manoeuvring.

1.2 Ship manoeuvring

All ship manoeuvres involves turning, except some stopping manoeuvres. When the rudder is deflected the rudder produces forces and moments, which can be divided into two parts:

- An initial transient part where significant surge, sway and yaw accelerations occur.
- A steady turning part where the rate of turn and forward speed is constant and the patch of the ship is circular.

The manoeuvring tests have two alternative purposes:

- Direct verification of manoeuvrability - fulfilment of IMO criteria.
- Establishment of hydrodynamic coefficients for the manoeuvring equations (usually followed by calculation of manoeuvrability in a manoeuvring prediction program).

IMO published "Interim Guidelines for Estimating Manoeuvring Performance in Ship Design" in 1985. These guidelines provided that the manoeuvring performance of all new ships above 100 meters (as well as gas carriers and passenger vessels) must be estimated, tested and verified. The manoeuvring capabilities should permit the ships in course, to turn, to check turns, to operate at acceptable slow speeds and to stop in a satisfactory manner. The significant qualities for evaluation of the manoeuvring characteristics are as follows [39]:

a) *Inherent dynamic stability:* If a ship is settling on a straight course after a small disturbance without correct course with rudder, the ship is dynamically stable on a straight course.

b) *Course-keeping ability:* Course-keeping quality is a measure of ability of the steered ship to maintain a straight path in a predetermined course direction without excessive oscillations of rudder or heading.

c) *Initial turning/course-changing ability:* The initial turning ability is defined by the change-of-heading response to a moderate helm, in turns of heading deviation per unit distance sailed (the P number) or in terms of the distance covered before realizing a certain heading deviation (such as the "time to second execute" demonstrated when entering the zig-zag manoeuvre).

d) *Yaw checking ability:* The yaw checking ability of the ship is a measure of the response to counter-rudder applied in a certain state of turning, such as the heading overshoot reached before the yawing tendency has been cancelled by the counter-rudder in a standard zig-zag manoeuvre.

e) *Turning ability:* Turning ability is the measure of the ability to turn the ship using hard-over rudder. The result being a minimum "advance at 90°change of heading" and "tactical diameter" defined by the "transfer at 180°change of heading". Analysis of the final turning diameter is of additional interest.

f) *Stopping ability:* Stopping ability is measured by the "track reach" and "time to dead in water" realized in a stop engine-full astern manoeuvre performed after a steady approach at full test speed. Lateral deviations are also of interest, but they are very sensitive to initial conditions and wind disturbances.

1.2.1 IMO standard manoeuvring tests

The IMO has defined three standard manoeuvring tests which ships over 100 meters (as well as gas carriers and passenger vessels) are required to perform. The three tests are the turning circle manoeuvre, the zig-zag manoeuvre and the stopping manoeuvre. These manoeuvres investigates all the mentioned manoeuvring characteristics above except for a) and b). However, a) is checked on the basis of the linear stability index, which is calculated from the hydrodynamic coefficients.

Turning circle manoeuvre

This manoeuvre is performed to both starboard and port with 35°or maximum rudder angle at a given test speed until the ship has changed its heading 360°. From the turning circle manoeuvre the tactical diameter, advance and transfer are obtained (see figure 1.1)

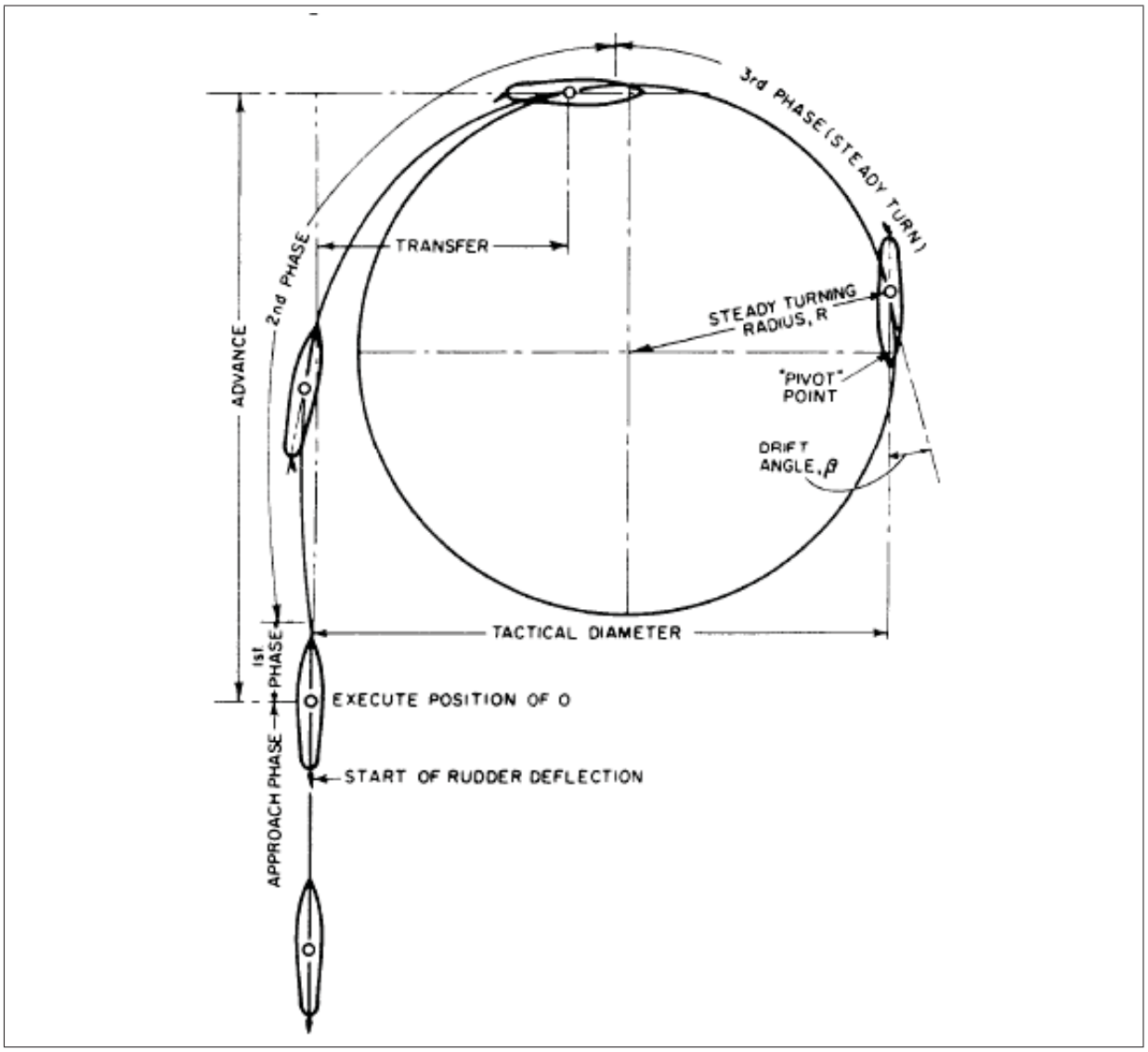

Figure 1.1: Turning circle [34]

The turning circle investigates the manoeuvring characteristic *turning ability* of the ship. The IMO criteria for the turning ability are:

- $Advance \leq 4.5L$
- $Tactical\ diameter \leq 5.0L$

Zig-zag manoeuvre

The zig-zag manoeuvre is to be done to both starboard and port with both 10°/10°and 20°/20°rudder and heading change. The rudder is put to an angle after a steady approach (first execute). When the heading has changed to the same angle the rudder is reversed to the opposite corresponding angle (second execute). From the zig-zag test the overshoot angles, initial turning time to second execute and the time to check yaw are obtained.

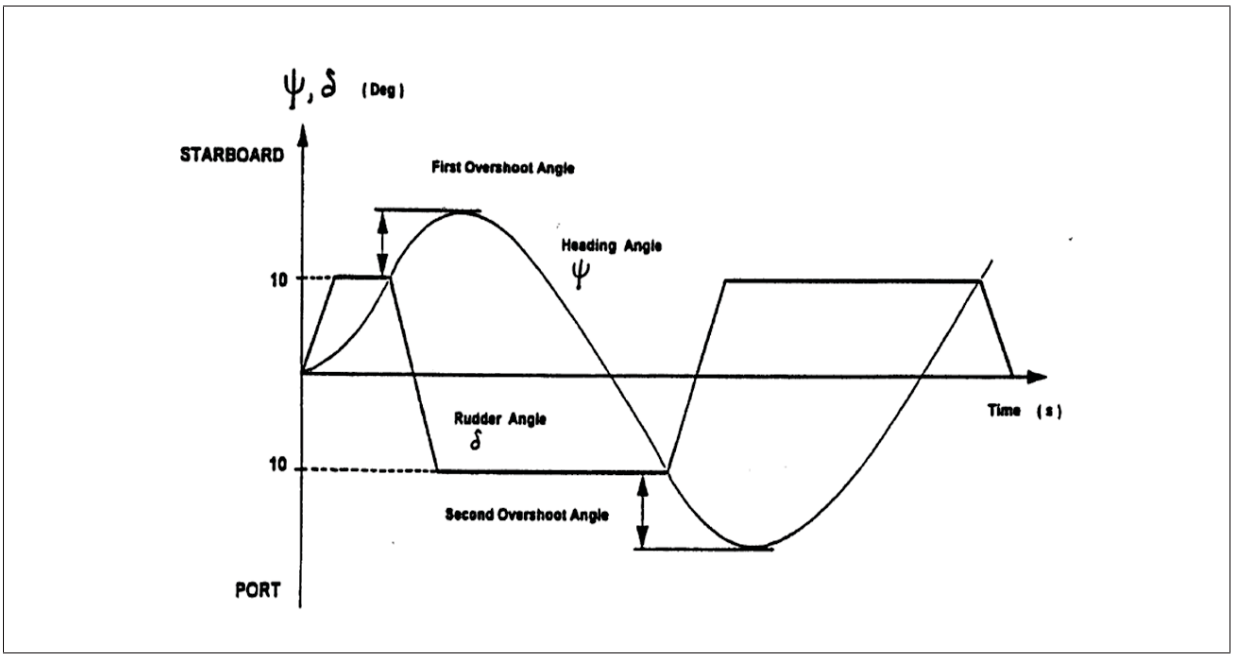

Figure 1.2: Zig-Zag test 10°/10°[39]

The zig-zag test investigates the manoeuvring characteristics *initial turning/course-changing ability* and *yaw checking ability*. The IMO criteria for the initial turning ability is:

- With 10°rudder angle to port or starboard, the ship should not have travelled more than 2.5 L by the time the heading has changed by 10°from its initial value.

The IMO criteria for yaw-checking and course-keeping abilities are:

1. The value of the first overshoot angle in the 10°/10°zig-zag test should not exceed:
   - 10°if L/V is less than 10 seconds.
   - 20°if L/V is 30 seconds or more.
   - 5+(1/2(L/V))degrees if L/V is 10 seconds or more, but less than 30 seconds. L and V are expressed in m and m/s.
2. The value of the second overshoot angle in the 10°/ 10°zig-zag test should not exceed:
   - 25°if L/V is less than 10 seconds
   - 40°if L/V is 30 seconds or more
   - (17.5+0.75(L/V)) degrees if L/V is 10 seconds or more, butt less than 30 seconds.
3. The value of the first overshoot angle in the 20°/20°zig-zag test should not exceed 25 degrees.

Stopping tests

The stopping test are performed by keeping the ship in steady course with steady speed, followed by a stop order (full astern engine order). From the stopping tests the track reach, head reach, lateral deviation and time to dead in water are obtained (see figure 1.3).

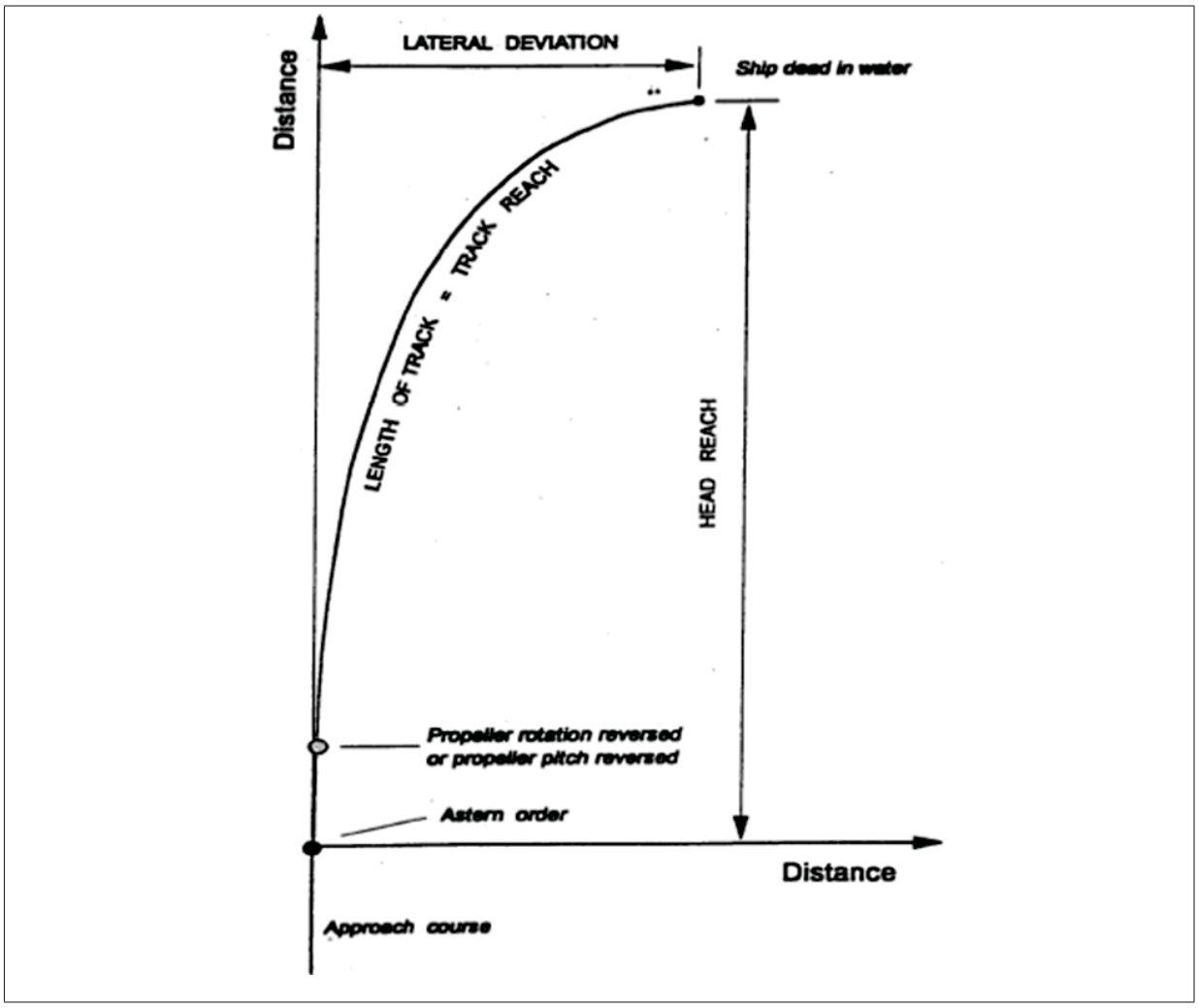

Figure 1.3: Stopping test [39]

The stopping test investigates the manoeuvring characteristic *stopping ability*. The IMO criteria for the stopping ability is that the track reach should not exceed 15 ship lengths. This criteria may be modified by the Administration where ships of large displacement make this criterion impracticable. However, the track reach should in no case exceed 20 ship lengths.

1.2.2 Conditions

The IMO standard manoeuvring tests should be evaluated under the standard conditions [39]:

- Deep, unrestricted waters
- Full load and even keel condition
- Calm environment
- Reasonable and practicable metacentric height
- Steady approach at the test speed

All tests have to be performed to both port and starboard.

1.2.3 Other manoeuvring tests

Other manoeuvring tests to determine the manoeuvring characteristics which have been proposed by the ITTC are the Pull-Out Manoeuvre, Diedonne's spiral manoeuvre and Bechs's Reverse spiral manoeuvre. The Pull-out manoeuvre are used to check whether a ship is straight-line stable or not. The manoeuvre is performed by applying a rudder angle of approximately 20°until steady turning has been reached. Rudder angle is returned to zero and the rate of turn decays to a value. If the decay value is the same for both starboard and port, the ship is straight-line stable. If not, the ship is unstable. The pull-out manoeuvre can also be done by the end of a turning circle.

The spiral manoeuvre checks straight-line stability and gives an indication of the validity range of linear theory and degree of stability. The manoeuvre is performed from a straight course turning the rudder angle 25°until steady yawing rate is obtained. The rudder angle is decreased in steps of 5°and held until steady yawing rates is obtained for all rudder angles. The manoeuvre is performed for both starboard and port.

The reverse spiral manoeuvre produces a non-linear manoeuvring characteristic for an unstable ship. The manoeuvre should be performed if the ship turns out to be unstable because of the hysteresis at small turning rates. The results of the manoeuvre indicates which rudder corrections that are required to stabilize the ship.

1.2.4 Manoeuvring problems

The understanding of physical processes which occurs around a manoeuvring ship is still insufficient in operational conditions like [22]:

- Manoeuvring with small under keel clearance (shallow water)
- Manoeuvring in harbours and at low speeds
- Manoeuvring strongly affected by hull-propeller-rudder interactions
- Passing near banks, approaching banks
- Passing and approaching other ships

1.3 Prediction methods

An overview of existing manoeuvring prediction methods is found in figure 1.4. These methods are generalized by the ITTC and based on the experience of the manoeuvring committee and insights obtained from the SIMMAN 2008 workshop. The red arrow illustrates the prediction methods of SIMAN and VeSim.

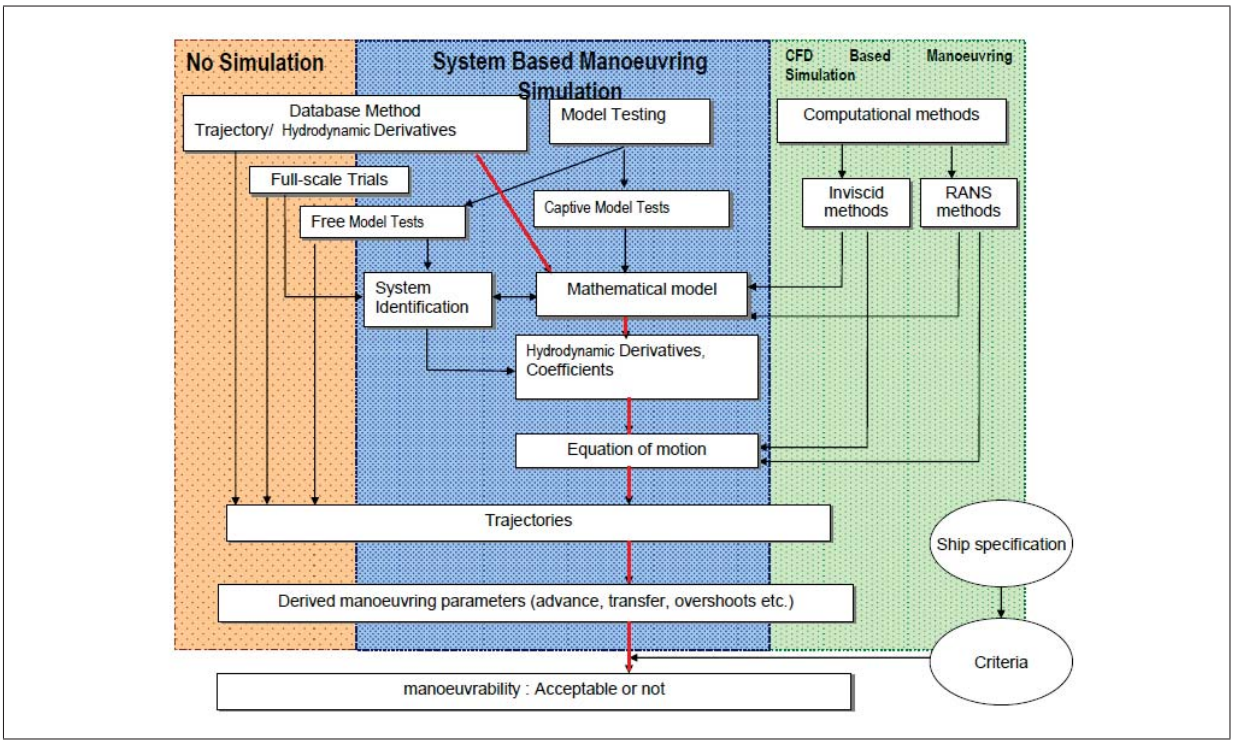

Figure 1.4: Overview of manoeuvring prediction methods [8]

Different prediction methods have different accuracies and cost, roughly given in figure 1.5.

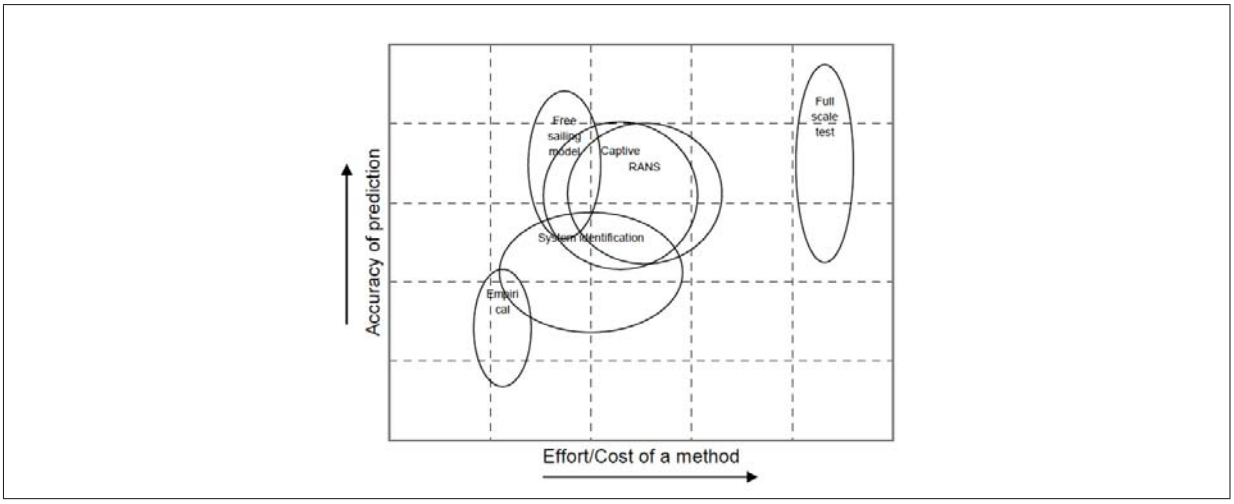

Figure 1.5: Effort/cost versus accuracy of manoeuvring prediction methods [8]

The prediction methods have their own advantages/disadvantages which are elaborated in [8].

Predictions based on free model tests

A scaled model of the ship is used to perform the relevant manoeuvre(s). This prediction method is generally believed to be the closest as possible to reality. Apart from possible scale effects there are no assumptions made which affects the results of the simulated manoeuvre.

Predictions based on captive model tests

Predictions are made from simulations based on captive model tests. The captive model tests may be PMM, CPMC, CMT/rotating arm or captive drift tests. Rudder force measurements could be included as well. The tests are analysed to obtain the mathematical model and the manoeuvring coefficients.

Predictions based on empirical/semi-empirical methods

These methods use a mathematical model and manoeuvring coefficients. The manoeuvring coefficients are usually based on empiricism or a mix of empiricism and semi-empirical/semi-theory. Empirical methods depends heavily on ships that the method is based on. ShipX's manoeuvring plug-in predicts manoeuvres based on this method, where slender body theory is used together with cross flow drag theory. The red arrows in figure 1.4 illustrates the sequence of this prediction method. Advantages of these predictions are [8]:

- Very quick and low costs.
- Easy to modify ship particulars in an early design stage.
- Depending on the mathematical model, it can be used for open-loop simulations (training and bridge simulations).

The disadvantages are:

- The accuracy and reliability of the results is fairly limited.
- Most of the models do not take into account the hull form details (such as details of the aft hull), which are often of importance in the assessment of the manoeuvrability.
- With shallower water, the results are less reliable.

Predictions based on system identification methods

System identification is based on free model tests. A number of manoeuvring tests are used to derive a mathematical procedure which optimises the hydrodynamic coefficients in a mathematical model so it can reproduce the manoeuvres. The larger number of manoeuvring tests (various tests as well as different speeds, rudder angles, drift angles and rotation rates) increases the method's quality.

Predictions using viscous flow CFD

There are two kinds of viscous flow CFD RANS (Reynolds-averaged Navier-Stokes) calculations. The most commonly used method is where RANS-calculations is used to simulate captive model tests. These calculations are analysed to obtain the manoeuvring coefficients to be applied in a mathematical model. The mathematical model is then used to predict manoeuvres. The other method is a full time domain simulation of the manoeuvres.

Predictions using potential flow CFD

Potential flow CFD are methods used for codes that are not RANS. The methods for determining the forces on a manoeuvring ship includes small aspect ratio wing theory, slender body theory and 3D panel methods.

1.4 Thesis organization

Chapter 2 presents the standard notation and coordinate systems used in manoeuvring. The equations of motion are derived from Newtons second law, which is valid in the earth-fixed coordinate system. These equations of motion are the basis of mathematical modelling in ship manoeuvring and can be divided into *formal mathematical models* and *modular mathematical models*. Empirical methods used to estimate the hydrodynamic derivatives are presented as well.

Chapter 3 is a literature review of shallow water effects. Adaptations to shallow water mathematical models are presented and assessed. Shallow water ratios to scale the hydrodynamic derivatives, added mass, propulsion and rudder induced forces are looked into. Esso Osaka full-scale manoeuvring trials and conclusions are presented.

Chapter 4 describes the aspects and governing mechanisms of low speed manoeuvring. Critics to the IMO standard criteria concerning lack of assessment of low speed manoeuvring are summarized. Specific low speed manoeuvres/criteria from Dand, Hwang et al. and ISO are presented. A brief section of low speed mathematical models is looked into.

Chapter 5 is dedicated to validation and verification theory and techniques. The recommended practice suggested by ITTC Manoeuvring Committee and available benchmark data are presented.

Chapter 6 describes the mathematical model and coordinate systems of SIMAN. The calculation method of hydrodynamic hull forces, propeller forces and rudder forces are described in detail. VeSim is described more briefly.

Chapter 7 presents the simulation model of KVLCC2. Input parameters are presented as well as the calculated non-dimensional hydrodynamic coefficients for deep and shallow water. Previous model test conducted with models of KVLCC2 are summarized.

Chapter 8 presents the simulation results in both SIMAN and VeSim. Turning circles, zig-zag tests and stopping tests are simulated in deep water with approach speed of 15.5 knots to both starboard and port. These are checked against the manoeuvring characteristics specified in IMO MSC Res. 137(70). Turning circles and zig-zag tests are simulated at water depth ratio (h/T) 1.2, 1.5, 1.8 and deep water with approach speed of 7.0 knots to starboard.

Chapter 9 compares the simulation results with with results from SIMMAN 2008, as well as the benchmark data from SIMMAN 2008 suggested by the 26th ITTC Manoeuvring Committee. The results are also compared to the results from MARINTEK's contribution in SIMMAN 2008 to look at differences due to plug-in alterations. Shallow water simulations trends are discussed and compared against full-scale trials of Esso Osaka. A sensitivity analysis of pa-

rameters and hydrodynamic coefficients in SIMAN is presented and discussed. An assessment of the linear velocity is done in deep and shallow water. Calculated drag coefficients, wake fraction and trust deduction are assessed briefly.

Chapter 10 contains conclusion and suggestions for further work.

Chapter 2

Mathematical modelling

2.1 Mathematical modelling

Mathematical models describing seakeeping and ship manoeuvrability are based on six equations of motions and an equation of ship propulsion equilibrium. The motion variables and coordinate system for a marine vessel is presented in figure 2.1.

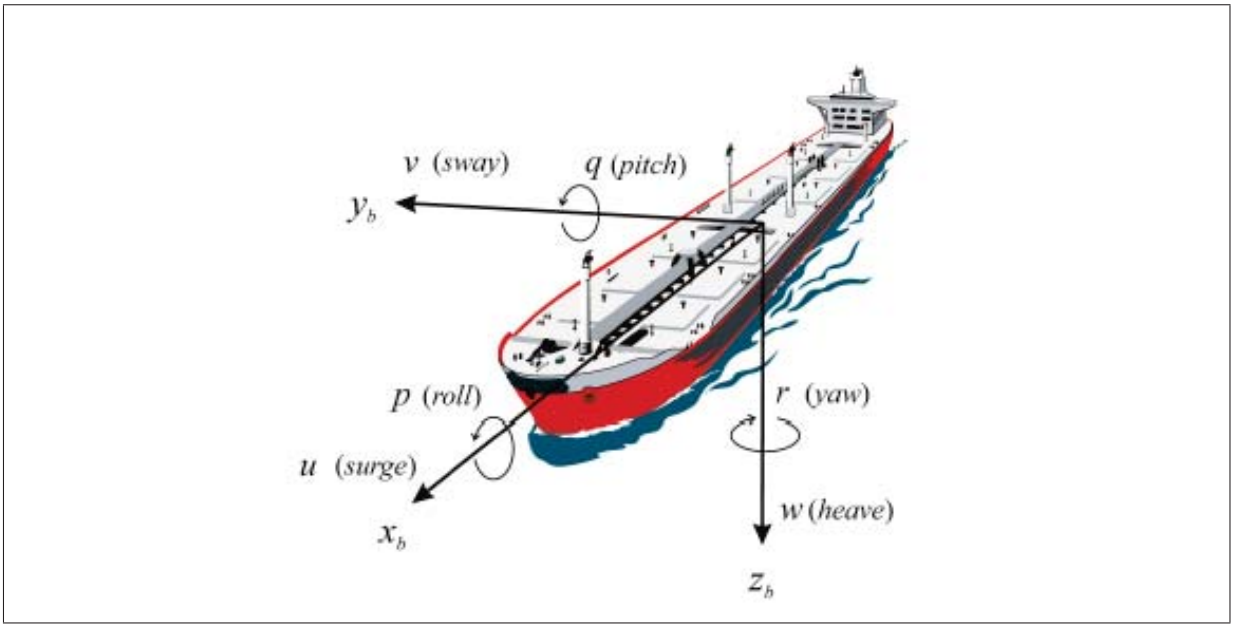

Figure 2.1: Motion variables for a marine vessel (SNAME 1950)

Manoeuvrability of surface ships only considers the horizontal motions (surge, sway and yaw). Roll motion can also be of significance for certain ship types with high speeds and low GM, such as container ships. Basic dynamics of the manoeuvring and course-keeping can be described using Newtons equations of motion and can be considered both in an earth-fixed axis and a body-fixed axis as in Figure 2.2. Euler-Lagrange equations can also be used. These equations are energy based and possess frame-indifference (can be used for any reference frame).

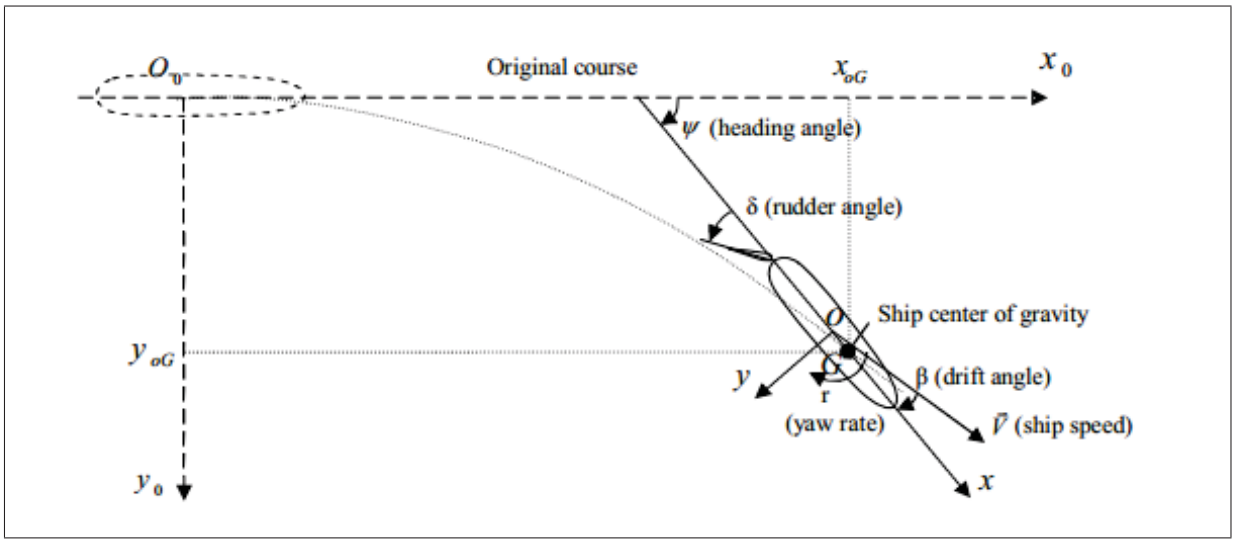

Figure 2.2: Orientation of fixed and moving axes [47]

Figure 2.2 shows the trajectory of a ship and displays various parameters. Two right-handed coordinate systems are used: an earth-fixed coordinate system $O_0 - x_0y_0z_0$ and a body-fixed coordinate system $O - xyz$. The body-fixed axis is moving with the body and the standard notation by SNAME and ITTC for positions, forces and velocities are given in table 2.1.

Motion	**Type**	**Position and angles**	**Velocities**	**Forces and moments**
Surge	Translation on x-axis	x	u	X
Sway	Translation on y-axis	y	v	Y
Heave	Translation on z-axis	z	w	Z
Roll	Rotation about x-axis	ϕ	p	K
Pitch	Rotation about y-axis	θ	q	M
Yaw	Rotation about z-axis	ψ	r	N

Table 2.1: Notation for body-fixed axis

The manoeuvring motion is described by the speed $\overrightarrow{V}$ of the translational motion and the yaw rate $r = \dot{\psi}$ of rotation motion around the z-axis. The angle between the directions of the earth fixed and body fixed x axis is defined as the heading angle ψ. The angle between the speed direction and the x-axis is the drift angle β. The speed components u and v are defined as:

$$\begin{aligned} u &= V\cos\beta \\ v &= -V\sin\beta \end{aligned} \tag{2.1}$$

Where

$$V = |\overrightarrow{V}| = \sqrt{u^2 + v^2} \tag{2.2}$$

The mathematical models (equation of motion) are usually derived from Newtons second law.

$$mass * acceleration = \sum external forces \tag{2.3}$$

$$mass\ moment\ of\ inertia * acceleration = \sum external\ moments \tag{2.4}$$

Newtons second law is valid in the earth-fixed coordinate system, which is an inertial frame. The equations of motions of this coordinate system are

$$\begin{aligned} X_0 &= m\ddot{x}_{0G} \\ Y_0 &= m\ddot{y}_{0G} \\ N_0 &= I_{zG}\ddot{\psi} \end{aligned} \tag{2.5}$$

Where X_0 and Y_0 are the external force components acting on the ship and $\ddot{x_0}$ and $\ddot{y_0}$ are the acceleration components in the x_0- and y_0-axes. N_0 is the external moment and I_{zG} is the moment of inertia of the ship about z-axis. $\ddot{\psi}$ is the yaw acceleration. It is more convenient to use the equations of motion in the body-fixed coordinate system when predicting manoeuvrability. A relationship between the motion parameters in the earth- and body-axis is applied. When the body-fixed coordinate system is fixed to the center of gravity CoG) the kinematic relationships are:

$$\begin{aligned} x_0 &= x_{0G} + x\cos\psi - y\sin\psi \\ y_0 &= y_{0G} + x\sin\psi + y\cos\psi \\ z_0 &= z \end{aligned} \tag{2.6}$$

In reverse the equation becomes:

$$\begin{aligned} x &= (x_0 - x_{0G})\cos\psi + (y_0 - y_{0G})\sin\psi \\ y &= -(x_0 - x_{0G})\sin\psi + (y_0 - y_{0G})\cos\psi \\ z &= z_0 \end{aligned} \tag{2.7}$$

Denoting $x_0' = x_0 - x_{0G}$, $y_0' = y_0 - y_{0G}$ and $z_0' = z_0$ the equations becomes:

$$\begin{aligned} x &= x_0'\cos\psi + y_0'\sin\psi \\ y &= -x_0'\sin\psi + y_0'\cos\psi \\ z &= z_0' \end{aligned} \tag{2.8}$$

And in reverse:

$$\begin{aligned} x_0' &= x\cos\psi - y\sin\psi \\ y_0' &= x\sin\psi + y\cos\psi \\ z_0' &= z \end{aligned} \tag{2.9}$$

The external force components in the directions of the x- and y-axis are now denoted as X_G and Y_G.

$$\begin{aligned} X_G &= X_0\cos\psi + Y_0\sin\psi \\ Y_G &= -X_0\sin\psi + Y_0\cos\psi \end{aligned} \tag{2.10}$$

The ship speed components in the directions of the x- and y-axis are denoted by u_G and v_G.

$$\begin{aligned} \dot{x}_{0G} &= u_G\cos\psi - v_G\sin\psi \\ \dot{y}_{0G} &= u_G\sin\psi + v_G\cos\psi \end{aligned} \tag{2.11}$$

Differentiating equation 2.11 with respect to time gives the accelerations.

$$\begin{aligned}\ddot{x}_{0G} &= \dot{u}_G \cos\psi - u_G\dot{\psi}\sin\psi - \dot{v}_G \sin\psi - v_G\dot{\psi}\cos\psi \\ \dot{y}_{0G} &= \dot{u}_G \sin\psi + u_G\dot{\psi}\cos\psi + \dot{v}_G \cos\psi - v_G\dot{\psi}\sin\psi\end{aligned} \tag{2.12}$$

Substituting equations 2.5 and 2.12 into equation 2.10 yields the equations of motion in the fixed ship origin coordinate system in the CoG are:

$$\begin{aligned}m(\dot{u}_G - v_G r_G) &= X_G \\ m(\dot{v}_G + u_G r_G) &= Y_G \\ I_{zG}\dot{r}_G &= N_G\end{aligned} \tag{2.13}$$

Where $r_G = \dot{\psi}$ is the yaw rate about the z-axis. Since the position of the centre of gravity changes with the loading condition a reference system with the origin at a midship point is preferred. The relationship between ship velocities, forces and moment of inertia midship and the ships centre of gravity are:

$$\begin{aligned}u &= u_G \\ v &= v_G - x_G r_G \\ r &= r_G \\ X &= X_G \\ Y &= Y_G \\ N &= N_G + Y_G x_G \\ I_{zz} &= I_{zG} + m x_G^2\end{aligned} \tag{2.14}$$

Where x_G is the longitudinal distance between the centre of gravity G and the midship point O. With the velocity and moment of inertia relationships the equations of motion can be expressed as:

$$X = m(\dot{u} - vr - x_G r^2) \tag{2.15}$$

$$Y = m(\dot{v} + ur + x_G\dot{r}) \tag{2.16}$$

$$N = I_{zz}\dot{r} + m x_g(\dot{v} + ur) \tag{2.17}$$

Where X, Y and N are the components of hydrodynamic forces and moment related to the midship origin. The various mathematical models have different ways of expressing these forces and moments. X, Y and N are functions of $(\dot{u}, \dot{v}, \dot{r}, u, v, r, n, \delta)$ where n is the propeller rate of turn and δ is the rudder angle.

The linear dynamic stability criterion is derived from the coupled linear equations for yaw and sway and is defined as:

$$s' = \frac{N'_r - m'x'_G}{Y'_r - m'} - \frac{N'_v}{Y'_v} \tag{2.18}$$

if s' is positive the ship is dynamically stable, whilst is s' is negative the ship is dynamically unstable. The criteria can also be written as [13]:

$$\frac{N'_r - m'x'_G}{Y'_r - m'} > \frac{N'_v}{Y'_v} \tag{2.19}$$

The term on the left hand side is called stability arm l'_r and the term on the right hand side is called stability are l'_v. l'_r and l'_v indicates the center of yaw damping and sway damping forces acting on a ship respectively. The course keeping stability becomes stable if the center of yaw damping force is greater than the center of sway damping force. It is advisable that a ship have a positive linear dynamic stability, but for certain kinds of ships it is almost impossible to achieve this. Especially those with high block coefficient.

2.1.1 Formal mathematical models

Abkowitz [12] introduced a mathematical model which is one of the first so-called formal or regression models. The mathematical model is also referred to as whole ship model which treats the ship/fluid interaction phenomenon as a black box. The equations of motion expresses the external forces and moments acting on the ship by using terms up to third order Taylor-series expansion. From considerations of magnitude one can ignore the terms of higher order than third (there are some objections to this, but this will not be assessed in this thesis). The theory assumes that forces at any instant are determined by the prevailing instantaneous motions of the ship [22]. The forces are functions of velocities and accelerations involved in a motion.

$$\begin{aligned}(m - X_{\dot{u}})\dot{u} &= f_1(u, v, r, \delta)\\ (m - Y_{\dot{v}})\dot{v} + (mx_G - Y_{\dot{r}})\dot{r} &= f_2(u, v, r, \delta)\\ (mx_G - N_{\dot{v}})\dot{v} + (I_{zz} - N_{\dot{r}})\dot{r} &= f_3(u, v, r, \delta)\end{aligned} \tag{2.20}$$

Where f_1,f_2 and f_3 is expressed as:

$$\begin{aligned}f_1(u, v, r, \delta) = X^0 + X_u\Delta u + \frac{1}{2}X_{uu}(\Delta u)^2 + \frac{1}{6}X_{uuu}(\Delta u)^3 + \frac{1}{2}X_{vv}v^2 +\\ (\frac{1}{2}X_{rr} + mx_G)r^2 + \frac{1}{2}X_{\delta\delta}\delta^2 + \frac{1}{2}X_{vvu}v^2\Delta u + \frac{1}{2}X_{rru}r^2\Delta u +\\ \frac{1}{2}X_{\delta\delta u}\delta^2\Delta u + (X_{vr} + m)vr + X_{v\delta}v\delta + X_{r\delta}r\delta + X_{vru}vr\Delta u +\\ X_{v\delta u}v\delta\Delta u + X_{r\delta u}r\delta\Delta u\end{aligned} \tag{2.21}$$

$$\begin{aligned}f_2(u, v, r, \delta) = Y^0 + Y^0_u\Delta u + Y^2_{uu}(\Delta u)^2 + Y_v v + \frac{1}{6}Y_{vvv}v^3 + \frac{1}{2}Y_{vrr}vr^2 +\\ \frac{1}{2}Y_{v\delta\delta}v\delta^2 + Y_{vu}v\Delta u + \frac{1}{2}Y_{vuu}v(\Delta u)^2 + (Y_r - mu_1)r + \frac{1}{6}Y_{rrr}r^3 +\\ \frac{1}{2}Y_{rvv}rv^2 + \frac{1}{2}Y_{r\delta\delta}r\delta^2 + Y_{ru}r\Delta u + \frac{1}{2}Y_{ruu}r(\Delta u)^2_\delta + \frac{1}{6}Y_{\delta\delta\delta}\delta^3 +\\ \frac{1}{2}Y_{\delta vv}\delta v^2 + \frac{1}{2}Y_{\delta rr}\delta r^2 + Y_{\delta u}\delta\Delta u + \frac{1}{2}Y_{\delta uu}\delta(\Delta u)^2 + Y_{\delta rv}\delta rv\end{aligned} \tag{2.22}$$

$$\begin{aligned}f_3(u, v, r, \delta) = N^0 + N^0_u\Delta u + N^0_{uu}(\Delta u)^2 + N_v v + \frac{1}{6}N_{vvv}v^3 + \frac{1}{2}N_{vrr}vr^2 +\\ \frac{1}{2}N_{v\delta\delta}v\delta^2 + N_{vu}v\Delta u + \frac{1}{2}N_{vuu}v(\Delta u)^2 + (N_r - x_G u_1)r + \frac{1}{6}N_{rrr}r^3 +\\ \frac{1}{2}N_{rvv}rv^2 + \frac{1}{2}N_{r\delta\delta}r\delta^2 + N_{ru}r\Delta u + \frac{1}{2}N_{ruu}r(\Delta u)^2 + N_\delta\delta + \frac{1}{6}N_{\delta\delta\delta}\delta^3\end{aligned} \tag{2.23}$$

The propeller rate of turn is incorporated in the terms depending on the variation of the longitudinal velocity component Δu. The odd powers in v, r and δ is missing in equation 2.21 due to symmetry about the x-axis. The hydrodynamic coefficients is denoted as the following derivatives:

$$X_u = \frac{\partial X}{\partial u}, Y_{\delta rv} = \frac{\partial^3 Y}{\partial \delta \partial r \partial v}, N_{uu} = \frac{\partial^2 N}{\partial u^2} \tag{2.24}$$

Norrbin (1971) tried to show the physical background of the hydrodynamic forces. The model was a link between pure regression models and modular mathematical models. Functions for propeller thrust, propeller torque, inflow rudder velocity are included.

There are certain disadvantages of the formal mathematical models:

- The hydrodynamic hull, rudder and propeller forces and moments are determined by global regression coefficients and do not directly allow for separate characteristics of these. This is unfortunate in the design stage of a ship.
- The regression model is based on experimental data with a fully appended model. Data fitting can lead to poor physical background of the models.
- Regression models differ between institutes which makes comparisons and data exchange impossible.
- Different combinations of ship speed and rudder action may lead to functions with enormous higher order terms which are not physically understandable.

2.1.2 Modular mathematical models

The basic idea of the modular mathematical model was launched by A. Basin and K. Fediaevsky in the 1960's. But it was the Japanese Mathematical Modeling Group (MMG) that proposed the widespread accepted method of expressing the hydrodynamic forces and moments in modules in the late 1970's. The MMG model decomposes the hydrodynamic forces and moment into three parts; parts acting on the ship hull, the propeller and the rudder. X, Y and N in equation 2.15, 2.16 and 2.17.

$$\begin{aligned} X &= X_H + X_P + X_R \\ Y &= Y_H + Y_P + Y_R \\ N &= N_H + N_P + N_R \end{aligned} \tag{2.25}$$

Where the terms with subscripts H, P and R represent hull forces, propeller forces and rudder forces. The hull, rudder and propeller are considered as interacting modules and the mathematical models are based on examination of the established hydrodynamic principles [22]. Other authors and institutes that contributed to the acceptance and development of the modular mathematical models as well as prediction of ship manoeuvrability has been [22]:

- Oltmann & Sharma, Germany, HSVA.
- Dand, United Kingdom, British Maritime Technology Ltd.
- Asinovsky, USA
- Ankudinov, USA

2.2 Hydrodynamic forces

Theoretical, semi-empirical as well as experimental methods are used to obtain the hydrodynamic forces [5]. The estimation of the various forces and moments affect the accuracy of the simulations in a big way. There are seven different ways of estimation of the hydrodynamic forces and moments, but these can be divided into two main methods; generic databases and ship specific data. When using the generic database method the ship type should be the same and the adequacy of the database should be evaluated carefully; the two methods are database (type ship concept) and regression equations from database. Five different methods can be used in ship specific data:

1. Captive model tests
2. Free model tests with system identification
3. Full scale trials with system identification
4. Calculation of forces resulting from prescribed kinematics by CFD techniques
5. On-line application of CFD techniques during simulation

2.2.1 Generic databases

In this thesis the focus will be on the generic database method: which expresses simple formulae for the hydrodynamic coefficients. These are empirical or semi-empirical methods where a database of model test results and/or alternative prediction methods are used to establish empirical expressions for the various hydrodynamic derivatives based on the principal characteristics of the hull [16]. Regression is often used from data sets (e.g. PMM tests). The empirical approaches provide a cost effective method of estimating the hydrodynamic forces and moments. They have a particular use in estimating the performance at the design stage since it is not necessary to build the ship model and small changes of the hull may easily be investigated for decision-making. Authors and researchers such as Oltmann, Wagner Smitt, Norrbin, Inoue et al., Clarke, Lee and Kijima has been relevant in proposing empirical formulas for the hydrodynamic derivatives. There are similar regression methods based on model tests that are used for prediction of added mass coefficients, flow straightening factor and wake fraction. A thing to keep in mind is that nearly all of the regression formulas proposed by the authors above were developed from a period where full-bodied bulk carriers and tankers were the dominating ship types. Global hull parameters like C_B, $\frac{L}{T}$, $\frac{B}{T}$ are usually used in the formula. Empirical formulae for the linear velocity derivatives are far more common than formulae for the non-linear or acceleration derivatives. A reason for this may be that the velocity derivatives are easier to identify. Burnay and Ankudinov (2003) [16] found the numbers of empiric formulae available for each of the derivatives. Twelve methods are available for prediction of the velocity derivatives whilst only four are available for the acceleration derivatives.

2.2.2 Strip theory

Clarke expresses the normalized velocity derivatives by integrating the horizontal added mass coefficients C_H from the two-parameter Lewis family [18] for the sections along the hull. The

hull shape is taken into consideration through the longitudinal added mass distribution. The expressions are given as:

$$
\begin{aligned}
-\frac{Y'_{\dot{v}}}{\pi(T/L)^2} &= \int_{X'_B}^{X'} C_H dX' \\
-\frac{Y'_{\dot{r}}}{\pi(T/L)^2} &= \int_{X'_B}^{X'} C_H X' dX' \\
-\frac{N'_{\dot{v}}}{\pi(T/L)^2} &= \int_{X'_B}^{X'} C_H X' dX' \\
-\frac{N'_{\dot{r}}}{\pi(T/L)^2} &= \int_{X'_B}^{X'} C_H X'^2 dX \\
-\frac{Y'_{v}}{\pi(T/L)^2} &= [C_H]_{X'} \\
-\frac{N'_{v}}{\pi(T/L)^2} &= [C_H X']_{X'} + \int_{X'_B}^{X'} C_H dX' \\
-\frac{Y'_{r}}{\pi(T/L)^2} &= [C_H X']_{X'} \\
-\frac{N'_{r}}{\pi(T/L)^2} &= [C_H X'^2]_{X'} + \int_{X'_B}^{X'} C_H X' dX'
\end{aligned}
\tag{2.26}
$$

C_H is the zero frequency added mass coefficient at station X', T is the draft of the ship and L is the length. The non-dimensional derivatives are found by integrating these from bow to stern. In [18] Clarke concluded with that it is a fair overall agreement with experiment and theory of the distributions of the velocity derivatives along the hull.

2.2.3 Empirical methods

Jones

Jones [29] used low aspect ratio wing theory to express the derivatives as functions of the draft to length ratio of the ship multiplied by constant factors. The theory make use of the assumption that the ship's hull may be considered to be a low aspect ratio wing turned on its side. The expressions for the linear velocity derivatives were:

$$Y'_v = -\pi \left(\frac{T}{L}\right)^2 (1) \tag{2.27}$$

$$Y'_r = -\pi \left(\frac{T}{L}\right)^2 (-0.5) \tag{2.28}$$

$$N'_v = -\pi \left(\frac{T}{L}\right)^2 (0.5) \tag{2.29}$$

$$N'_r = -\pi \left(\frac{T}{L}\right)^2 (0.25) \tag{2.30}$$

The equations applies only to a thin ship and the last term in the brackets is a function of hull shape in reality.

Wagner Smitt

Wagner Smitt (1970/71) proposed empirical formulae for prediction of the velocity derivatives from regression of 30 data sets from complete hull PMM tests:

$$
\begin{aligned}
Y'_v &= -\pi \left(\frac{T}{L}\right)^2 1.59 \\
Y'_r &= -\pi \left(\frac{T}{L}\right)^2 (-0.32) \\
N'_v &= -\pi \left(\frac{T}{L}\right)^2 0.62 \\
N'_r &= -\pi \left(\frac{T}{L}\right)^2 0.21
\end{aligned} \tag{2.31}
$$

Norrbin

Norrbin investigated similar database as Wagner Smitt and proposed the following expressions for the velocity derivatives:

$$Y'_v = -\pi \left(\frac{T}{L}\right)^2 \left(1.69 + 0.08 \frac{C_B}{\pi} \frac{B}{T}\right) \tag{2.32}$$

$$Y'_r = -\pi \left(\frac{T}{L}\right)^2 \left(-0.645 + 0.038 \frac{C_B}{\pi} \frac{B}{T}\right) \tag{2.33}$$

$$N'_v = -\pi \left(\frac{T}{L}\right)^2 \left(0.64 - 0.04 \frac{C_B}{\pi} \frac{B}{T}\right) \tag{2.34}$$

$$N'_r = -\pi \left(\frac{T}{L}\right)^2 \left(0.47 - 0.18 \frac{C_B}{\pi} \frac{B}{T}\right) \tag{2.35}$$

$$\tag{2.36}$$

Clarke

Clarke et al. [20] collected the results of 72 captive model tests and performed a multiple regression analysis. The final results were:

$$
\begin{aligned}
Y'_v &= -\pi \left(\frac{T}{L}\right)^2 \left(1 + 0.40 \frac{C_B B}{T}\right) \\
Y'_r &= -\pi \left(\frac{T}{L}\right)^2 \left(-\frac{1}{2} + 2.2 \frac{B}{L} - 0.08 \frac{B}{T}\right) \\
N'_v &= -\pi \left(\frac{T}{L}\right)^2 \left(\frac{1}{2} + 2.4 \frac{T}{L}\right) \\
N'_r &= -\pi \left(\frac{T}{L}\right)^2 \left(\frac{1}{4} + 0.039 \frac{B}{T} - 0.56 \frac{B}{L}\right)
\end{aligned} \tag{2.37}
$$

Inoue

Inoue et al. (1981) proposed empirical formulae for the hydrodynamic derivatives. The formulae are valid in deep water and the forces and moments are non-dimensionalized respectively by $\frac{1}{2}\rho L^2U^2$ and $\frac{1}{2}\rho L^3U^2$. The linear velocity derivatives formulae were approximated by [6]

$$\begin{aligned} Y'_v &= -(\frac{\pi}{2}k + 1.4C_B\frac{B}{L})\frac{T}{L} \\ Y'_r &= \frac{\pi}{4}k\frac{T}{L} \\ N'_v &= -k\frac{T}{L} \\ N'_r &= -(0.54k - k^2)\frac{T}{L} \end{aligned} \tag{2.38}$$

Where $k = 2T/L$, which is the effective aspect ratio of the hull in deep water.

Lee

Lee [25] presented formulas for the hydrodynamic derivatives from a database from PMM tests for modern hulls including various ship types and drafts. A simple parameter representing stern hull form is introduced. The ranges of ship particulars are:

- C_B: 0.55 - 0.87
- T/L: 0.022 - 0.071
- L/B: 5.0 - 8.8
- $C_B(B/L)$: 0.075 - 0.166

The forces and moments are normalized by dividing the sway and yaw equations with $\frac{1}{2}\rho LTU^2$ and $\frac{1}{2}\rho L^2TU^2$. Lee's formulas are multiplied by $\frac{T}{L}$ to normalize them the same way as the other hydrodynamic derivatives as the other [45].

$$\begin{aligned} Y'_v &= -\left(0.145 + 2.25\frac{T}{L} - 0.2\Delta_{SR}\right)\frac{T}{L} \\ Y'_r &= -(0.282 + 0.1\Delta_{SR})\frac{T}{L} + 0.0086\Delta_{B/L} + 0.004 + m'\frac{T}{L} \\ N'_v &= -(0.222 + 0.1\Delta_{SR})\frac{T}{L} + 0.00484 \\ N'_r &= -(0.0424 - 0.03\Delta_{SR})\frac{T}{L} - 0.004\Delta_{Cb} + 0.00027 \end{aligned} \tag{2.39}$$

where:

$$\begin{aligned}
\Delta_{Cb} =& 1 - \frac{C_B}{P_{C_B}} \\
P_{C_B} =& 1.12\frac{T}{L} + 0.735 \\
\Delta_{B/L} =& 1 - \frac{B/L}{0.18} \\
\Delta_{SR} =& 1 - \frac{S_R}{P_{SR}} \\
P_{SR} =& 28.7\nabla' + 0.54 \\
S_R =& \frac{B_{P07}}{B_{PS}} \\
\nabla' =& \frac{\nabla}{L^3} \\
m' =& \frac{\Delta}{0.5\rho L^2 T}
\end{aligned} \tag{2.40}$$

B_{PS} is half breath of the vessel at the height of the propeller shaft in 2.0 station, B_{P07} is half breadth at the height of 0.7R (propeller radius) in 2.0 station as seen in figure 2.3.

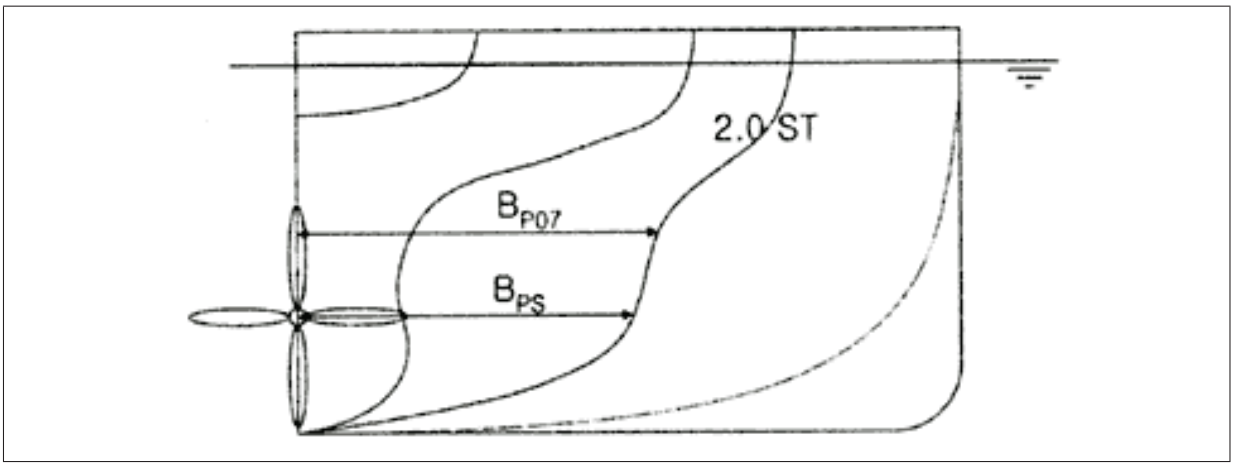

Figure 2.3: Stern Hull Form [25]

Kijima

Kijima and Nakiri [31] proposed prediction formulae of the hydrodynamic derivatives with coefficients that express the characteristics of the aft hull form; fullness of aft run e_a, aft sections fullness metric σ_a and the form factor K. These were obtained from a database consisting of 15 kinds of ships (container ship, bulk carrier, tanker, cargo ship, etc.) and their 48 loading conditions, as well as theoretical investigation. Kijima proposed originally expressions for Y'_β

and N'_β. Y'_v and N'_v are obtained by multiplying the expressions for Y'_β and N'_β by (-1) [45].

$$\begin{aligned}
Y'_v =& -\left(\frac{1}{2}\pi K + 1.9257\frac{C_B B}{L}\sigma_a\right)\frac{T}{L} \\
Y'_r =& \left(\left(\frac{1}{4}\pi K + 0.052e'_a - 0.457\right) + (m' + m'_x)\right)\frac{T}{L} \\
N'_v =& -K\left(15.0668\left(T\frac{1-C_B}{B}e'_a K\right)^2 - 23.819T\frac{1-C_B}{B}e'_a K + 1.802\right)\frac{T}{L} \\
N'_r =& (-0.54K + K^2 - 0.0477e'_a K + 0.0368)\frac{T}{L}
\end{aligned} \tag{2.41}$$

Where:

$$\begin{aligned}
e_a =& \frac{L}{B}(1 - C_{pa}) \\
e'_a =& \frac{e_a}{\sqrt{\frac{1}{4} + \frac{1}{(B/T)^2}}} \\
\sigma_a =& \frac{1 - C_{wa}}{1 - C_{pa}} \\
K =& \left(\frac{1}{e'_a} + \frac{1.5}{L/B} - 0.33\right)(0.95\sigma_a + 0.40) \\
m_x =& \left(\frac{2.7\rho}{L^2}\right)(C_B LBT)^{5/3}
\end{aligned} \tag{2.42}$$

The mass m and added mass m_x are dimensionless by dividing it with $1/2\rho L^2 T$. C_{wa} and C_{pa} are the water plane area coefficient and prismatic coefficient of aft half hull between APP and ship station five. The coefficients are calculated as:

$$\begin{aligned}
C_{wa} &= \frac{A_{wa}}{L_a B_a} \\
C_{pa} &= \frac{\nabla_a}{A_a L_a}
\end{aligned} \tag{2.43}$$

where A_{wa} is the water plane area of the aft section. A_a is the cross-sectional area equal to the largest underwater section of the aft hull. ∇_a is the displacement of the aft hull. B_a is the vessel's breadth of the aft hull and L is its length. Kijima et a. (1990) also proposed a correction formulae for the velocity derivatives if the ship is trimmed.

Chapter 3

Shallow water effects

3.1 Shallow water effects

Due to larger ships sizes with deeper draft more ships experience the effect of shallow waters in several ports and harbours. This has led to an increased need for research within shallow water manoeuvring. The effect of the water depth on ship manoeuvrability is mostly illustrated by comparing standard manoeuvres at different water depths. These comparisons are usually based on simulations because the IMO standard manoeuvres are always carried out in deep water. Full-scale trials in shallow water are so rare that the ships involved are well known (Esso Osaka). The water depth affects the ship manoeuvring capabilities but is mostly related to other applications than the standard manoeuvres. Studies of ship behaviour in shallow water are often related to course keeping in channels/canals, swinging, berthing, unberthing, tug assistance, slow, reversed speed and propeller rate [6]. Manoeuvring descriptions of shallow water are more complicated due to depth/draft ratio and parameters (e. g. forward speed, drift angle, rate of turn, rudder angle and propeller rate) have a more extended range. An arbitrary distinction is made dealing with water depths (PIANC, 1992):

- deep water: h/T>3.0
- medium deep water: 1.5<h/T<3.0
- shallow water: 1.2<h/T<1.5
- very shallow water: h/T<1.2

The ship starts to feel the effect of the depth already at medium deep water. The reason for this is that the water depth changes the pressure distribution around the vessel and leads to increasing hydrodynamic forces. At shallow water the effect is very significant and in very shallow water the effect of the depth dominates. In figure 3.1 it is clearly shown that an increase in the hydrodynamic forces with smaller UKC (under keel clearance).

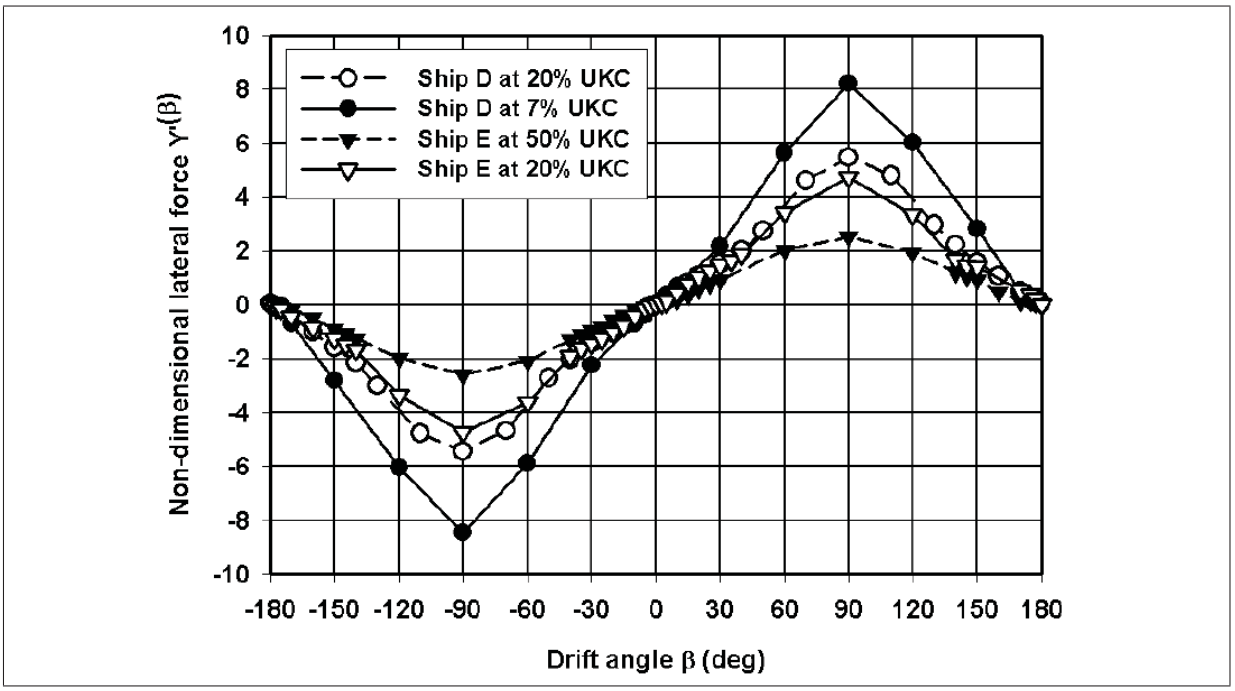

Figure 3.1: Influence of water depth on non-dimensional lateral force Y due to oblique towing for a containership (ship D) and a tanker (ship E) [22]

This leads to a decrease in the ships manoeuvrability, depending on the ship type. For instance a container ship execution of a turning circle gets larger as the water gets shallower as seen in figure 3.2.

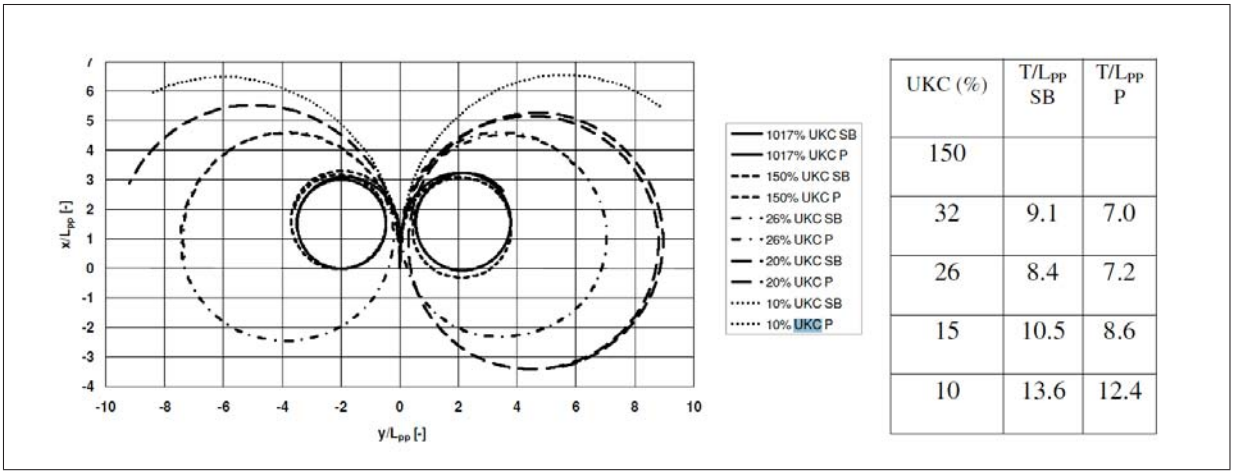

UKC (%)	T/L_{PP} SB	T/L_{PP} P
150		
32	9.1	7.0
26	8.4	7.2
15	10.5	8.6
10	13.6	12.4

Figure 3.2: Free-running turning circle model tests with a 6000 TEU container ship in deep and shallow water compared with the tactical diameter prediction (table) from captive model test [23]

Yasukawa and Kobayashi [27] investigated the shallow water effect on turning performance based on free-running model test for four different ship types. The ship principal particulars of tested ship models were:

	Ship A	Ship B	Ship C	Ship D
Ship type	**Container**	**LNGC**	**Special cargo**	**Tanker(Esso Osaka)**
Ship length (m)	4.200	5.000	5.500	4.600
Breath (m)	0.709	0.809	1.531	0.751
Draft (m)	0.209	0.210	0.240	0.308
Block coefficient	0.64	0.73	0. 88	0.83
No. of propeller	1	1	2	1
Propeller dia. (m)	0.158	0.158	0.137	0.130
No. of rudder	1	1	2	1
Approach speed (m/s)	0.77	0.36	0.37	0.31
Water depth (h/d)	1.3, 1.5, 16.3	1.3, 1.5, 16.2	1.25, 1.5, 14.3	1.2,1.5,11.3

Table 3.1: Ship particulars of tested ship models

It was observed that the depth/draft ratio has a different effect on the turning circle for the different ships as seen in figure 3.3.

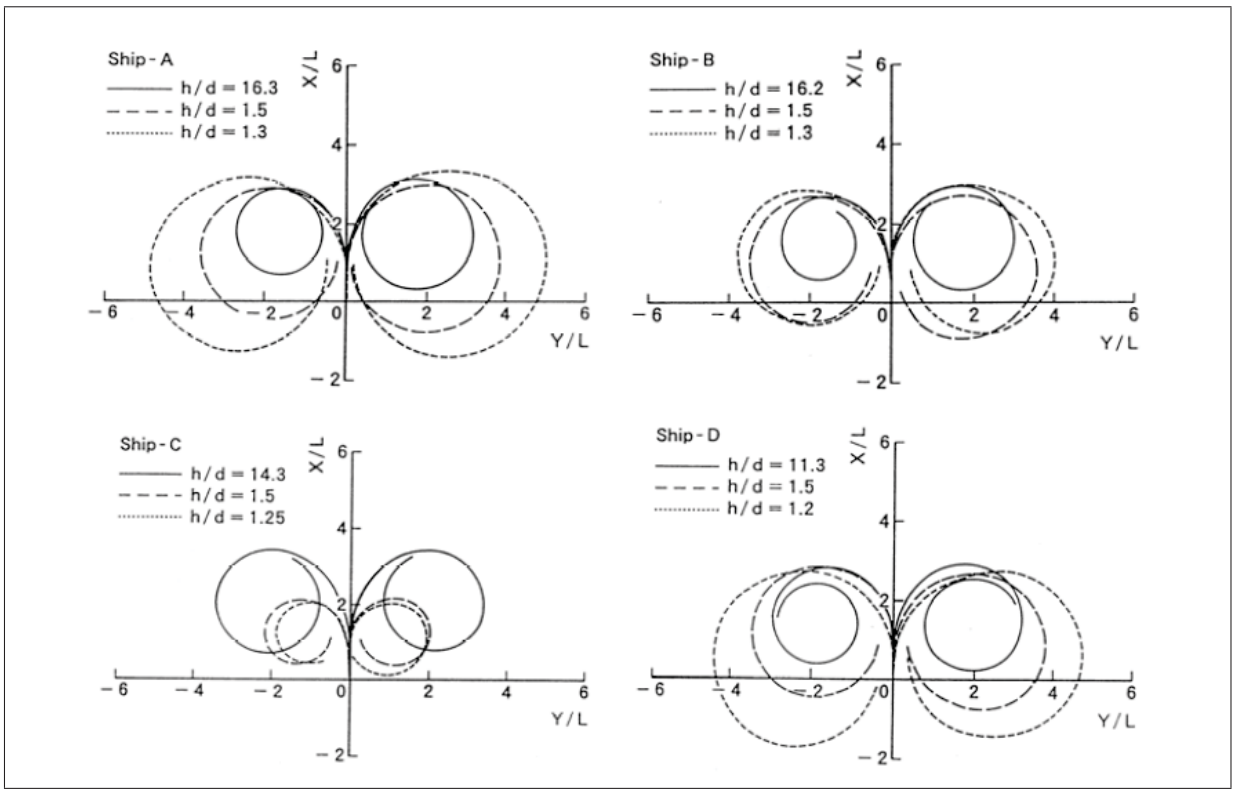

Figure 3.3: Comparisons of ship trajectories in shallow and deep waters [8]

The results led to a proposed classification into three different ship types:

- Type-N (normal): the turning circle becomes larger monotonously with decreasing water depth. This shallow water effect is found for slender ships like container ships with block coefficients C_B lower than 0.75 (Ship A and B).
- Type-U (unstable): the turning circle becomes larger with decreasing water depth, however the course keeping instability appears in medium deep water. This could be found

for the tanker Esso Osaka (Ship D) and is generally adopted for full ship forms.

- Type-S (small): the turning circle becomes smaller with decreasing water depth (Ship C). Due to increase of the rudder normal force at decreasing water depth a wide beam and small draft ship (L_{PP}/B is lower than B/d) turns easier in shallow than deep water.

Another outcome of Yasukawa and Kobayashi was that for conventional ships (Type-N and Type-U) the shallow water effect is especially expected to affect the hull forces while the rudder forces are considered unaffected. Another factor in the different manoeuvring characteristics in shallow water is the position of the acting points of yaw damping and sway damping forces, which depends on the hull form.

Another aspect of shallow water effects is that the changing pressure field around the hull can cause trim and sinkage of the body. The sinkage increases considerably in shallow water and this phenomenon is known as squat. This will however not be assessed in this thesis.

3.2 Adaptations to shallow water mathematical models

Norrbin incorporated the effect of water depth by adding equations depending on a parameter z which is defined by:

$$z = \frac{T}{h - T} \tag{3.1}$$

Where T is the draft and h is the water depth. The force and moment contributions to the equation of motions of Norrbins model [37]:

$$\begin{aligned} X_{conf} =& X_{\dot{u}z}\dot{u}z + X_{uuz}u^2z + X_{vrz}vrz + X_{vvzz}v^2u^2 \\ Y_{conf} =& Y_{\dot{v}z}\dot{v}z + Y_{urz}urz + Y_{uvz}uvz + Y_{v|v|z}v|v|z + Y_{c|c|\beta|\beta||\delta|z}c|c|\beta|\beta||\delta|z \\ N_{conf} =& N_{\dot{r}z}\dot{r}z + N_{urz}urz + N_{uvz}uvz + N_{r|v|z}r|v|z + N_{c|c|\beta|\beta||\delta|z}c|c|\beta|\beta||\delta|z \end{aligned} \tag{3.2}$$

The last term in of the lateral force and the yawing moment in equation 3.2 shows that contributions from the rudder is included as well.

Several authors incorporate the shallow water effect by including ratios of shallow to deep water values to scale the hydrodynamic derivatives, provided that these are available. Most of the contributions of the hydrodynamic derivatives are based on slender-body strip theory methods, using two-dimensional horizontal added mass coefficients along the hull. Therefore most of the formulas that account for shallow water are based on an analytical approach of the influence of the presence of a bottom on the 2D horizontal added mass of circular, elliptical and rectangular body sections [6]. The 23rd ITTC Manoeuvring Committee divided the formulations into:

- Formulations based on Sheng's formulae

- Formulations based on the MMG model

3.2.1 Formulations based on Sheng's formulae

Sheng (1981) showed that the elliptical horizontal added mass coefficients can be corrected by a deep to shallow water ratio:

$$\frac{C_H}{C_{H\infty}} = K_0 + K_1\frac{B}{T} + K_2\left[\frac{B}{T}\right]^2 \tag{3.3}$$

Where:

$$\begin{aligned} K_0 =& 1 + \frac{a_0}{F^2} + \frac{b_0}{F^3} \\ K_1 =& \frac{a_1}{F} + \frac{b_1}{F^2} + \frac{c_1}{F^3} \\ K_2 =& \frac{a_2}{F} \end{aligned} \tag{3.4}$$

$F = \frac{h}{T} - 1$ is a function of water depth and draft. a_0, b_0, a_1, b_1, c_1 and a_2 are predetermined constants. Clarke et al. (1983) obtained the following deep to shallow water ratio by integrating the equations 2.26.

$$\begin{aligned} \frac{Y'_{\dot{v}}}{Y'_{\dot{v}\infty}} =& K_0 + \frac{2}{3}K_1\frac{B}{T} + \frac{8}{15}K_2\left[\frac{B}{T}\right]^2 \\ \frac{N'_{\dot{r}}}{N'_{\dot{r}\infty}} =& K_0 + \frac{2}{5}K_1\frac{B}{T} + \frac{24}{105}K_2\left[\frac{B}{T}\right]^2 \\ \frac{Y'_{v}}{Y'_{v\infty}} =& K_0 + K_1\frac{B}{T} + K_2\left[\frac{B}{T}\right]^2 \\ \frac{N'_{v}}{N'_{v\infty}} =& K_0 + \frac{2}{3}K_1\frac{B}{T} + \frac{8}{15}K_2\left[\frac{B}{T}\right]^2 \\ \frac{Y'_{r}}{Y'_{r\infty}} =& K_0 + \frac{2}{3}K_1\frac{B}{T} + \frac{8}{15}K_2\left[\frac{B}{T}\right]^2 \\ \frac{N'_{r}}{N'_{r\infty}} =& K_0 + \frac{1}{2}K_1\frac{B}{T} + \frac{1}{3}K_2\left[\frac{B}{T}\right]^2 \end{aligned} \tag{3.5}$$

He was not able to obtain expressions for $Y'_{\dot{r}}$ and $N'_{\dot{v}}$. Clarke (1997) revised this method by publishing new values for a_0, b_0, a_1, b_1, c_1 and a_2. Clarke's expressions above are valid for $1.25 < h/T < \infty$.

Ankudinov et al. [46] proposed a water depth correction matrix based on the ratios in 3.5. The expressions are valid for $1.085 < h/T < 5$ and $C_B \leq 0.85$. The linear sway-yaw terms are gives as:

$$\begin{aligned} \frac{Y'_{\dot{v}}}{Y'_{\dot{v}\infty}} =& gv\ ,\ \frac{Y'_{\dot{r}}}{Y'_{\dot{r}\infty}} = gv \\ \frac{N'_{\dot{v}}}{N'_{\dot{v}\infty}} =& gv\ ,\ \frac{N'_{\dot{r}}}{N'_{\dot{r}\infty}} = gnr \\ \frac{Y'_{v}}{Y'_{v\infty}} =& fyv\ ,\ \frac{Y'_{r}}{Y'_{r\infty}} = fyr \\ \frac{N'_{v}}{N'_{v\infty}} =& fnv\ ,\ \frac{N'_{r}}{N'_{r\infty}} = fnr \end{aligned} \tag{3.6}$$

The surge terms are given as:

$$\begin{aligned}\frac{X'_{\dot{u}}}{X'_{\dot{u}\infty}} =& gv \ , \ \frac{X'_{rr}}{X'_{rr\infty}} = gnr \\ \frac{X'_{vr}}{X'_{vr\infty}} =& frv \ , \ \frac{X'_{vv}}{X'_{vv\infty}} = frv\end{aligned} \tag{3.7}$$

with

$$\begin{aligned}gv =& K_0 + \frac{2}{3}K_1\frac{B_1}{T} + \frac{8}{15}K_2\left[\frac{B_1}{T}\right]^2 \\ gnr =& K_0 + \frac{8}{15}K_1\frac{B_1}{T} + \frac{40}{105}K_2\left[\frac{B_1}{T}\right]^2 \\ fyv =& 1.5fnr - 0.5 \\ fyr =& K_0 + \frac{2}{5}K_1\frac{B_1}{T} + \frac{24}{105}K_2\left[\frac{B_1}{T}\right]^2 \\ fnv =& K_0 + K_1\frac{B_1}{T} + K_2\left[\frac{B_1}{T}\right]^2 \\ fnr =& K_0 + \frac{1}{2}K_1\frac{B_1}{T} + \frac{1}{3}K_2\left[\frac{B_1}{T}\right]^2\end{aligned} \tag{3.8}$$

where

$$\begin{aligned}K_0 =& 1 + \frac{0.0775}{F^2} - \frac{0.0110}{F^3} + \frac{0.000068}{F^5} \\ K_1 =& -\frac{0.0643}{F} + \frac{0.0724}{F^2} - \frac{0.0113}{F^3} + \frac{0.0000765}{F^5} \\ K_2 =& \frac{0.0342}{F} \ for \ \frac{B}{T} \leq 4 \\ K_2 =& \frac{0.137}{F}\frac{T}{B} \ for \ \frac{B}{T} > 4\end{aligned} \tag{3.9}$$

$F = \frac{h}{T} - 1$ is a function of water depth and draft. $B_1 = C_B B\left(1 + \frac{B}{L}\right)^2$ is a function of breadth, length and block coefficient.

3.2.2 Formulations based on the MMG model

Velocity derivatives

Hirano et al. (1985) included the shallow water effect in for the empirical linear velocity derivatives formulae proposed by Inoue (1981) in equation 2.38. The effective aspect ratio of the hull in deep water is simply replaced by a ratio in deep water.

$$k_e = \frac{k}{\frac{Tk}{2h} + \left(\frac{\pi T}{2h}\cot\frac{\pi T}{2h}\right)^\lambda} \tag{3.10}$$

The coefficient λ must be adjusted experimentally, but proposed values are $\lambda = 2.3$ for Y'_v, $\lambda = 1.7$ for N'_v and $\lambda = 0.7$ for Y'_r and N'_r. Kijima et al. (1990) proposed a correction for shallow water conditions, which is also based on equation 2.38:

$$D_{shallow} = f\left(\frac{T}{h}\right) D_{deep} \tag{3.11}$$

Where f is a correction factor depending on the draft, water depth and a factor n (varying with which derivative which is considered):

$$f\left(\frac{T}{h}\right) = \frac{1}{\left(1 - \frac{T}{h}\right)^n} - \frac{T}{h} \tag{3.12}$$

The linear damping derivatives have the following n formulas:

$$\begin{aligned} D = Y'_v \;&\Rightarrow\; n = 0.40 C_B \frac{B}{T} \\ D = N'_v \;&\Rightarrow\; n = 0.425 C_B \frac{B}{T} \\ D = N'_r \;&\Rightarrow\; n = -7.14 \frac{2T}{L} + 1.5 \end{aligned} \tag{3.13}$$

The correction expression for Y'_r is inclusive the non dimensional mass and the surge acceleration derivative.

Added inertia coefficients

Deep water to shallow water ratios for added inertia coefficients has been proposed by Li & Wu (1990):

$$\begin{aligned} \frac{m_{11}}{m_{11\infty}} &= 1 + \frac{3.77 + 1.14\frac{B}{T} - 0.233\frac{L}{T} - 3.43 C_B}{F^{1.30}} \\ \frac{m_{22}}{m_{22\infty}} &= 1 + \frac{0.413 + 0.032\frac{B}{T} + 0.0129(\frac{B}{T})^2}{F^{0.82}} \\ \frac{m_{66}}{m_{66\infty}} &= 1 + \frac{0.413 + 0.0192\frac{B}{T} + 0.00554(\frac{B}{T})^2}{F^{0.82}} \end{aligned} \tag{3.14}$$

Where $F = (h/T - 1)$.

Resistance and propulsion

The hull resistance in shallow water can be accounted for by correcting the form factors. Millward (1989) proposed:

$$k_{shallow} = k_{deep} + 0.644\left(\frac{T}{h}\right)^{1.72} \tag{3.15}$$

Yasukawa proposed a shallow water ratio for the wake factor based on model experiments with single propeller and single rudder in 1998. The wake factor increases significantly with decreasing water depth.

$$\frac{w_h}{w_{h\infty}} = 1 + a(C_B)\left(\frac{T}{h} - 0.2\right)^{b(C_B)},\ for\ \frac{T}{h} > 0.5 \tag{3.16}$$

Where:

$$\begin{aligned} a(C_B) &= 6.6 - 7.0C_B \\ b(C_B) &= 5.4C_B - 2.2 \end{aligned} \tag{3.17}$$

Equation 3.17 is not valid for ships with low C_B.

Effect on rudder induced forces

The MMG model expresses usually the rudder induced forces and moment as:

$$\begin{aligned} X_R &= -(1 + a_X)F_N \sin\delta \\ Y_R &= -(1 + a_H)F_N \cos\delta \\ N_R &= -(x_R + a_H x_H)F_N \cos\delta \end{aligned} \tag{3.18}$$

The rudder normal force can be written as

$$F_N = \frac{1}{2}\rho A_R U_R^2 C_N \sin\alpha_R \tag{3.19}$$

Where α is the effective rudder inflow angle and $U_R = \sqrt{u_R^2 + v_R^2}$ is the effective rudder velocity. The rudder normal force is mostly affected by the influence of the hull force factor a_H which increases significantly in shallower water. The longitudinal coordinate x_H of the hull force application point have a tendency to more forward when h/T decreases. Hirano et al (1985) showed these tendencies as seen in figure 3.4 and figure 3.5.

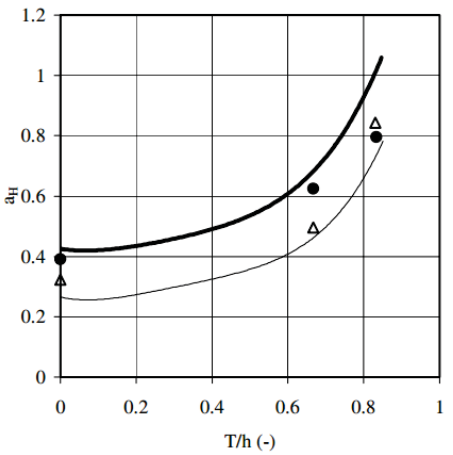

Figure 3.4: Influence of water depth on hull force factor [6]

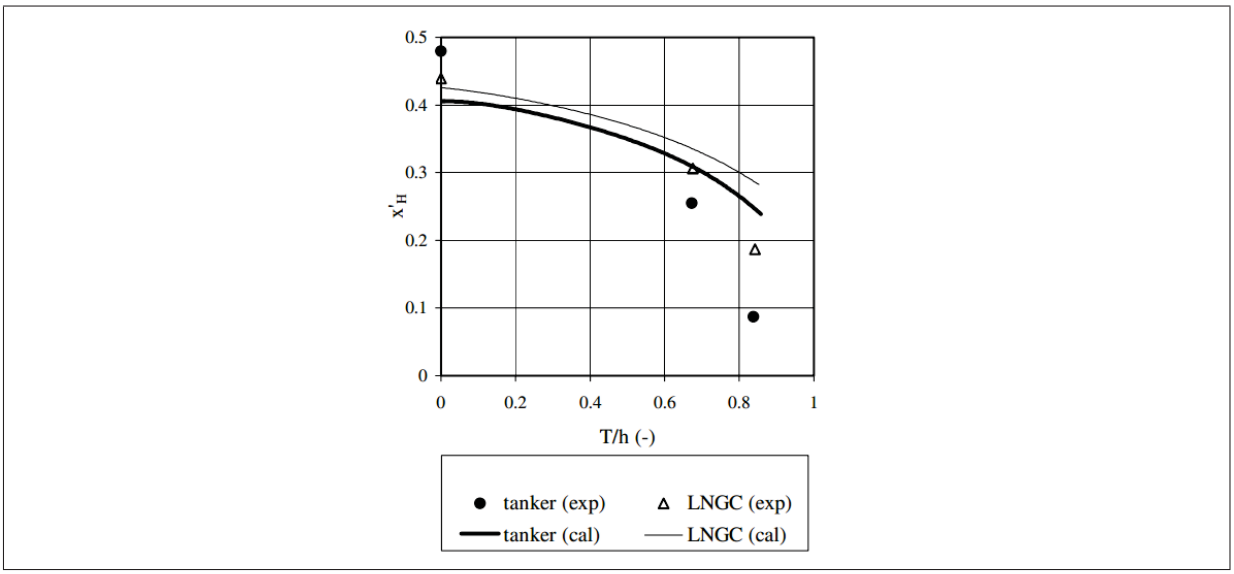

Figure 3.5: Influence of water depth on hull-rudder interaction [6]

Water depth influences the inflow velocities of the rudder:

$$\begin{aligned} u_R =& \epsilon u_P \sqrt{1 + \kappa \frac{8K_T}{\pi J^2}} \\ v_R =& U f(v' + l'_R r') \end{aligned} \tag{3.20}$$

Kobayashi included the shallow water effect on κ, ϵ and $f(v' + l'_R r')$ by applying the formulae:

$$\frac{(Coefficient)_{shallow}}{(Coefficient)_{deep}} = 1 + q_5 \left(\frac{T}{h}\right)^{q_6} \tag{3.21}$$

Where q_5 and q_6 is defined for each of the coefficients.

Experimental methods

An example an experimental method is a power law function on the hydrodynamic coefficients f by Gronarz (1999):

$$f = c_0 + c_n (\frac{T}{h})^n \tag{3.22}$$

c_0 is a constant term indicating deep water, c_n is a term depending on the water depth or ratio $\frac{T}{h}$. c_0, c_n and n has to be determined experimentally. Gronarz demonstrated a simple and easy way of consideration of water depths effects in the manoeuvring simulation.

A review of the empirical shallow water correction methods was made by the 23rd ITTC manoeuvring committee. The results of the review are attached in appendix A.3. The conclusion was that the various methods differ considerably when going towards shallow water. When the water becomes very shallow the methods have varying asymptotic expressions with some of the derivatives even going towards infinity. The flow becomes a 2D flow since no cross-flow can occur in very shallow water. In general, the Ankudinov formulae appear to results into a fair approximation for N_{ur} and $N_{\dot{r}}$ [6]. Kobayashi's expressions perform very well for slender ships. It should be noticed that Kijima's formulae generally tend to underestimate the linear velocity coefficients, while the non-linear coefficients are overestimated. The experimental data for very shallow water range are very scarce because of practical difficulties.

3.3 Esso Osaka

Full-scale manoeuvring trials were conducted in 1977 with the tanker Esso Osaka. The trials were sponsored by US Maritime Administration, the US Coast Guard and the American Institute of Merchant Shipping, and were managed by Exxon International Company [1]. The results were published by Crane et al. (1979). The trials consisted of standard manoeuvres in three different water depths, 20%, 50% and 320% UKC. Figure 3.6 presents the manoeuvres which were chosen for the trials.

TYPE OF MANEUVER OR CALIBRATION RUN	SPEED OF APPROACH TO MANEUVERS, knots		
	Depth/ Draft 1.2	Depth/ Draft 1.5	Depth/ Draft 4.2
1. *Maneuvers*	Shallow	Medium	Deep
Turn, port, 35-deg L rudder	5, 7	7	7
Turn, stbd, 35-deg R rudder	5, 7	7	7, 10
Turn, accelerating, 35-deg R rudder	0+	0+	–
Turn, coasting, 35-deg R rudder	5	5	5
Z-maneuver, 20/20	7	7	7
Z-maneuver, 20/20 coasting	5	5	5
Z-maneuver 10/10	7	7	7
Biased Z-maneuver	7	7	7
Spiral	7	7	7
Stop, 35-deg L rudder	3.5		3.5
Stop, 35-deg R rudder	3.5	3.5	3.5
Stop, controlled heading	3.5	–	3.5
Stop, steering for constant heading			3.5
2. *Calibration Runs*			
Speed/rpm, taken during steady runs prior to chosen maneuvers	3.5, 6, 8.5	5, 7.5	7, 10
Total runs	17	12	15

Figure 3.6: Esso Osaka full-scale trials [1]

Esso Osaka was previously selected as a benchmark ship by the ITTC for various reasons [38]:

- Unusual extensive set of trials had been conducted with unusual attention to measurement accuracy.
- The trials were conducted in deep and finite (shallow) water.
- Free running model tests and captive model tests had been done by at least 20 different laboratories, using models with different scales (lengths ranging from 1.65 to 8.125

meter).

- Detailed drawings of hull, propeller and rudder had been made available by EXXON, which was needed for RANS calculations.

Esso Osaka is a Type-U ship, which is unstable. Comparisons of spiral tests for model and full scale of Esso Osaka shows the course keeping instability appearing in medium water depths as shown is figures 3.7 and 3.8.

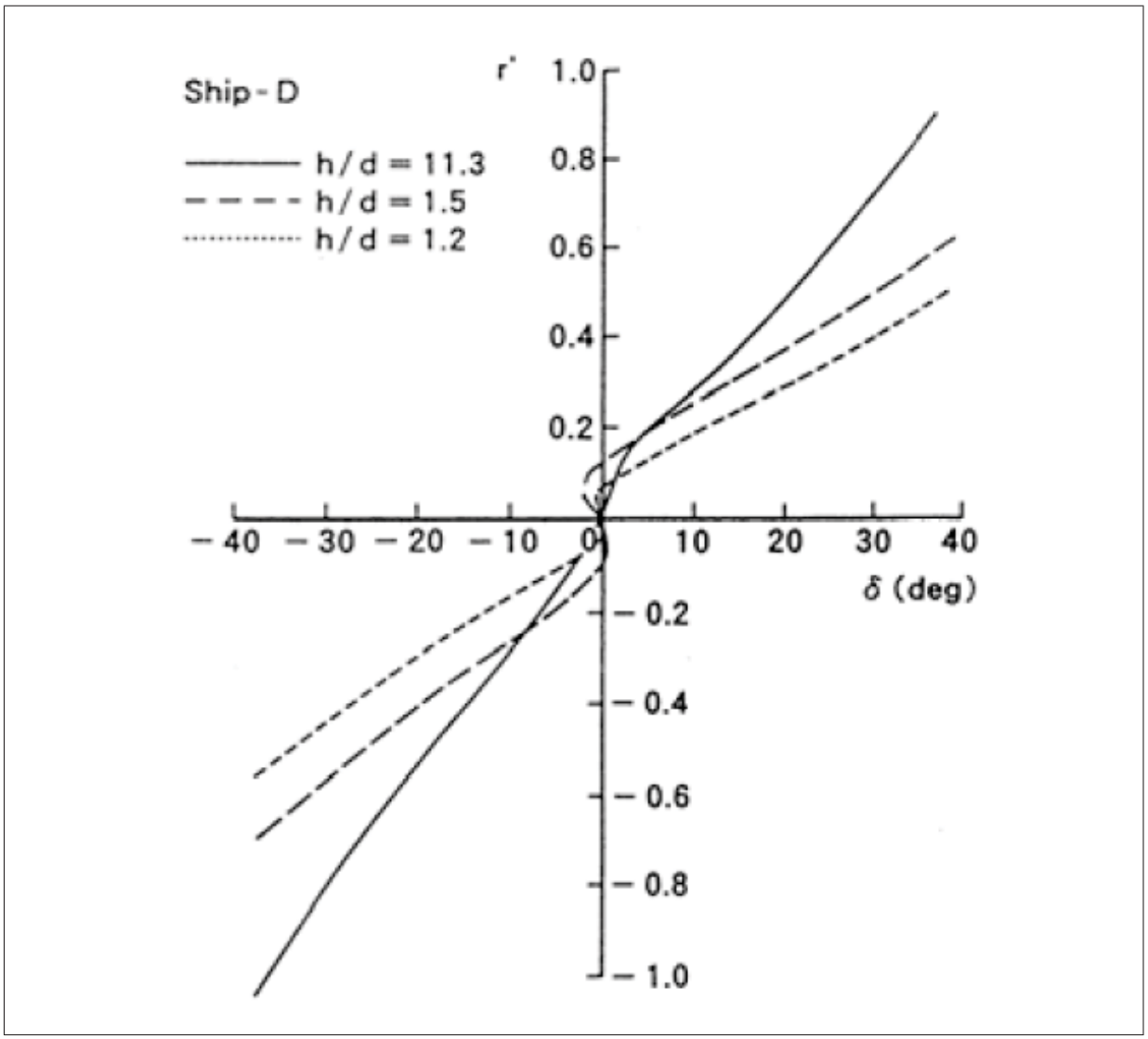

Figure 3.7: Spiral test characteristics in model scale [8]

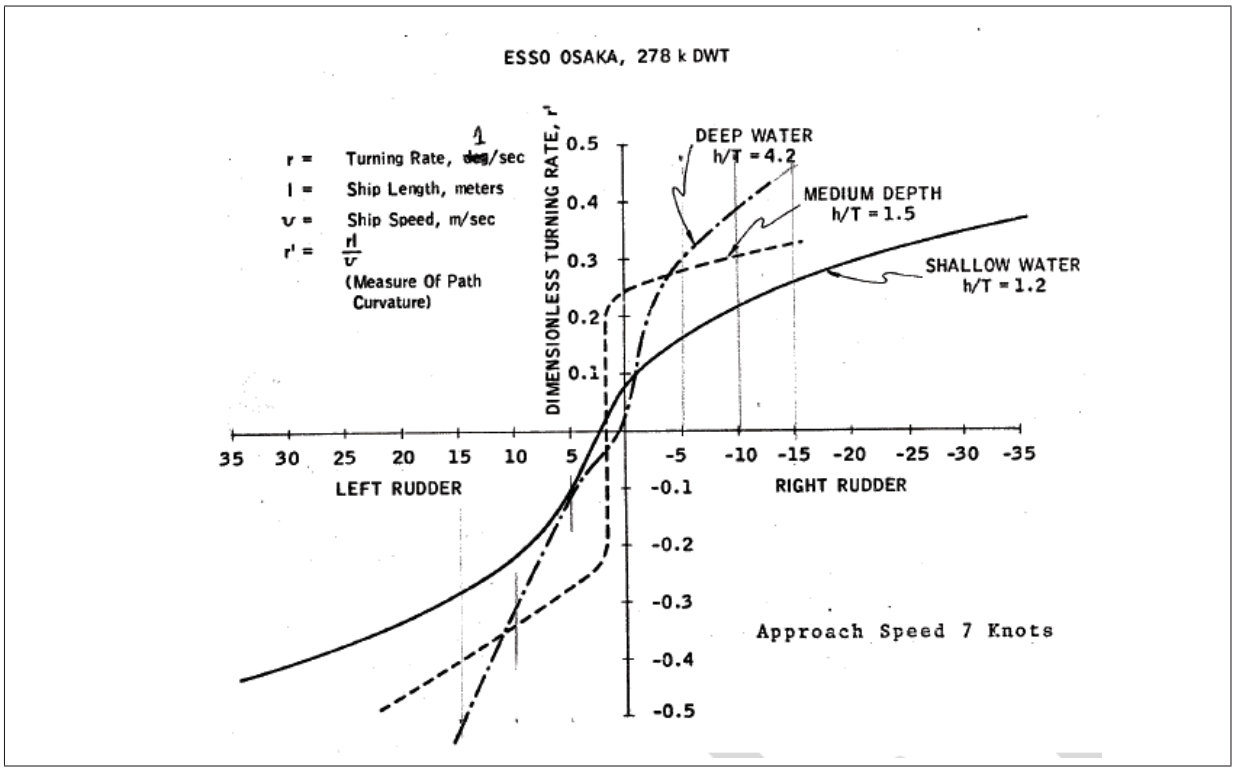

Figure 3.8: Spiral test characteristics in full-scale [8]

The main conclusions from the complete published set of trial results were summarised by the 16th ITTC Manoeuvrability Committee [1]:

- *"In shallow water, turning circle tactical diameter increase by as much as 75% with 20% under keel clearance, while drift angle and related speed loss reduce relative to turning in deep water. With 50% bottom clearance, the changes from deep water turning were much less."*

- *"Checking and counter turning ability are reduced as water depth decreases from deep water to an intermediate depth (50% bottom clearance) and then increase again at more shallow depths, becoming better than in deep water at 20% under keep clearance in these trials. This phenomenon is closely related to the apparent reversal in controls fixed course stability shown by the trial results, where stability first decreases when moving from deep to medium water depths and then increases again as water depth becomes very shallow."*

- *"The greatest effect of decreasing water depth on the stopping of this single-screw tanker from slow speed, is an increase in heading deviation to starboard, which varies from 18 to 50 and then to 88 degrees in deep, medium and shallow water, respectively. Stopping distance is substantially independent of water depth."*

Uncertainties in the environmental conditions makes the full-scale sea trials hard to use fas benchmark data. The wind and waves were slight but the average current was 0.4 knots (ranging from 0.1 to 0.8 knots), varying with time, location and depth [1]. The deep water trials were performed on h/T=4.2 where bottom effects could exist, as well as water depth was not constant in the shallow water trials. ITTC's specialist Committee on Esso Osaka tried to discuss the full-scale trial tests against model tests in shallow water, but were not able to get sufficient data

because lack of information on experiments and analyzing procedures. The available data sets are small and the scatter of the results are more diverse. A comparison of the hydrodynamic forces from different sources were made. The conclusion was that the results did not correlate well. The results showed evidence of scale effects of the hydrodynamic side force which seemed to increase for decreasing model size. Esso Osaka will not be used for validation of the shallow water model of KVLCC2, but shallow water trends will be compared.

Chapter 4

Low speed manoeuvring

4.1 Low speed manoeuvring

According to Eloot (2006) the term “low” or “slow” can mostly be interpreted in two ways in papers dealing with ship manoeuvring:

- *”Reports dealing with modified expressions for the hull forces due to the existence of large drift angles and/or yaw rate angles when ships are for example laterally shifted or turned by tug boats”* [22]

- *”Reports dealing not only with wide ranges of kinematic parameters but also with all possible combinations of propeller operation and consequently rudder operation”* [22]

Course changes are seldom made in shallow water or in proximity to other ships or land, but radical manoeuvres a ship makes occur. Ship operations may require low speed manoeuvres with high yaw rate angle and drift angle, as well as large ahead and astern propeller loadings. Most ship accidents occur near harbours with shallow and restricted waters at low speed. The lateral force depends significantly on the yaw rate angle and drift angle, which traditional manoeuvring models usually do not account for at high angles. The dominant force during large drift angles is cross flow drag forces which are caused by flow separation as seen in figure 4.1.

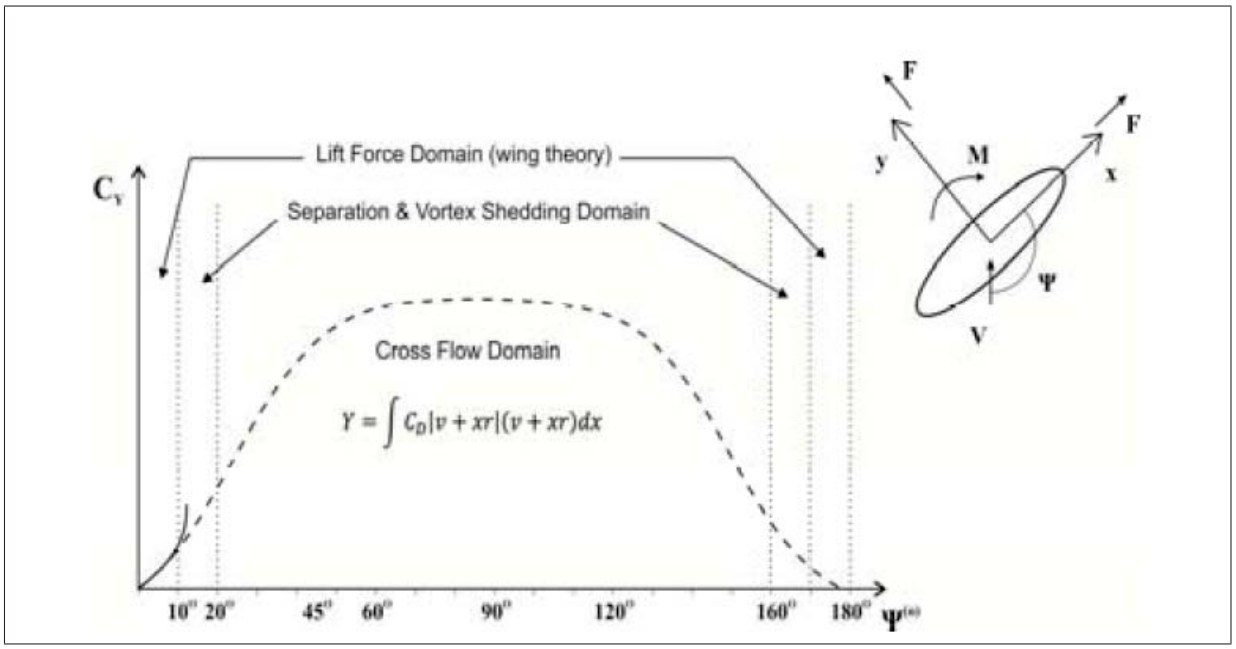

Figure 4.1: Lateral force variation with drift angle [10]

The governing mechanisms of low speed ship hydrodynamics according to Hwang et al. [24]: The tactical diameter becomes larger for most ships are a function of Froude Number. For the MARAD full-form series, both damping coefficient ratio and yaw damping coefficient ratio drop as Froude Number becomes smaller [24]. Resistance coefficient increases with decreasing ship speed for low speed operation. A result of this is an increase propeller loading which can cause an increase in propeller wash and make the rudder more effective.

There are yet no standards for low speed manoeuvring criteria, but the need for these has been raised for a long time. The need for expanding performance indices from service speed to low speed has evolved gradually from needs of operation and simulator facilities [24]. The standardized manoeuvre indices do not provide sufficient information about the ship low speed manoeuvring performance, and the lack of standardized manoeuvres and performance indices is a problem for the validation of low speed mathematical models. Low speed manoeuvres are not amongst the central concerns for design of most ships for ship owners and shipyards but they are crucial to safe operations. Critics of the IMO standards have been raised by Dand (2003) and Quadvlieg and Coevorden (2003). Dand [21] summarized the shortcomings of the IMO standards as:

- *IMO standard may not be valid for low speed manoeuvring in ports, because they are for deep water and design speed only."*
- *"They are for calm conditions only and give no indication of the qualities in wind, current or waves."*
- *"They cover standard manoeuvres only and do not necessarily cover the type of manoeuvring normally carried out by most merchant ships."*
- *"The full astern stopping test on trials puts to much strain on the prime mover and propulsion train."*

- *"The criteria are derived from databases heavily biased toward tankers and bulk carriers."*

Quadvlieg and Coevorden [40] had concerns regarding the IMO standards which for safety reasons have to be further investigated

- *"Adequate manoeuvrability in shallow waters."*
- *"Maximum achievable wind forces for harbour manoeuvring."*
- *"Low-speed manoeuvring capabilities."*
- *"Steering in wind and waves at relatively high speeds including ability to execute 180 degrees turn in waves."*
- *"Limited heel angles."*

4.2 Specific low speed manoeuvres/criteria

As mentioned earlier the IMO standards manoeuvres may not be valid for low speed manoeuvres. How can a ship be judged to manoeuvre satisfactory using the IMO standards when it appears to have poor manoeuvrability in harbours where most of the manoeuvres take place? One low speed manoeuvre has previously been recommended by IMO (A.601), SNAME (1989) and Japan (RR) is the Zig-Zag Manoeuvre test at low speed. The manoeuvre is used to acquire the minimum speed at which the ship does not respond to the helm. The execution of the test should be carried out as follows [30]:

1. Establish a steady ship speed and steady course.
2. Stop the engine and let the propeller idle. Order the rudder to be moved to 35°right.
3. When the ship turns to 1°starboard heading, reverse the rudder angle to 35°left.
4. After the ship reverses turning direction and the approach heading reaches 1°port, reverse the rudder angle to right 35°.
5. Repeat steps three and four until the rudder is no longer active and the ship does not respond to the rudder.

There are also some other recommended manoeuvres in the IMO manoeuvring booklet, but these are not criteria. The manoeuvres suggested does not cover the all the four quadrants of operation as in figure 4.2.

4.2.1 Dand

Typical manoeuvres which are expected of a ship at low speed are according to Dand [21]:

- Controlled loss of speed
- Emergency stop

- Control and course stability at very low speeds
- Sideslipping/Breasting/Crabbing
- Kick ahead
- Swing checking
- Astern performance
- Controlling bank effects
- Control during low speed transfers
- Control using currents
- Control in wind

Due to the difficulty of performing low speed manoeuvres in shallow water with constant depth for full scale sea trials, Dand proposed to use a combination of simulation and suitable indices for assessing the low speed manoeuvrability criteria of ships. He suggested indices derived from the geometry of the ship, as well as operation indices. Examples of indices of the geometry of the ship could be:

- Rudder area ratio
- Lateral area ratio
- Lateral and longitudinal above-water aspect ratios

The operational indices could be:

- Limiting Froude Depth number, $F_{Nh} = \frac{V}{\sqrt{gh}}$, which indicates whether transit speeds expected of the ship are possible, bearing in mind increases in resistance associated with sub-critical speeds in shallow water.
- Lateral thruster power per square meter, which says something about ships self-berthing abilities and windage-ability.
- Depth/draft ratio, which limit operations due to squat and motions.

Dand proposed low speed manoeuvring criteria for the stopping, breasting and kick ahead manoeuvre.

Stopping

The ability to stop under control within a specified distance in shallow water should be assessed at the design stage. Criteria for both head reach and lateral deviation should be set. The stopping manoeuvre should be performed from harbour speed and the track reach should be less then in the IMO criteria. Lateral deviation should be small, preferably less than a beam and certainly less than one ship length.

Breasting

A breasting criterion could be decided in terms of a desired beam wind (and/or current) speed. Dand proposes wind speeds of 15 to 25 knots and the manoeuvre should be carried out at very low forward speed. This criterion would be of great value for self-berthing ships.

Kick ahead

This manoeuvre is invaluable in low speed manoeuvring. The purpose is to change vessel heading without moving ahead appreciably [21]. A kick ahead criterion could be checked in shallow port approaches during builder's trials. A specified shaft rpm could be applied for a specified time while the heading change is noted.

4.2.2 Hwang

Other studies have been made to determine how to characterize low speed manoeuvring performance. The objective of SNAME Panel H-10 panel was to identify and develop a set of low speed manoeuvres based on relatively simple and effective test procedures [24]. Senior mariners, simulator operators and other relevant professionals were surveyed to collect information on the characteristics of low speed manoeuvring. Eleven basic low speed manoeuvres in table 4.1 was suggested. Additional low speed test for twin-screw ships and test for bow and stern thrusters are given in [24] as well, but these are not relevant for KVLCC2. Test conditions for these tests include: deep and 1.2 depth/draft shallow water, calm weather, moderate uniform current as well as loaded and ballast draft. A problem with these tests are the economic aspect of performing all of these. If all the 11 bast test is to be conducted in deep and shallow water, for loaded and ballasted draft the total number of runs would be 44. In addition to the fact that some test are to be conducted to both starboard and port. Actually, the full-scale trials with Esso Osaka summarized in figure 3.6 clearly correspond to some of the low speed manoeuvres suggested by Hwang et al.

4.2.3 ISO

ISO (the International Organization for Standardization) published new manoeuvring standards in 2013 (ISO 13643). It consists of six parts:

- Part 1: General concepts, quantities and test conditions
- Part 2: Turning and yaw checking
- Part 3: Yaw stability and steering
- Part 4: Stopping, acceleration, traversing
- Part 5: Submarine specials
- Part 6: Model test specials

All the IMO standard manoeuvres are included in the standards, but the ISO documentation are far more detailed. The ISO manoeuvring standards which can be connected with low speed manoeuvring are listed below (found in ISO 13643:2-13643:4). Further details about conducting the test, as well as data and analysis of the tests are described in detail in the standards.

Name of manoeuvre	**Test purposes**
Minimum Effective Rudder (MER)	-Least rudder angle that can be applied and still effect yaw checking at speeds ranging from cruising to slow speed at each engine order.
Crash Stop from HALF AHEAD (HAHD) speed	-Ship's stopping capabilities from a speed which is relevant in harbour operation -Ship's dynamic response to throttle order when operation in transition from Quadrant 1 $\rightarrow$ 4 -Paddlewheel Effect/Stern Walk
Acceleration/Deceleration Combinations (start from and back to DEAD IN WATER (DIW))	-Ship's dynamic response to throttle order when operating in transition from Quadrant 1 $\rightarrow$ 4 $\rightarrow$ 3 -Paddlewheel Effect/Stern Walk
Backing/Stopping Combinations (start from and back to DIW)	-Ship's dynamic response to throttle order when operating in transition from Quadrant 3 $\rightarrow$ 2 $\rightarrow$ 1 -Paddlewheel Effect/Stern Walk
35°Accelerating Turn Starting from DIW with SLOW AHEAD (SAHD) bell	-Ship's ahead turning capability during acceleration at slow speed
35°Coasting Turn from SAHD speed	-Ship's ahead turning capability at slow speed during deceleration with propeller(s) wind milling or possibly stopped.
20°/20°Overshoot Test with SAHD approaching speed	Ship's yaw checking capability at a speed which is relevant in harbour operation
20°/20°Accelerating Overshoot Test Starting from DIW with SAHD bell	-Ship's yaw checking capability during accelerating ahead at slow speed
20°/20°Coasting Overshoot Test with SAHD or HAHD approaching speed	-Ship's yaw checking capability at slow speed during coasting ahead with propeller(s) wind milling or possibly stopped
Back and Fill with Fill First (for both Starboard Filling and Port Filling)	-Ship's manoeuvrability in tight space -Interactions between hull, propeller and rudder when operating in transition from Quadrant 1 $\rightarrow$ 4 $\rightarrow$ 3
Back and Fill with Back First (for both Starboard Filling and Port Filling)	-Ship's manoeuvrability in tight space -Interactions between hull, propeller and rudder when operating in transition from Quadrant 3 $\rightarrow$ 2 $\rightarrow$ 1

Table 4.1: Suggested Basic Slow Speed Manoeuvres [8]

Accelerating turn test

Test to determine the ship's behaviour when accelerating from stand-still and simultaneously applying the manoeuvring devices hard over.

Thruster turning test

Test to determine the ship's capability to turn at zero speed by using its thrusters. The thruster turning test ahead determines the limiting speed where no more turning effect from bow thrusters can be obtained. For ships having low or moderate block it can be required for a thruster turning test astern.

Astern test

Test to determine the ability of the ship to maintain course while going astern.

Astern zig-zag test

Test to determine the ability of the ship to maintain course while going astern by assessing the efficiency of the manoeuvring devices from a zig-zag test.

Coasting stop test

Test to determine the ship's behaviour after the propulsion plant has been shut down.

Acceleration test

Test to determine ship's performance under positive/negative acceleration.

Test conditions

The tests may be started in any direction for very calm conditions (wind force not exceeding Beaufort 2). For winds exceeding Beaufort 2 the approach should be made into the wind for the following tests: coasting stop test, acceleration test, turning circle test, accelerating turning test, astern test, zig-zag test and sine test. Significant wave height should be $H_S \leq 0.01L$ and the wind speed should be $V_W \leq V_0$ (or mean speed if the manoeuvre contains major speed changes). Water depths should exceed five times the mean draft of the ship if shallow water effects is not considered. The test should be conducted in sea areas with low current speeds.

4.3 Mathematical models of low speed and large drift angles

It is also a need for mathematical models for low speed manoeuvres. Standard manoeuvres have drift angles up to 30 degrees and uses conventional mathematical models. Low speed manoeuvres have large drift angles (ranging from -180 to 180 degrees) and large yaw rate angle (ranging from -90 to 90 degrees). The fluid flow is complicated where hull, propeller and rudder interacts. Especially when the ship operates in low speed with frequent piloting commands eighter headway or sternway while the propeller is thrusting ahead or astern as seen in figure 4.2. These four combinations of ship velocity and propeller rate are called the four quadrants of operation definition.

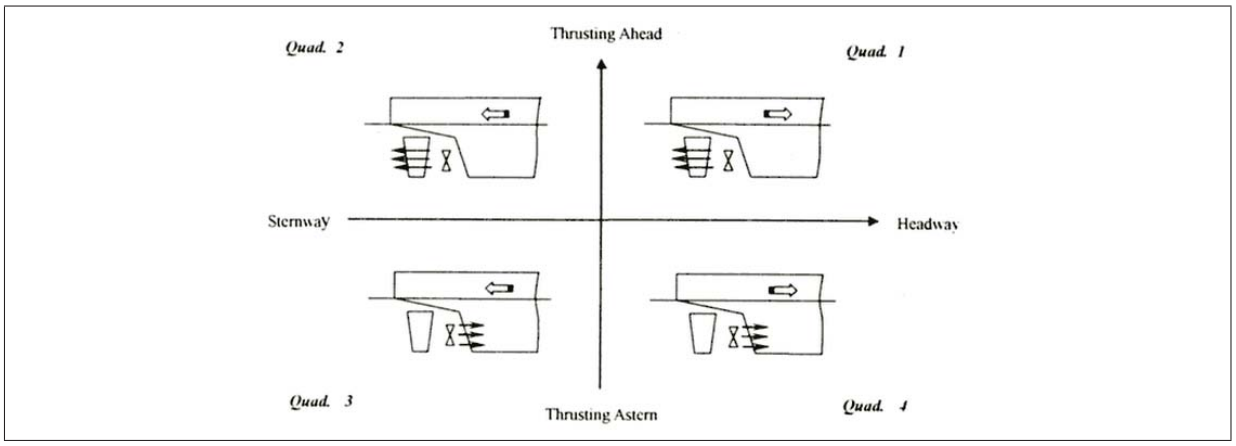

Figure 4.2: Four quadrants of operation [24]

Several approaches have been used to obtain mathematical models of low speed and large drift angles the last three decades. Several authors have proposed different approaches to obtain mathematical models for low speed flow and large drift angles [9]: Obokata (1983, 1987), Oltmann and Sharma (1984), Jiang et al. (1987), Kobayashi and Assai (1987), Wichers (1988), Takashina and Hirano (1990), Sohn (1992), Hooft (1994), Simos et al. (2001), Tannuri et al. (2001). Kobayashi and Assai [32] divided the hydrodynamic forces acting on the hull into four mathematical expressions classified within the following speed ranges:

- Ordinary advance speed model, which is for the speed range larger than a specified Froude number $F_n \geq F_{nmin1}$
- Low speed model with three speed ranges:
  - Low advance speed model for the speed range: $0 \leq F_n < F_{nmin2}$
  - Averaged model of the two mathematical models of the ordinary advance speed model and the low speed model with speed range: $F_{nmin2} \leq F_n \leq F_{nmin1}$
  - Astern model for backing: $F_n < 0$

The hydrodynamic forces of averaged model is a combination of the forces from the ordinary advance speed model and the low speed model.

$$\begin{bmatrix} X_H \\ Y_H \\ N_H \end{bmatrix} = g_1 \begin{bmatrix} X_H \\ Y_H \\ N_H \end{bmatrix}_{ordinary} + g_2 \begin{bmatrix} X_H \\ Y_H \\ N_H \end{bmatrix}_{low}$$

Where g_1 and g_2 are Froude number ratios expressed by:

$$g_1 = \frac{F_n - F_{nmin2}}{F_{nmin1} - F_{nmin2}} \tag{4.1}$$

$$g_2 = \frac{F_{nmin1} - F_n}{F_{nmin1} - F_{nmin2}} \tag{4.2}$$

3-DOF mathematical models have been used traditionally and hydrodynamic force coefficients are estimated by two different formulations. One formulation is based on cross flow models and the other is based on traditional force derivatives, but for low speed manoeuvring models.

Cross flow models

Cross flow (drag) models have been studied by several authors. Although some differences between the models and applications, the concept is the same. The difference may be how the pure turning is to be defined. The non-linear part of the horizontal hull forces and moment are given as (Obokata(1983)):

$$
\begin{aligned}
C(t) =& \frac{\partial \phi}{\partial t} + \frac{1}{2}|\Delta\phi|^2 + \frac{P}{\rho} + gy \\
X'_H =& -\frac{1}{2}\rho T \int_{-L/2-x_G}^{L/2-x_G} Cd_x(\psi_{crx}) V_{crx}^2 dx \\
Y'_H =& -\frac{1}{2}\rho T \int_{-L/2-x_G}^{L/2-x_G} Cd_y(\psi_{crx}) V_{crx}^2 dx \\
N'_H =& -\frac{1}{2}\rho T \int_{-L/2-x_G}^{L/2-x_G} \left[Cd_y(\psi_{crx}) V_{crx}^2 - Cd_y(\psi_{cr}) V_{cr}^2 \right] x dx - \frac{1}{2}\rho D L^2 Cd_z(\psi_{cr}) V_{cr}^2
\end{aligned}
\tag{4.3}
$$

Where:

$$
\begin{aligned}
V_{cr}^2 &= u_r^2 + v_r^2 \\
V_{crx} &= \sqrt{u_r^2 + (v + xr + V_c \sin\psi_{cr})^2} \\
\psi_{crx} &= \tan^{-1}\left(\tfrac{v + xr + V_c \sin\psi_{cr}}{u_r}\right)
\end{aligned}
\tag{4.4}
$$

An aspect of these models is that which tends to be forgotten in academic studies; the cross flow drag coefficient is not a constant as a function of drift angles, or the velocity that is used is not constant [9].

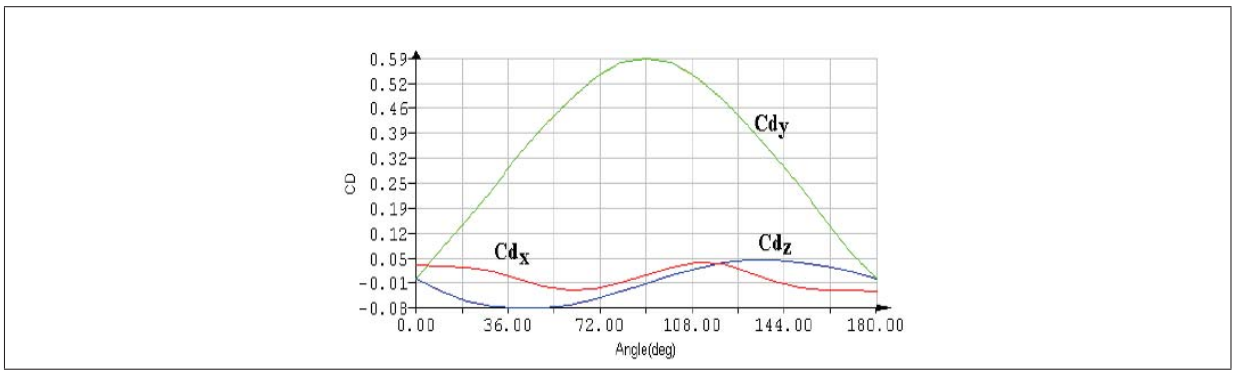

Figure 4.3: Drag coefficient curves by Nishimoto et al. [9]

Polynomial models

Polynomial models represent hydrodynamic forces due to flow and ship motion using hydrodynamic force derivatives. These models originates from Abkowitz and Norrbin models. The hydrodynamic derivatives are obtained from different towing tank tests combined with traditional PMM tests [9]. The yaw rotating test obtains the hydrodynamic forces in low speed and high drift angles. The main difference between this model and the formal models is that it represents the hydrodynamic force derivatives in higher drift angles. An example is the equations

proposed by Takashina and Hirano (1990) for the hydrodynamic forces and moment on the hull:

$$\begin{aligned} X_H &= \frac{1}{2}\rho LTU^2(X'_u u' + X'_{vr} v' r') \\ Y_H &= \frac{1}{2}\rho LTU^2(Y'_v v' + Y'_{vvv} v'^3 + Y'_{vvvvv} v'^5 + Y'_{ur} u' r' + Y'_{ur|r|} u' r'|r'| + Y'_{v|r|} v'|r'| \\ N_H &= \frac{1}{2}\rho L^2 TU^2(N'_v v' + N'_{uv} u' v' + N'_{vvv} v'^3 + N'_{uvvv} u' v'^3 + N'_r r' + N'_{r|r|} r'|r'| \\ &\quad + N'_{ur|r|} u' r'|r'| + N'_{vvr} v'^2 r' \end{aligned} \tag{4.5}$$

The coefficients in the equations above are the non-dimensional hydrodynamic force derivatives. u', v' and r' are non-dimensional surge, sway and yaw velocities which are defined as:

$$u' = \frac{u}{U},\ v' = \frac{v}{U},\ r' = \frac{rL}{U},\ U = \sqrt{u^2 + v^2} \tag{4.6}$$

A disadvantage with the equations in 4.5 is that these may approach infinity when $U = 0$ and $r \neq 0$.

Other low speed models

Other low speed models are Fourier Expansion Models, Tabular Manoeuvring Models and Models based on RANS CFD. Fourier Expansion models consider the hull forces as a combination of sinus and cosinus expansions. The model has recently been utilized by Toxopeus (2007,2011) and is a mix of the robustness of cross flow models and the accuracy of polynomial models at smaller drift angles [9]. Tabular models are based on interpolation of experimental results. Low speed models based on CFD methodologies like URANS or DES can be used to determine the forces or coefficients for low speed manoeuvring models.

4.3.1 Application and validation

Several papers have been published concerning simulation of manoeuvring associated with low speed and large yaw angles recent years. Usually, these do not present the manoeuvring model, only the simulation results. This is a big problem when comparing results because of the diversity of the mathematical models. There are no common benchmark data to validate the manoeuvring models, because of the lack of standard low speed manoeuvres. The mathematical models are usually validated on a force level, not motions.

4.4 Case specific low speed manoeuvres

From the literature study of low speed manoeuvres there are no definite standard low speed manoeuvres which are used widely. Both Dand and Hwang et. al have suggested low speed manoeuvring criteria and manoeuvres based on relatively simple and effective test procedures. ISO standards (ISO 13643-1:2013(E)) published in 2013 contains some manoeuvres which are connected to low speed manoeuvring. Many of these manoeuvres are suitable case specific low speed manoeuvres that can be used in model validation. There are however little validation data for these manoeuvres. Some of the full-scale trials with Esso Osaka corresponds clearly with the suggested manoeuvres of Hwang et al., but due to test uncertainties it is suggested to

not use these as validation data. One of the 27th ITTC Manoeuvring Committee's objectives is to study possible criteria for manoeuvring at low speed. The outcome of this study will be of high relevance for case specific low speed manoeuvres. In the SIMMAN 2014 workshop a free sailing model tests for shallow water depths are specified. The tests which to be conducted is zig-zag tests (10°/2.5°and 20°/5°), as well as a 35°turning circle test. The approach speed is 7 knots, which corresponds to Froude Number 0.064. The shallow water test have been conducted at:

- h/T=1.2
- h/T=1.5
- h/T=1.8

The results of these free model tests are not available for the moment, but they will be available after the workshop in December 2014. The tests assesses shallow water as well as low speed manoeuvring. These case specific low speed manoeuvres shall be used for model validation later.

Chapter 5

Validation and verification

5.1 Validation and verification

Simulation models are increasingly being used to solve problems and to aid in decision making. The correctness of the models and its results are a factor users and developers are concerned about. The evaluation of the simulation models used for engineering studies is to a certain degree parallel to the evaluation needed for training simulators [14]. The major items of these evaluations are:

- Simulation fidelity
- Simulation verification
- Simulation validation

Simulation fidelity is the level of realism that the simulator is presenting to the user. Verification is usually defined as the process of assessing that a model is operating as intended. Validation is the process of assessing that the conclusions reached from a simulation are the same as those obtained from the real-world system being modelled [14].

Pegden (1995) defined validation and verification as: “Validation is the process of determining that we have built the right model, whereas verification is designed to see if we have built the model right” ([17] , p. 129).

A simulation model should be developed for a purpose and its validity should be determined with respect to that purpose. If this purpose is to answer a variety of questions, the validity of the model needs to be determined with respect to each question [43]. A model may be valid in one set of experimental conditions (domain) and invalid in another. The models accuracy is also something to be considered, what amount of accuracy does the model require? Verification and validation are usually a part of the total model development process. A compromise needs to be done between the cost of validation versus model value of the user (the confidence of the model) as seen in figure 5.1.

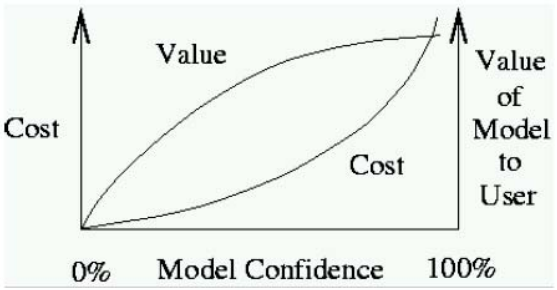

Figure 5.1: Model confidence [43]

The cost can be significant when high model confidence is required. It is often too costly and time consuming to determine that a model is absolutely valid over its complete domain of its intended applicability. As a minimum, Sargent (2011) [44] recommended eight steps that should be performed when validating a model:

1. *"An agreement should be made in advance between the model development team, the model sponsors and (if possible) the users that specifies the basic validation approach and a minimum set of specific validation techniques to be used in the validation process."*

2. *"Specify the amount of accuracy required of the simulation model's output variables of interests for the model's intended application prior to starting the development of the model or very early in the model development process."*

3. *"Test, wherever possible, the assumptions and theories underlying the simulation model."*

4. *"In each model iteration, perform at least face validity on the conceptual model."*

5. *"In each model iteration, at least explore the simulation model's behaviour using the computerized model."*

6. *"In at least the last model iteration, make comparisons if possible, between the simulation model and system behaviour (output) data for a few sets of experimental conditions, and preferably for several sets."*

7. *"Develop validation documentation for inclusion in the simulation model documentation.*

8. *"If the simulation model is to be used over a period of time, develop a schedule for periodic review of the model's validity."*

5.1.1 Basic approaches

There are four different approaches deciding model validity. Each of these approaches requires the model development team to conduct verification and validation as a part of the model development process [43].

- The model development team decides subjectively if the simulation model is valid.
- Users of the model and the model development team decides if the simulation model is valid.

- A third, independent party decides whether the simulation model is valid (IV&V, "independent verification and validation").

- Using a scoring model.

5.1.2 Paradigms

The relationship with verification and validation to a model development process are usually viewed in two ways: a simple view and a complex view. The complex view is presented in figure 5.2.

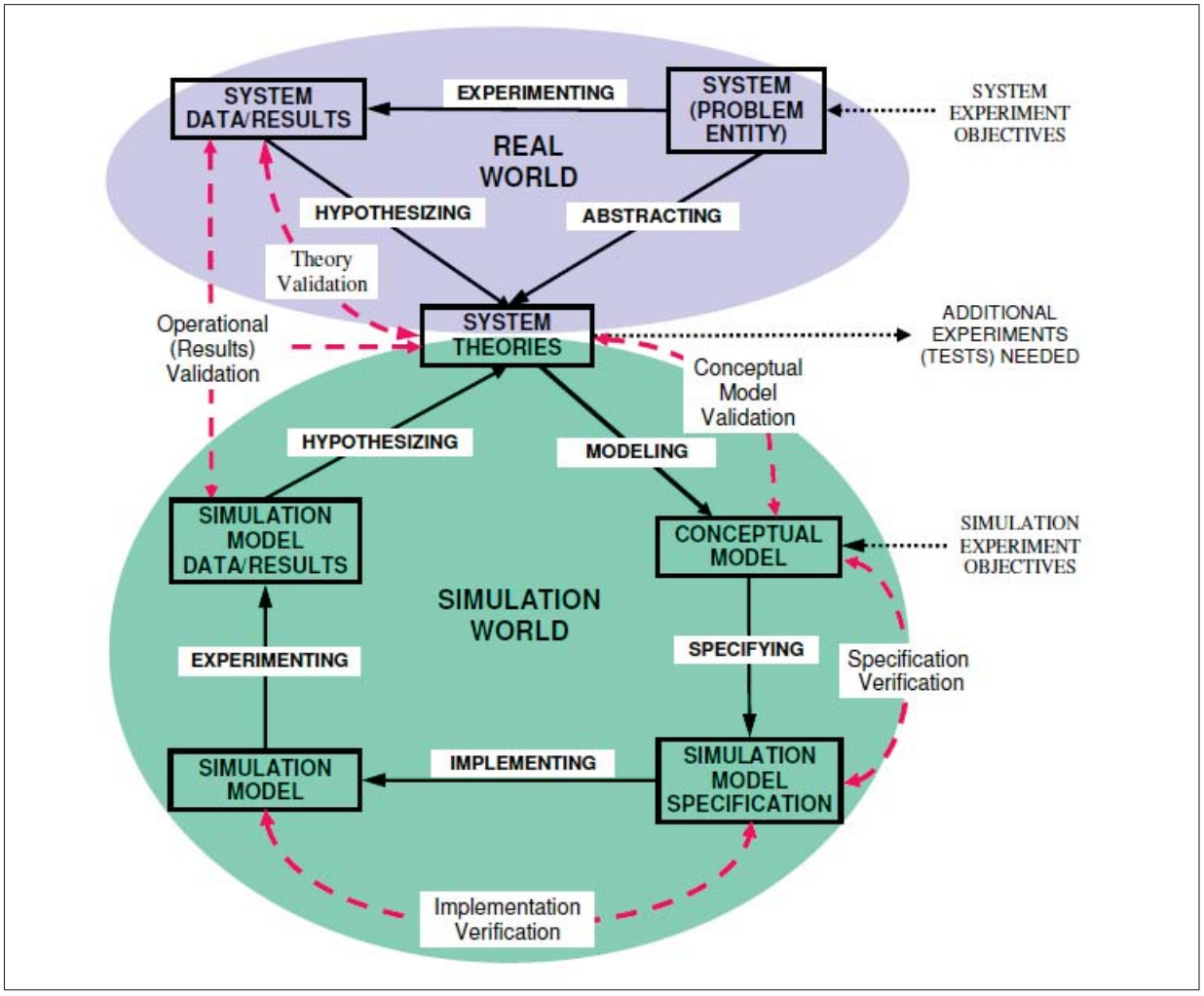

Figure 5.2: Real world and simulation world relationships with verification and validation [43]

Figure 5.2 relates verification and validation in development of simulation models and system theories in a detailed manner. This paradigm shows a real world and a simulation world and shows different types of validation and verification within the simulation world, and how it is connected with the real world. It shows the iterative processes for developing valid system theories and valid simulation models.

5.1.3 Validation techniques

There are several validation techniques and tests which are used in model verification and validation. They can be used subjectively or objectively, where objectively is that some mathematical or statistical tests are used on sub models and/or overall model.

- *Animation:* Graphically displayed behaviour of the model
- *Comparison to Other Models:* Various results of the simulation model are compared with results to other valid models.
- *Event Validity:* The events of occurrences of the simulation model are compared to the occurrences of the real system to determine if they are similar.
- *Extreme Condition Tests:* The simulation models output should be plausible for any extreme and unlikely factors in the system.
- *Face Validity:* Knowledgeable individuals about the system validate the model.
- *Historical Data Validation:* Part of historical data is used to build the model and the remaining data are used to test whether the model behaves as the system does (if historical data exists).
- *Multistage Validation:* Validation based on three steps:
  1. Developing the models assumptions on theory, observations and general knowledge.
  2. Validation the models assumptions by empirically testing them.
  3. Testing the input/output relationships of the model to the real system.
- *Operational Graphics:* Values of various performance measures.
- *Parameter Variability - Sensitivity Analysis:* Change of input values and internal parameters to determine the effect of the models behaviour or output. The input values or parameters that are most sensitive for output changes should be made sufficiently accurate.
- *Predictive Validation:* System behaviours are predicted using the simulation model and compared with the real behaviour of the system.
- *Turing Tests:* Knowledgeable individuals about the operations are asked if they can discriminate between system and model output.

5.2 ITTC recommended procedures and guidelines

The ITTC has written recommended procedures and guidelines for validation of manoeuvring simulation models. This was last updated in 2011 (procedure 7.5_ 02 06-03, rev. 2) A distinction between manoeuvring simulation models can be divided into two types of models [10]:

- Models for prediction of ship manoeuvrability
- Models for use in simulators

The models for prediction of ship manoeuvrability is used at the design stage of a ship to check that the ship has the desired manoeuvring capabilities. The manoeuvring capabilities may be defined by the ship owner, the IMO or local authorities. The models for use in simulators are time-domain models and can be used for various purposes, conditions and waters. The two models requires to be validated on different levels. The models for use in simulators are generally described more extensively, hence validated more extensively. According to the ITTC the generation of a manoeuvring models is based on seven steps, where each step must be validated and documented. These steps are as follows [10]:

1. Ship particulars
2. Prediction of the hydrodynamic forces
3. Modelling of forces in the mathematical model (derivatives, coefficients, tables, direct simulation of forces)
4. Mathematical model structure
5. Integration method
6. Simulation software
7. Simulated manoeuvres

Each of the steps above is elaborated in the project thesis [33]. When documenting a simulation model it should be clear which methods and assumptions that are used. The operational range and parameters should be given and the simulated standard manoeuvres should be presented and discussed in terms of accuracy. The documentation must include the models purpose, nomenclature and coordinate systems.

5.3 Benchmarking

Full-scale manoeuvring benchmark data should be used to validate manoeuvring prediction methods. There is a lack of high quality sea trial data for model validation work [14]. The benchmark data should include full ship documentation and accurate full-scale trial results. The problem is that there are little benchmark data available since the ship owners or shipyard mostly keep this confidential. Another problem is the environmental influences when performing full-scale trials, which is difficult to measure and model exact. Trials with Esso Osaka are the only widely cited full-scale trials, but due to old ship design and measuring instruments ITTC recommends not to use this data as validation material [10]. With this conclusion the 24th ITTC requested a new set of benchmark data. Four different ship hulls were selected:

- MOERI KVLCC1 tanker
- MOERI KVLCC2 tanker
- MOERI KCS container ship
- Naval combatant

These benchmarking models have modern hull forms with full geometrical data for hull, propeller, rudder and other appendages. None of the ships exists in full-scale.

Chapter 6

Simulation software

6.1 SIMAN

The hydrodynamic workbench ShipX is developed at MARINTEK. The ShipX Manoeuvring Plug-In consists of two software tools, SIMAN and HullVisc. The Plug-In is used to estimate the manoeuvring capabilities of a vessel in an early design stage. It is described as an empirical modular model with cross flow drag and slender body theory. SIMAN can predict all standard manoeuvres for a single rudder and twin rudder common merchant type mono hull displacement ship. The Plug-In gives prediction results of acceptable results for slender type ship hulls to full type with conventional stern. The input required in the plug-in are [42]:

- Hull description including main dimensions, body plan, bow and stern contours.
- Rudder description including dimensions, type and location.
- Propeller description including dimensions, pitch ratio, blade area ratio and location.
- Propulsion engine description including engine type. The choice of engine type is restricted to directly coupled diesel engine characteristics or constant rate of revolution in the manoeuvre.
- Environmental forces including wind and current and the effect of limited water depth.

HullVisc is a pre-processor to SIMAN and calculates the hydrodynamic coefficients for the vessel, including added mass, linear damping and non-linear damping. The basis for these calculations are based on general arrangement and the loading condition of the vessel. The rudder, propeller and environment conditions are defined in SIMAN.

6.1.1 Coordinate systems

SIMAN uses two different coordinate systems for input and for calculation and reporting [41]. The coordinate system used for input is dependent on how SIMAN is started. If SIMAN is started from ShipX the ships z-axis is pointing upward, the x-axis is pointing forward and the y-axis pointing towards starboard (The origin is at the baseline at the APP). If SIMAN is started separate from ShipX the ships coordinate system is a right-handed Cartesian coordinate system (The origin of the x-axis is in the waterline at midships). The coordinate system for calculations

and results is a global right-handed Cartesian coordinate system with Zo-axis pointing downward, the same local coordinate system is used for the ship as shown in 6.1. The wind, current and waves are relative to the global coordinate system.

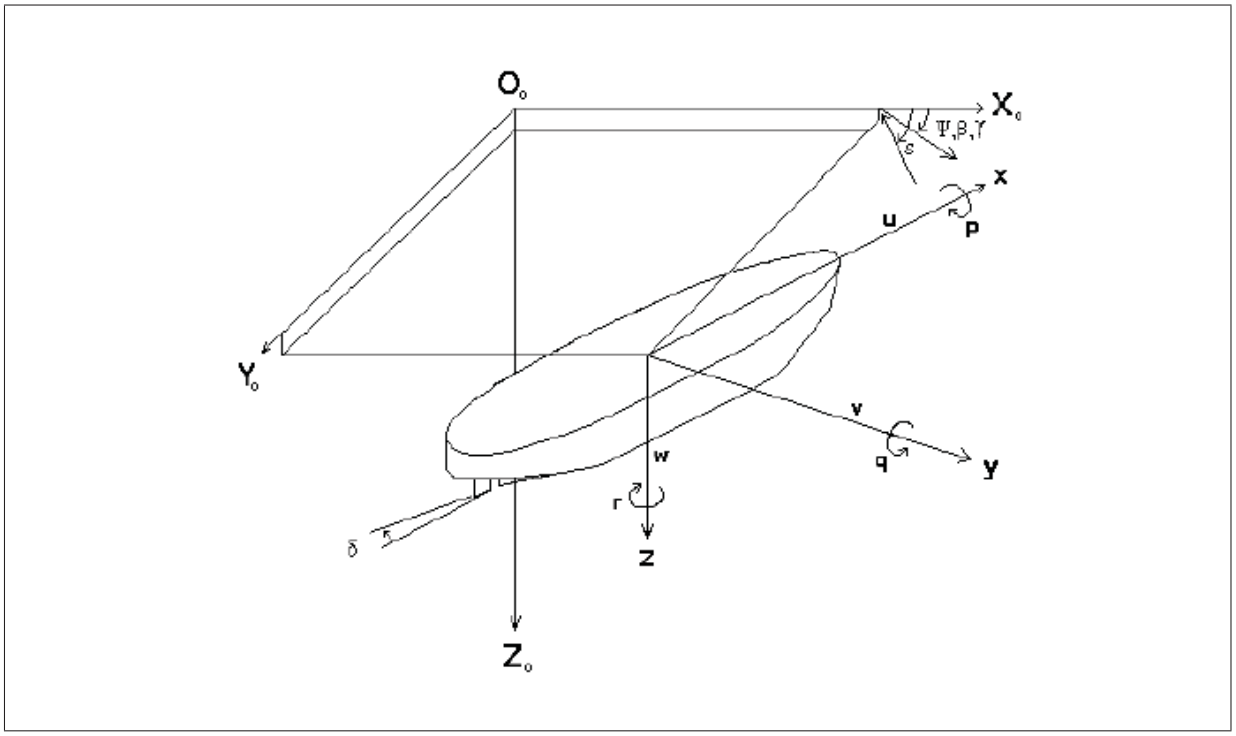

Figure 6.1: Global and local coordinate system [41]

Where:
X_0, Y_0, Z_0, x, y, z are global and ship fixed coordinates.
u, v, w, p, q, r are the 6-DOF.
δ, ψ are the rudder angle and ship heading.
ϵ, γ, β are wind, wave and current directions.

6.1.2 Method

SIMAN uses a 3-DOF(surge, sway and yaw) non-linear mathematical model and the equations of motions are of the form:

$$\begin{aligned}(m - X_{\dot{u}}) \cdot \dot{u} =&(m + X_{vr}) \cdot vr + (mx_g + X_{rr}) \cdot r^2 + X_{res} + X_{vv} \cdot v^2 + X_{vvvv} \cdot v^4 \\ &+ X_{prp} + X_{rud} + X_{thr} + X_{wi} + X_{cu} + X_{wa} + X_{tug}\end{aligned} \tag{6.1}$$

$$\begin{aligned}(m - Y_{\dot{v}}) \cdot \dot{v} + (mx_g - Y_{\dot{r}}) \cdot \dot{r} = &-mur + Y_v \cdot v + Y_{Uv} \cdot Uv + Y_r \cdot r + Y_{Ur} \cdot Ur \\ &- X_{\dot{u}} \cdot ur + Y_{cf} + Y_{prp} + Y_{rud} + Y_{thr} + Y_{wi} + Y_{cu} + Y_{wa} + Y_{tug}\end{aligned} \tag{6.2}$$

$$\begin{aligned}(I_{zz} - N_{\dot{r}}) \cdot \dot{r} + (mx_g - N_{\dot{v}}) \cdot \dot{v} = &-mx_g ur + N_r \cdot r + N_{Ur} \cdot Ur + N_v \cdot v + N_{Uv} \cdot Uv \\ &+ N_{cf} + N_{prp} + N_{rud} + N_{thr} + N_{wi} + N_{cu} + N_{wa} + N_{tug}\end{aligned} \tag{6.3}$$

Where:
m, I_{zz} are ship mass and mass moment of inertia
Y_v, N_r are linear sway and yaw damping derivatives
Y_r, N_v are sway and yaw damping coupling derivatives
$Y_{Uv}, Y_{Ur}, N_{Uv}, N_{Ur}$ are Froude number influence
$X_{\dot{u}}, Y_{\dot{v}}, N_{\dot{r}}$ are acceleration derivatives
$Y_{\dot{r}}, N_{\dot{v}}$ are acceleration cross coupling derivatives
$\dot{u}, u, U$ are surge acceleration, velocity and total ship speed
$\dot{v}, v$ are sway acceleration and velocity
$\dot{r}, r$ are yaw acceleration and velocity
x_g is the distance of centre of gravity from midship
X_{res} is ship resistance
X_{vr}, X_{rr} are coefficients for ideal fluid force contribution
X_{vv}, X_{vvvv} are coefficients for force contribution at drift angle
The subscripts stands for:
cf is cross-flow non-linear damping
prp, rud, thr are contributions from propeller, rudder and tunnel thrusters
wi, cu, wa, tug are external contributions from wind, current, waves and tugs

6.1.3 Hydrodynamic hull forces

The linear damping derivatives in sway and yaw are based on slender body theory. Added mass coefficients are calculated by strip theory, using the method of Clarke [18]. The sectional added mass in sway is integrated from the FP to a given section in the after-body. Due to large discrepancy from neglecting the viscous effects a correction based on the waterline angle in the fore-body is done. The hull cross sections were increased in size from bow to stern by adding a boundary layer on a flat plate corrected to consider a curved ship hull. Another correction for the integration of the added mass distribution is also the use of empirical data for linear manoeuvring derivatives from 25 ship models. The following procedures are used in ShipX to calculate the hydrodynamic coefficients [35]:

- $Y_{\dot{v}}, Y_{\dot{r}}, N_{\dot{v}}$ and $N_{\dot{r}}$ are set equal to the added masses or added moments of inertia as calculated by the strip theory applied.
- $X_{\dot{u}}$ is found from an estimation formula and the value is normally in the range 5-10 $\%$ of ship mass.
- Y_v is found by applying the maximum value of the CH-distribution.
- Y_r is found by applying the CH-value at a section $0.1\ x\ L_{pp}$ forward of the aft perpendicular.
- N_v and N_r are found by applying the CH-value at a section $0.1\ x\ L_{pp}$ forward of the aft perpendicular and carrying out the remaining integration from the forward perpendicular and to this section.

The four linear velocity derivatives are corrected by formulas based on regression analysis. The correction formulas includes two parameters taking account for the afterbody shape. The first

parameter is a function of the ratio between the prismatic coefficient and the waterline area coefficient of the part of the aft. The other is a function of the half-breadths at two different vertical positions on a section a little forward of the propeller [35].

The non-linear damping according to the cross-flow principle is of quadratic form. A cross-section in the aft-body is defined as the point where the flow separation will occur. This cross-section is located at the maximum curvature of the aft-body when the ship has small drift angle. Cross-flow drag occurs only aft of this section, whilst in front there are no non-linear transverse forces. The sectional cross-flow drag coefficients C_{cf} are obtained from different literature sources and depend on the breadth-to-draught ratio B/T.

$$Y_{cf} = \frac{1}{2}\rho \int U^2(x) C_{cf}(x) T(x) \mathrm{d}x \tag{6.4}$$

The assumption made when the drift angle is large is that the flow separation section moves forward with increasing drift angle. A similar assumption is made with regard to the yaw velocity angle. The complete hull is subjected to cross-flow force and moment when the drift angle or yaw angle is 90°.

The longitudinal resistance X_{res} in the surge equation are calculated by Holthrops method modified by MARINTEK if the resistance data for the ship or similar ships are not available.

The coefficients Y_{Uv}, Y_{Ur}, N_{Uv} and N_{Ur} takes the effect of Froude number on linear damping into account, but due to calculation difficulties they are neglected. The effect of drift angle on the longitudinal force is taken into account by the coefficients X_{vv} and X_{vvvv}.

6.1.4 Propeller forces

The propeller module is based on analytical expressions based on Strøm-Tejsen and Porter (1972). The performance is a function of blade-area ratio, blade pitch setting and any combination of propeller rate, direction of revolution, ship speed and direction of motion [36]. The four quadrants of operation as seen in figure 4.2 are fulfilled. The propeller module is validated against a number of propellers and it is assumed that the module is satisfactory for manoeuvring prediction and simulation purposes. The flow straightening effect and the wake of the hull are accounted for as functions of local drift angle at the propeller position. Sway force and yaw moment from the propeller are calculated from functions of propeller thrust and local drift angle at the propeller position. These are based both on model test performed at MARINTEK as well as information from literature.

6.1.5 Rudder forces

Rudder lift and drag are calculated from free stream characteristics of a conventional rudder based on works of Whicker and Fehlner (1958). The rudder module is validated against results from wind tunnel tests. After calculating the free stream lift and drag coefficient the effective aspect ratio is calculated as a function of the gap between hull surface and the top of the rudder. The flow velocity is calculated as a weighted average of the flow velocities above, in and below the propeller race. The wake fraction at the rudder is calculated by the wake fraction at the

propeller by:

$$w_R = 0.5788 w_P^2 - 0.1395 w_P + 0.2599 \tag{6.5}$$

The flow velocity of the rudder part above the propeller race the wake fraction is set to $w_{AR} = 2w_R$ given that $1 - w_R \geq 0$. For the rudder part below the propeller race the wake fraction is set to $w_{BR} = 0.5 w_R$ [36]. The rudder/hull interference is accounted for by using the effect of a flap on a wing. The lift slope for the rudder is multiplied by a factor $1 + a_H$.

$$a_H = 0.0563 \exp^{2.9185 C_B} \tag{6.6}$$

Variations of the lift coefficient can be expressed as a function of the ratio of speed of advance to race velocity. This ratio can be expressed as rudder-loading angle:

$$\xi = atan\big[\frac{U(1 - w_R)}{U_{race}}\big]\frac{180}{\pi} \tag{6.7}$$

A partly new rudder routine has been added. The deviation from the rudder routine in [36] are not known to the author.

SIMAN was extended to a ship-handling model based on the prediction model due to the markets interest in full ship-handling models. The manoeuvring plug-in consists of modules for all four quadrants of ship operation as seen in figure 4.2. The ship-handling model has shown satisfactory results in all speed ranges. The linear damping coefficients take drift angles up to 90°at ahead and atern ship speeds into account. Shallow water has been accounted for by including the effects from shallow water depths: the values of added mass and linear damping changes due to water depth, which is accounted for. The rudder and propeller forces have also been modified due to the shallow water effects of these according to theory.

6.1.6 Dimensionless hydrodynamic coefficients

The hydrodynamic coefficients are made dimensionless by:

$$Y'_{\dot{v}} = \frac{Y_{\dot{v}}}{\frac{1}{2}\rho L_{PP}^3} \qquad Y'_{\dot{r}} = \frac{Y_{\dot{r}}}{\frac{1}{2}\rho L_{PP}^4} \qquad N'_{\dot{v}} = \frac{N_{\dot{v}}}{\frac{1}{2}\rho L_{PP}^4} \tag{6.8}$$

$$N'_{\dot{r}} = \frac{N_{\dot{r}}}{\frac{1}{2}\rho L_{PP}^5} \qquad Y'_v = \frac{Y_v}{\frac{1}{2}\rho L_{PP}^2 U} \qquad Y'_r = \frac{Y_r}{\frac{1}{2}\rho L_{PP}^3 U} \tag{6.9}$$

$$N'_v = \frac{N_v}{\frac{1}{2}\rho L_{PP}^3 U} \qquad N'_r = \frac{N_r}{\frac{1}{2}\rho L_{PP}^4 U} \qquad X'_{rr} = \frac{X_{rr}}{\frac{1}{2}\rho L_{PP}^4} \tag{6.10}$$

$$X'_{\dot{u}} = \frac{X_{\dot{u}}}{\frac{1}{2}\rho L_{PP}^3} \qquad X'_{vr} = \frac{X_{vr}}{\frac{1}{2}\rho L_{PP}^3} \tag{6.11}$$

6.1.7 Sensitivity analysis

The sensitivity of simulated manoeuvres to each mathematical parameter will generally depend on [5]:

- the mathematical model itself
- the hydrodynamic of the ship

- the manoeuvre that is investigated

A sensitivity analysis identifies the parameters which are most important, thus where to put the focus of research. As part of the development of SIMAN a sensitivity analysis were performed on the hydrodynamic coefficients and other parameters. The various coefficients and parameters were divided into three degrees of importance [36]: *Important parameters (1), less important parameters(2) and parameters of small importance(3)*:

1. $Y_v,\ Y_r,\ N_v,\ N_r,\ Y_{\dot{v}},\ I_{zz},\ X_{res}$, sectional cross-flow drag coefficient, section for flow separation on hull, open water drift angle at propeller position, effect of propeller on the angle of flow to the rudder and correction of lift in case of rudder with horn.

2. $X_{\dot{u}},\ N_{\dot{r}},\ w_R,\ w_{AR},\ w_{BR}$, wake fraction at service speed, propeller side force and w_P at instantaneous speed as a function of drift angle.

3. $Y_{\dot{r}},\ N_{\dot{v}},\ X_{vr},\ X_{rr}$, distance between propeller and rudder stock, wake at instantaneous speed as fraction of wake at service speed, thrust deduction at instantaneous speed as fraction of thrust deduction at service speed, initial gap between rudder and hull surface, increase with rudder angle of gap between rudder and hull surface, and rudder sweep angle.

It should be mentioned that this sensitivity analysis were performed on a case vessel with two different bodyplan configurations. The case vessel is half the breath than KVLCC2, but the sensitivity analysis could still be of interest to indicate the importance of the various coefficients and parameters.

6.2 VeSim

ShipX has another plug-in called Vessel Simulator (VeSim). The simulation model uses data from a Vessel Response Run and a Manoeuvring Run. It combines the vessel hydrodynamics from both seakeeping and manoeuvring problems simultaneously. An overview of how the Vessel Simulator collects information from runs and sets up a Ship Model Run, which is reused by the Simulator Setup Runs is shown in figure 6.2.

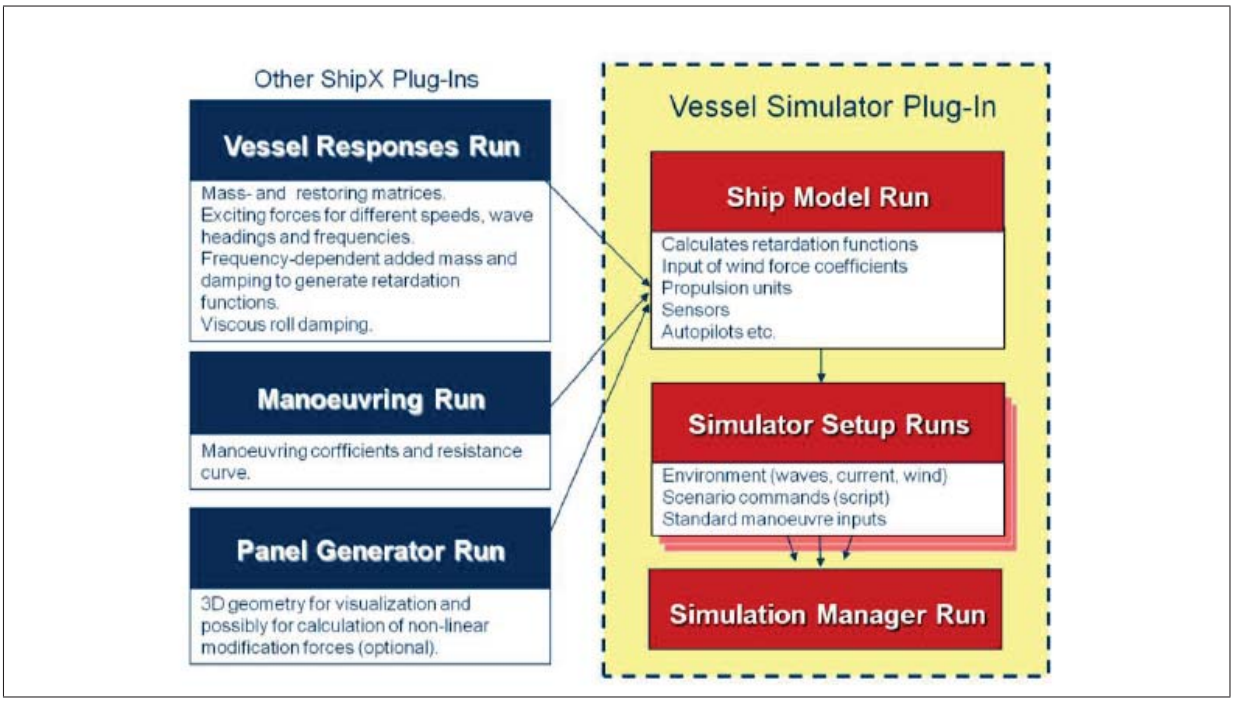

Figure 6.2: Overview of the various ShipX Plug-Ins and Runs available to generate a Simulator Setup [26]

VeSim uses three reference frames; two for ship motions and one to describe positions on the vessel itself. For ship motions the north-east-down (NED) and the body-fixed reference frame are used, while for positions the naval reference frame is used. The vessel model neglects hydroelastic effects and assumes that the vessel is moving as a rigid body. The model of the vessel is 6-DOF. The equation of motion is written as:

$$(\mathbf{m} + \mathbf{A}_\infty)\ddot{\eta} + \mathbf{C}(\dot{\eta})\dot{\eta} + \mathbf{D_1}\dot{\eta} + \mathbf{D_2}\mathbf{f}(\dot{\eta}) + \mathbf{K}\eta + \int_0^t \mathbf{h}(\mathbf{t}-\tau)\dot{\eta}(\tau)\mathbf{dt} = \mathbf{q}(t,\eta,\dot{\eta}) \quad (6.12)$$

Where η is 6-DOF motion vector, m is body mass matrix, A_∞ is the added mass at infinite frequency, C is the Coriolis matrix, D_1 is linear damping matrix, D_2 is quadratic damping matrix. f is vector function where each element is given by $f_i = \dot{\eta}_1|\dot{\eta}_1|$, K is the restoring matrix, $h(\tau)$ is retardation function and q is the excitation forces [26]. The excitation forces q consists contributions from wind, waves (O and O^2), propulsion, manoeuvring and other forces. Validation of the modules in VeSim is based on model tests within resistance, propulsion, seakeeping and manoeuvring using free-sailing models in the ocean basin at NTNU.

6.2.1 Manoeuvring forces

The source of the horizontal damping force comes mainly from friction and viscosity. The force in longitudinal direction is caused mostly by friction and wave resistance, while the force in transverse direction is caused by cross flow separation. The relative velocity is

$$u_D^{(i)} = u_w^{(i)}(\theta, x) + u_c^{(i)}(x) - u_v^{(i)}(x),\ i = 1, 2 \quad (6.13)$$

Where: i is 1 for surge motion and 2 for sway motion
x is longitudinal coordinate of vessel

$u_w^{(i)}$ is wave particle velocity at centre of buoyancy. It is assumed constant along the length of the vessel.
$u_c^{(i)}$ is current velocity
$u_v^{(i)}$ is vessel velocity (including yaw induced surge and sway motion).

The longitudinal resistance in surge is estimated using normal procedures for ship resistance in still water. VeSim uses a polynomial that are generated from a resistance model test or empirical method.

The cross flow drag forces in sway and yaw are based on cross flow principle which assumes that flow separates at the lee side of a structure.

$$f_D^{(2)}(\theta, x) = C_D(\theta, x) u_D^{(2)}(\theta, x) |u_D^{(2)}(\theta, x)| \tag{6.14}$$

C_D is the cross flow drag coefficient and $u_D^{(2)}$ is the vessels relative sway velocity with the surrounding fluid. The cross flow drag coefficient is calculated based on empirical formulas. The cross flow drag force over the whole length of the vessel is obtained by integration:

$$F_D^{(2)}(\theta) = \frac{1}{2}\rho \int_L c_D(\theta, x) D(x) u_D^{(2)}(\theta, x) |u_D^{(2)}(\theta, x)| dx \tag{6.15}$$

$$F_D^{(6)}(\theta) = \frac{1}{2}\rho \int_L c_D(\theta, x) D(x) x u_D^{(2)}(\theta, x) |u_D^{(2)}(\theta, x)| dx \tag{6.16}$$

Other manoeuvring forces are linear damping forces/moments and non-linear surge forces. Most hydrodynamic coefficients are obtained from the manoeuvring run. However, the linear damping derivatives Y_v, Y_r, N_v and N_r are calculated in VeSim. A low speed manoeuvring model is applied when simulated manoeuvre is at zero and low speed (F_N<0.04). Linear ramping is used in the intermediate speed range (0.04 < F_N < 0.1).

6.2.2 Propulsion model

The propulsion model which is suited for KVLCC2 is "Propeller and Conventional Rudder". This model is valid for the four quadrants of operation. The model calculates the forces that are generated by an open propeller combined with a conventional rudder. The physical effects included in the model are [26]:

- Hull straightening effect on the inflow
- Rudder hull interaction (single screw)
- Effect of head box lift and drag
- Rudder stall
- Propeller race turbulent mixing
- Gap between rudder and head box

Physical effects which are not covered are rudder hull interaction (twin screw), rudder horn (semi-spade rudders) and rudder and propeller at different transverse positions. Corrections due to shallow water are not implemented in the model.

Chapter 7

Simulation model

7.1 KVLCC2

The ITTC Manoeuvering Committee decided to arrange the SIMMAN workshop to benchmark the prediction capability of different ship simulation methods. Amongst the ships to be investigated were the MOERI VLCC tanker forms; KVLCC1 and KVLCC2. KVLCC2 is the second variant of the MOERI tanker and has more U-shaped stern frame-lines. No full-scale ship exist, only as models to use as a benchmark ship. The advantages of selecting these models as benchmark models are [7]:

- Modern hull forms
- Lines, propeller and rudder data are available
- Captive and free model test data are available
- They are already selected as benchmark ships for resistance and propulsion

KVLCC2 has a high geometrical metacentre so that the 4th degree of freedom (roll) is not of importance. The ship particulars are given in table 7.1. The shape of the hull is given from are presented in 7.1 and 7.2.

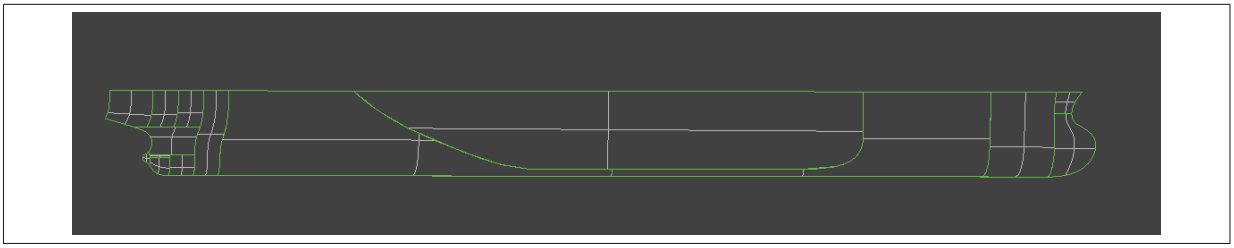

Figure 7.1: KVLCC2: side view [4]

Ship Particulars	Fullscale
Main particulars	
Scale	1.000
Lpp (m)	320.0
Lwl (m)	325.5
Bwl (m)	58.0
D (m)	30.0
T (m)	20.8
Displacement (m^3)	312622
S w/o rudder (m^2)	27194
CB	0.8098
CM	0.9980
LCB (%), fwd+	3.48
Rudder	
Type	Horn
S of rudder(m^2)	273.3
Lat. area (m^2)	136.7
Turn rate (deg/s)	2.34
Propeller	
Type	FP
No. of blades	4
D (m)	9.86
P/D (0.7R)	0.721
Ae/A0	0.431
Rotation	Right hand
Hub ratio	0.155

Table 7.1: Ship Particulars KVLCC2 [4]

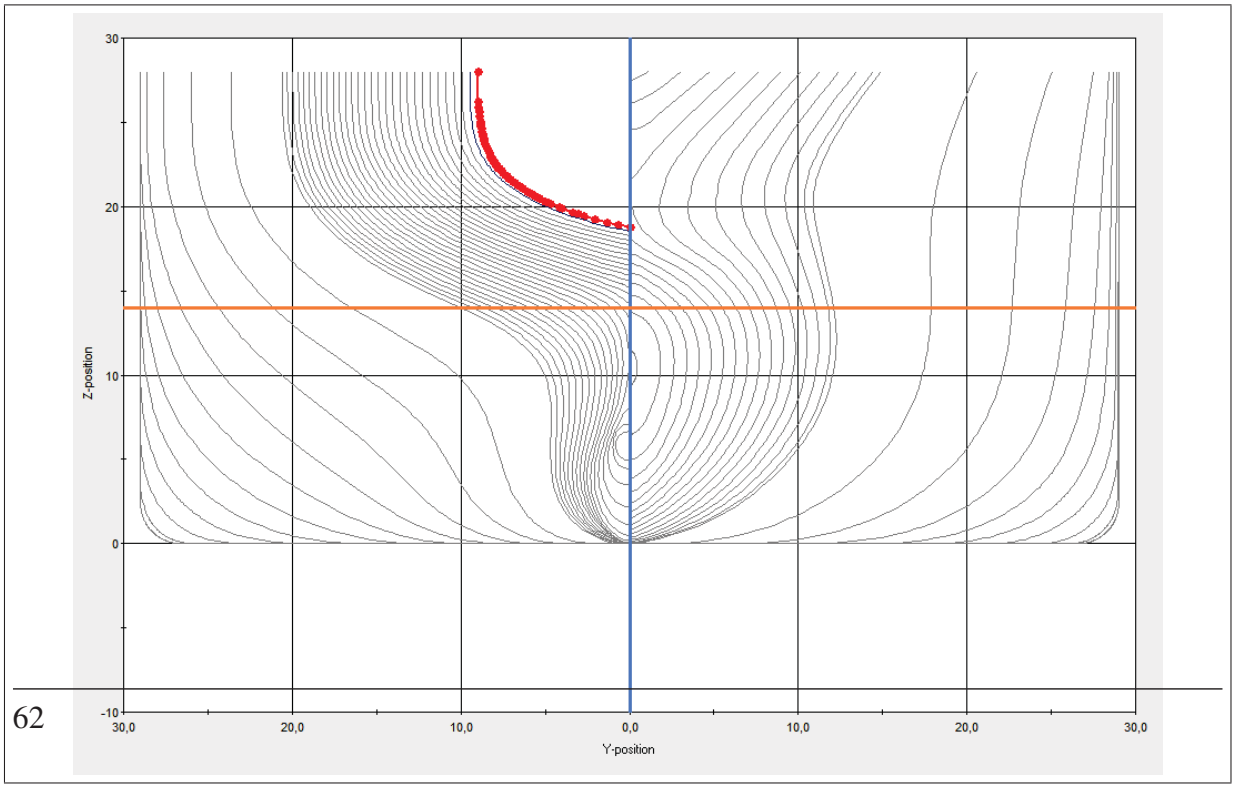

Figure 7.2: KVLCC2: body plan

The test conditions for the simulated manoeuvres are given in table 7.2.

Test conditions	**Fullscale**
T (m)	20.8
Displacement (m^3)	312622
S with rudder (m^2)	27467
LCG (m)	11.1
GM (m)	5.71
ixx/B (m)	0.40
izz/Lpp (m)	0.25

Table 7.2: Test conditions [4]

7.1.1 ShipX

MARINTEK had a hull model of KVLCC2 available; shipx_ geometry.mgf. When loading the hull model in ShipX it is possible to define various loading conditions. A loading condition with draft 20.8 meters is chosen according to the test condition. Trim and heel angle are set to zero. The principal hull data is attached in appendix A.1. ShipX calculates the hull hydrostatics which are attached in appendix A.2. To run the model in HullVisc some corrections to the hull geometry had to be done. Some of the fore sections had y-values of 0.001 at the keel which led open sections under water. These values are corrected to 0.000. There were also some troubleshooting when running Vessel Response Calculation for the Ship Model in Vessel Simulator. Some sections had zero thickness, which had to be corrected by setting the thickness to 0.001 meters.

7.1.2 HullVisc parameters

HullVisc have the following input parameters:

- Service speed
- Wake fraction
- Presence of skeg
- Tunnel thrusters
- Foils
- Water depths
- Calculation method of resistance

Skeg, tunnel thrusters and foils are not included in the simulation model. The option for different water depths is chosen to obtain the shallow water ratios. There are three methods when calculating the longitudinal resistance. A simplified empirical method based on [28]. The two others are automatic or manual polynomial. The manual polynomial method uses user-defined

coefficients the generate the polynomial, whilst the automatic generates the coefficients based on the empirical method. Automatic polynomial is chosen for the simulations and the polynomial is given in figure 7.3.

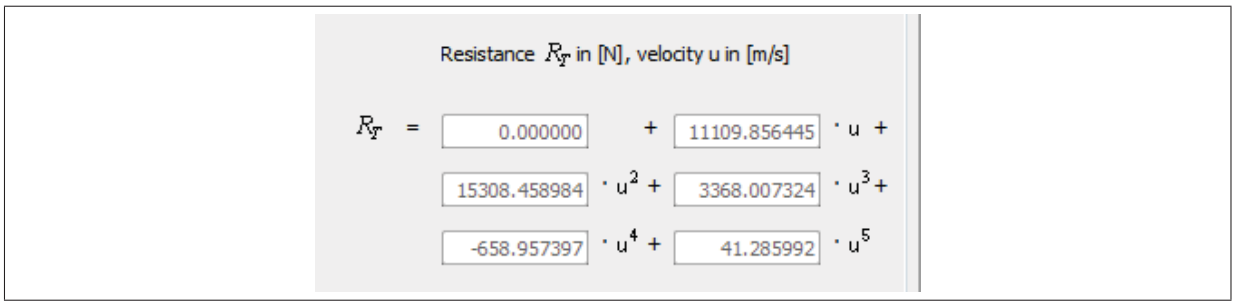

Figure 7.3: Longitudinal resistance polynomial

The wake fraction of the hull has to be defined by the user and is set to 0.150 [-] which has previously been used for KVLCC2 by MARINTEK.

Deep water coefficients

The calculated non-dimensional hydrodynamic coefficients of KVLCC2 for the test conditions in HullVisc are given in table 7.3. The linear stability index at infinite water depth is calculated

Coefficient	Value [-]
Y'_v	-0.02096
Y'_r	0.00497
N'_v	-0.01113
N'_r	-0.00276
$Y'_{\dot{v}}$	-0.01679
$Y'_{\dot{r}}$	-0.00039
$N'_{\dot{v}}$	-0.00039
$N'_{\dot{r}}$	-0.00110
X'_{rr}	0.00039
$X'_{\dot{u}}$	-0.00139
X'_{vr}	0.00289
X'_{vv}	-0.00129
X'_{vvvv}	0.04512

Table 7.3: Hydrodynamic coefficients

as $-8,51 * 10^{-5}$. This indicates that KVLCC2 is unstable, which is not uncommon for tankers.

Shallow water coefficients

The hydrodynamic coefficients for shallow water are partly based on Falch (1982) and are summarized in table 7.4. The ratios between the coefficients between deep and shallow water are shown in figure 7.4 and the linear stability index with the varying water depths are shown in figure 7.5.

$\frac{h}{T}$	Y'_v	Y'_r	N'_v	N'_r	$Y'_{\dot{v}}$	$Y'_{\dot{r}}$	$N'_{\dot{v}}$	$N'_{\dot{r}}$
1.10	-5.832E-2	1.305E-2	-3.261E-2	-6.794E-3	-4.60E-2	-9.32E-4	-9.32E-4	-2.83E-3
1.15	-5.219E-2	1.103E-2	-2.939E-2	-5.902E-3	-4.09E-2	-9.05E-4	-9.05E-4	-2.50E-3
1.20	-4.761E-2	9.773E-3	-2.686E-2	-5.318E-3	-3.71E-2	-8.62E-4	-8.62E-4	-2.27E-3
1.30	-4.118E-2	8.272E-3	-2.320E-2	-4.583E-3	-3.20E-2	-7.76E-4	-7.76E-4	-1.96E-3
1.5	-3.383E-2	6.832E-3	-1.890E-2	-3.83E-3	-2.63E-2	-6.53E-4	-6.53E-4	-1.62E-3
1.70	-2.980E-2	6.146E-3	-1.650E-2	-3.458E-3	-2.33E-2	-5.77E-4	-5.77E-4	-1.45E-3
2	-2.642E-2	5.627E-3	-1.447E-2	-3.164E-3	-2.07E-2	-5.10E-4	-5.10E-4	-1.31E-3
2.60	-2.341E-2	5.220E-3	-1.264E-2	-2.925E-3	-1.85E-2	-4.46E-4	-4.46E-4	-1.19E-3
3.70	-2.171E-2	5.032E-3	-1.159E-2	-2.807E-3	-1.73E-2	-4.09E-4	-4.09E-4	-1.13E-3
5	-2.095E-2	4.972E-3	-1.113E-2	-2.765E-3	-1.68E-2	-3.92E-4	-3.92E-4	-1.10E-3

Table 7.4: Shallow water coefficients

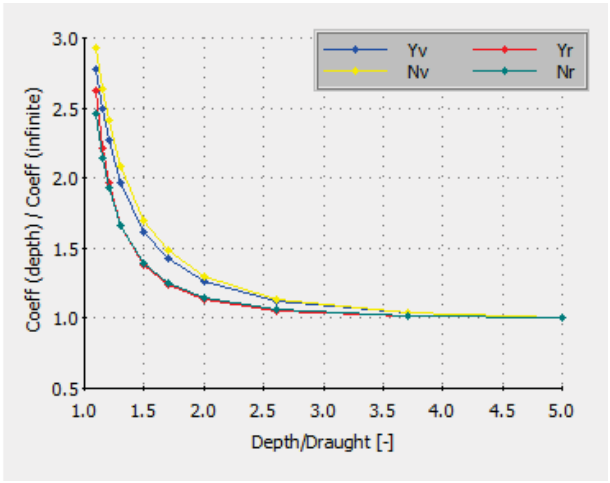

Figure 7.4: Velocity coefficients ratios at different water depths

The shallow water effects on the hydrodynamic coefficients are clearly shown giving larger damping forces when the water becomes shallower.

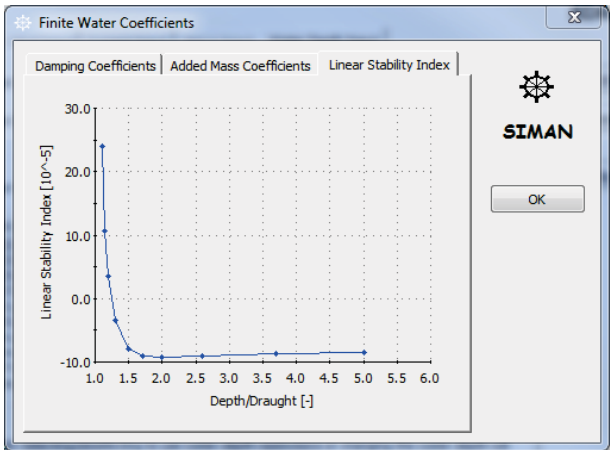

Figure 7.5: Linear instability index for various water depths

The linear stability index decreases from shallow water ratio h/T=5.0 to h/T=2.0 From h/T=2.0 to h/T=1.1 the linear stability increases significantly, and becomes positive around h/T=1.25.

7.1.3 SIMAN parameters

The input parameters for rudder and propulsion in SIMAN are set to the same as used in MARINTEKS contribution in SIMMAN 2008. The rudder and propulsion input parameters have been checked against the drawings of the propeller and rudder in AutoCAD-format from the SIMMAN website and are consistent. The software Rhinocerus 5.0 were used. The input values in figures 7.6 and 7.7 are used in the simulations.

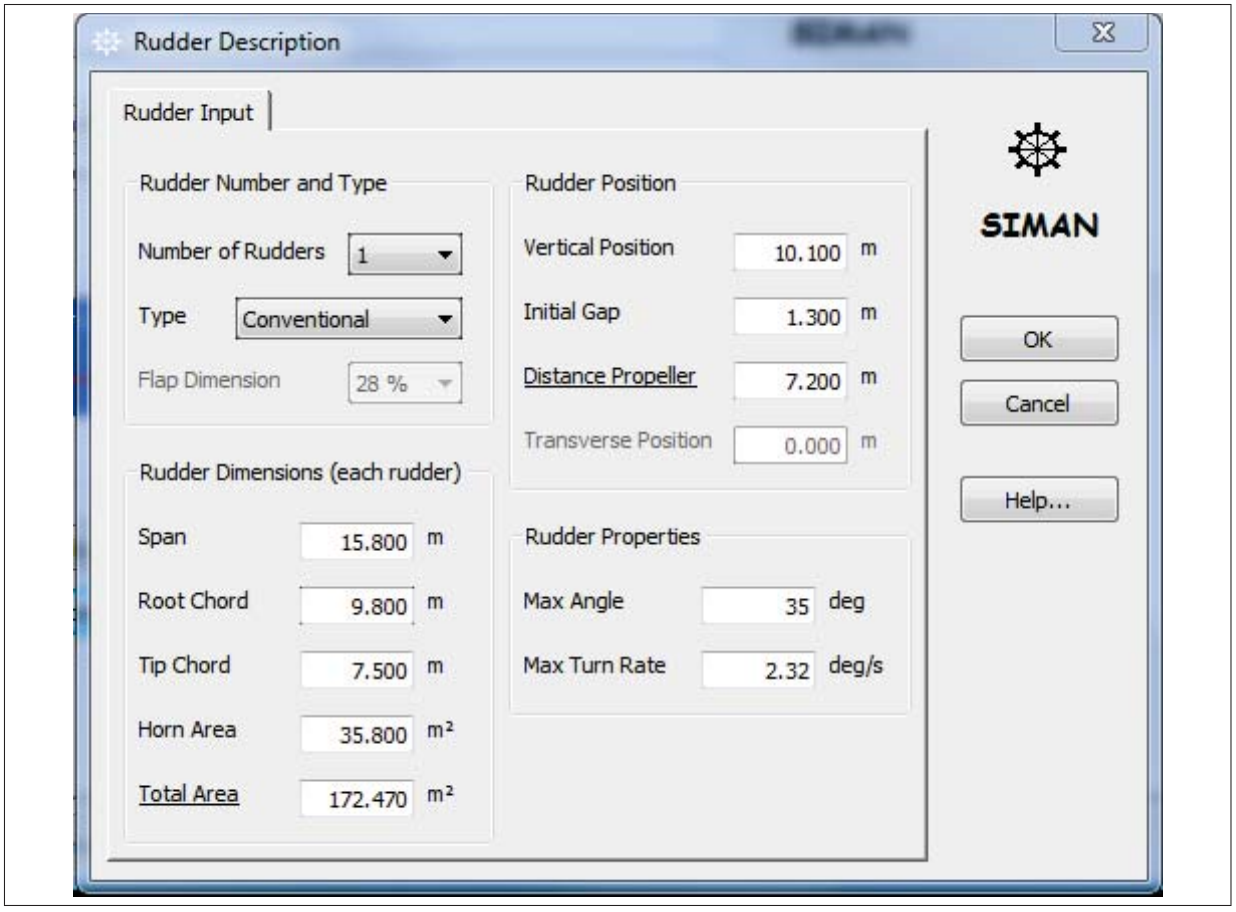

Figure 7.6: Input for rudder description

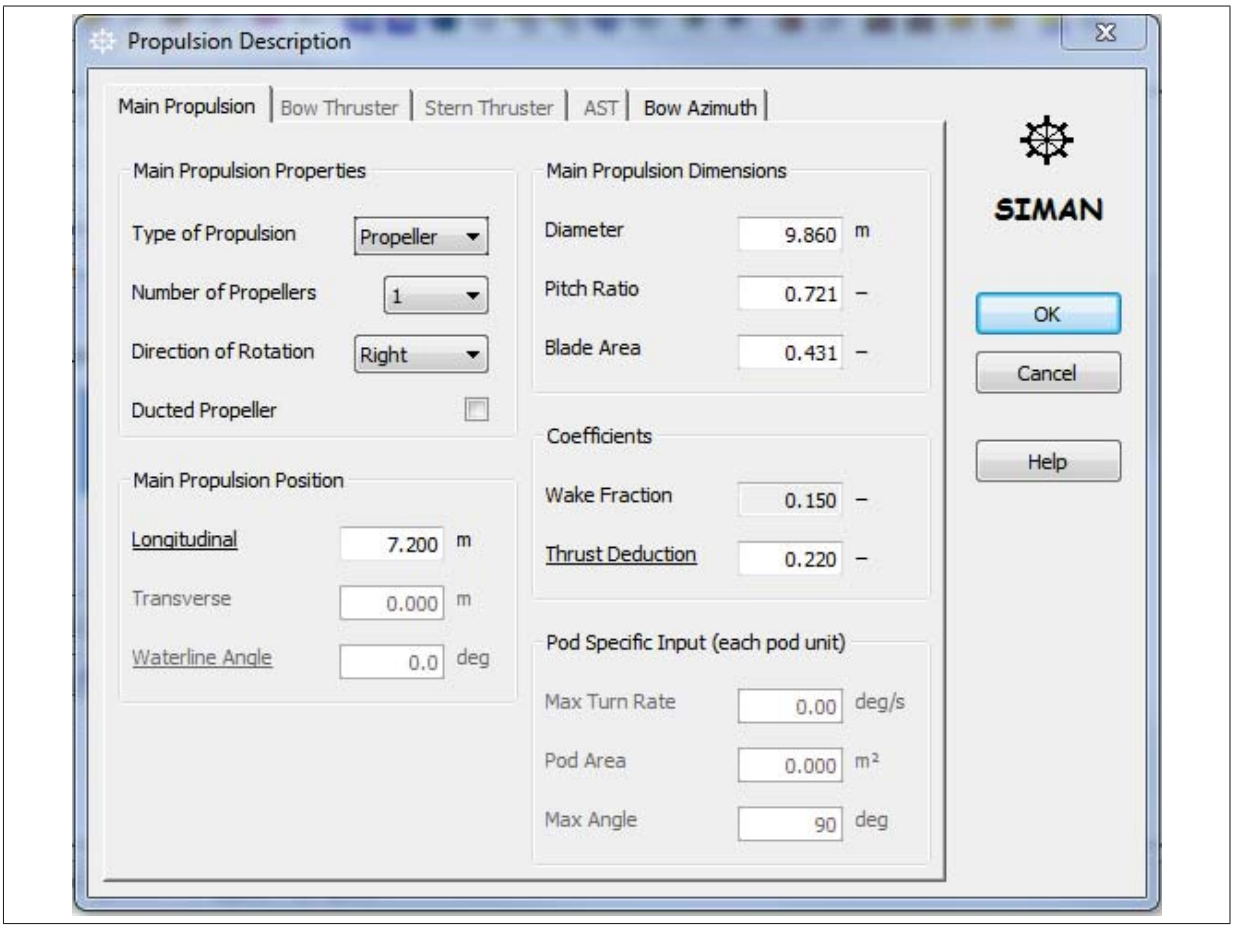

Figure 7.7: Input for propulsion description

Total rudder area and thrust deduction are calculated by default formulas. The trust deduction coefficient is a primitive estimate because it is a function of propellers only. Diesel engine is chosen and the total moment of inertia is 300000 kgm^2. The calculated service speed condition is:

- Propeller power = 21870 kW
- Propeller revolutions = 80.8 rpm
- Total thrust = 2015 kN

Before running test the engine must be tuned, since the tuning is vital to the results of the manoeuvres. This is calculated in the Tune Engine Input in the Manoeuvre frame.

7.1.4 Ship model in Vessel Simulator

The Ship Model for the vessel uses a Vessel Response Run to provide input of ship motion characteristics and wave drift force coefficients to the simulator, while a Manoeuvring Run provides the input of ship manoeuvring characteristics. Retardation functions can be calculated with a regular quality model or an high-quality model. High-quality model for calculation of retardation functions is chosen. The radius of gyration in roll(R_{44}) is calculated to be 20.3 meter. Other inputs in the Ship Model are wind force, propulsor and sensor inputs. In the propulsion

input a propeller and conventional rudder is used. Rudder and propulsion input are the same as in SIMAN, but there are some other parameters as well. The propulsor input are attached in appendix A.4. There were some problems with engine input, but the engine input attached in appendix A.5 provides a satisfactory engine for an approach speed of 15.5 knots. This can be fine-tuned if it is desirable.

7.1.5 Model tests

An overview of model test series from SIMMAN 2008 workshop as well as tests performed for the planned second SIMMAN 2014 workshop [9]. Bare and app. are two different model

Captive	
PMM app. deep	MOERI (1999), INSEAN (2006), BSHC (2011)
PMM app. shallow	INSEAN (2006), FHR (2010)
PMM bare deep	INSEAN (2006)
PMM bare shallow	INSEAN (2006), FHR (2010)
CMT app. deep	NMRI (2006)
Free	
Free app. deep	HSVA (2006), CTO (2007), MARIN (2007)
Free app. shallow	FHR(2010)

Table 7.5: Model test series for KVLCC2

configurations. The first covers the bare hull (hull alone without rudder). The second covers the appended hull (hull appended with rudder). Thee free appended hull model test for deep water will be used as benchmark data. During SIMMAN 2008 three faculties performed free sailing tests with the same models at nominal condition: HSVA, MARIN and CTO. All faculties used the same KVLCC2 model for the free model tests constructed by INSEAN. The model is manufactured of wood to a linear scale ratio of 1:45.714. Turbulence was stimulated using studs at the bow. Turning circle tests were only performed by MARIN and CTO. Only MARIN had enough results present to create figures for steady turning conditions. All faculties used propulsion point on the model. MARIN and HSVA used constant propeller RPM during their simulations, whilst CTO used constant torque delivered by the propeller during the simulation [2]. This plays a role for the prediction results, but the quantitative influence is not fully clarified [8]. FHR uses a model which has a scale of 1:75.000 for the free shallow water tests. All the shallow water tests have been conducted at:

- h/T=1.2
- h/T=1.5
- h/T=1.8

The approach speed is 7.0 knots, giving Froude number to be 0.064.

$$F_N = \frac{V}{\sqrt{gL_{PP}}} \tag{7.1}$$

The test to be conducted in shallow water is [19]:

- 10°/2.5°zig-zag tests including at least the first two overshoots with first execute of rudder to both port and starboard.
- 20°/5°zig-zag tests including at least the first two overshoots with first execute of rudder to both port and starboard.
- 35°turning circle tests with rudder to both port and starboard including pull-out, where rudder is put back at 0 degree after steady state has been reached.

Unfortunately, the free model results test at shallow water will not be available until after the SIMMAN 2014 workshop in December.

Chapter 8

Simulation results

8.1 Deep water simulations

The deep water simulations in SIMAN have been conducted in the project thesis. The manoeuvres in VeSim has to begin after 130 seconds into the simulation due to transient effects coming from "pushing" the ship to the correct approach speed. When setting the initial speed to 15.5 knots in VeSim all the manoeuvres had an approach speed of 15.3 knots. Correcting the initial speed to 15.7 knots gave an approach speed of 15.5 knots.

8.1.1 Turning circle

Turning circle manoeuvres are simulated in SIMAN and VeSim with 35 degree rudder angle, 360 degree max heading to both starboard and port. The results are presented in table 8.1.

Turning circle results				
Plug-In	**SIMAN**		**VeSim**	
Parameter	**35°SB**	**35°PT**	**35°SB**	**35°PT**
Approach speed [kn]	15.5	15.5	15.5	15.5
Advance/Lpp [-]	2.45	2.44	2.44	2.41
Transfer/Lpp [-]	1.03	1.02	1.04	1.06
Tactical diameter/Lpp [-]	2.55	2.54	2.50	2.51
Final Turning Radius/Lpp [-]	0.64	0.63	0.66	0.65
Drift Angle at 360°[°]	32.5	-32.9	28.9	-29.3
Final Speed/Approach Speed [-]	0.16	0.16	0.22	0.22
Final Rate of Turn [-]	1.56	-1.58	1.52	-1.55

Table 8.1: Turning circle results

The turning circle simulations of KVLCC2 fulfils the IMO criteria of turning ability in both SIMAN and VeSim.

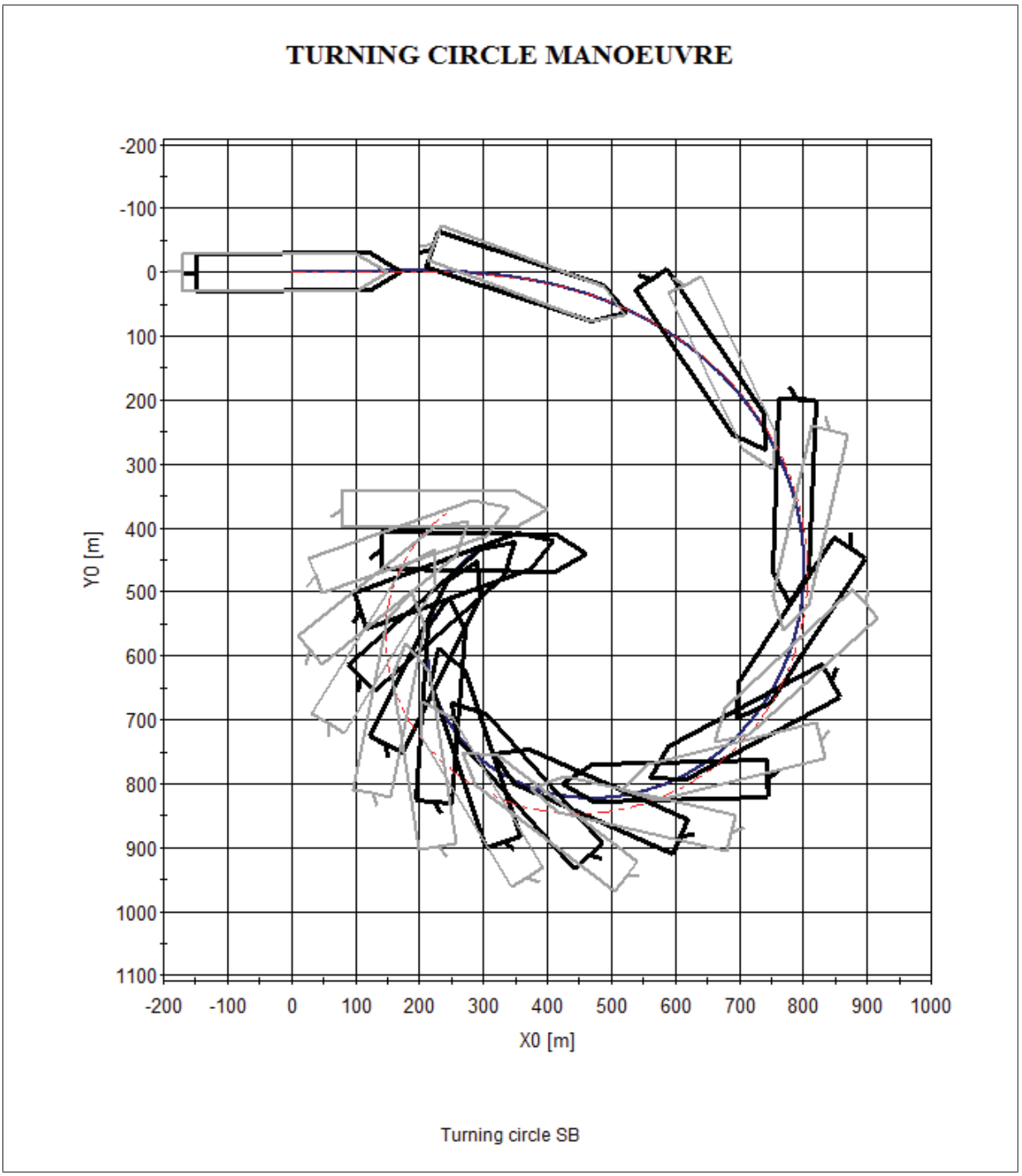

Figure 8.1: Track plot of turning circle for SIMAN (grey) and VeSim (black)

It is small differences between SIMAN and VeSim, this is not surprising as SIMAN uses a 3-DOF model, while VeSim uses a 6-DOF model. The roll angle during the manoeuvre is shown in figure 8.2.

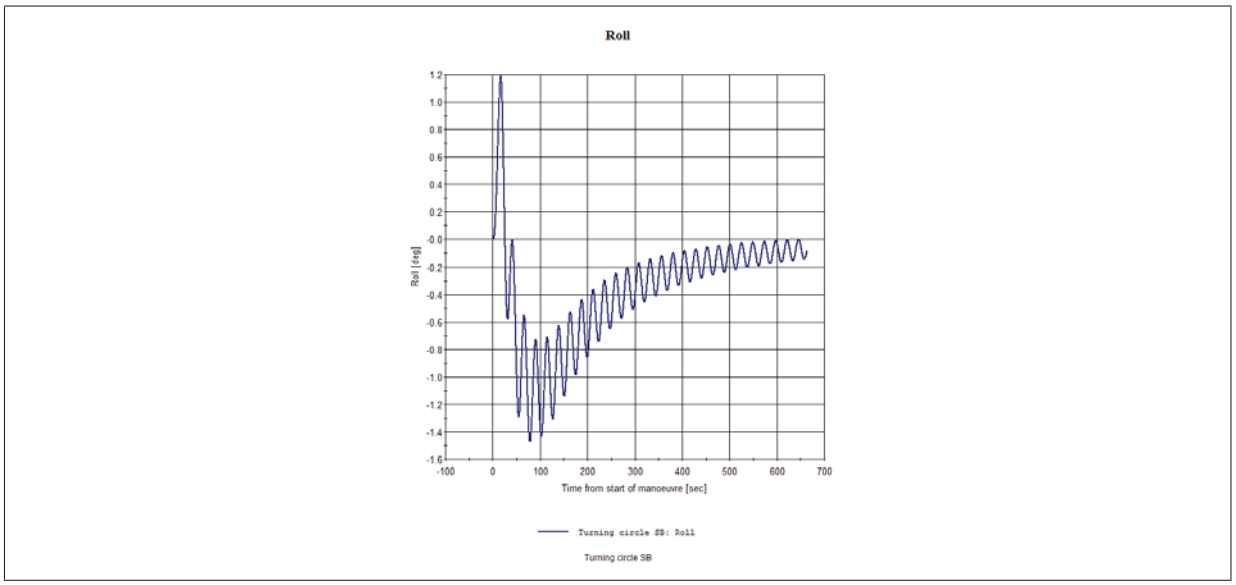

Figure 8.2: Roll angle 35° turning circle starboard

The shorter indices from the turning circle could be because of roll damping. Most of VeSim's manoeuvring forces are obtained from the manoeuvring run. The linear velocity derivatives are calculated within VeSim. The methods of calculation of these are not known to the author, but it seems like they are within a close range due to the similar results. But these could also be a reason for the small differences.

8.1.2 Zig-zag tests

10°/10°and 20°/20°zig-zag tests are simulated with 15.5 knots approach speed with first turn to both starboard and port. The results are presented in table 8.2. The zig-zag simulations of

SIMAN				
Parameter	**10°SB**	**10°PT**	**20°SB**	**20°PT**
Approach speed [kn]	15.5	15.5	15.5	15.5
1st overshoot angle [deg]	6.0	6.2	12.0	12.2
2nd overshoot angle [deg]	9.2	8.9	14.0	13.8
3rd overshoot angle [deg]	9.0	9.3	12.5	12.8
Initial turning time [-]	1.39	1.39	1.49	1.48
Vesim				
Parameter	**10°SB**	**10°PT**	**20°SB**	**20°PT**
Approach speed [kn]	15.5	15.5	15.5	15.5
1st overshoot angle [deg]	5.8	5.7	11.7	11.7
2nd overshoot angle [deg]	8.5	8.2	13.3	13.0
3rd overshoot angle [deg]	8.2	8.6	12.1	12.4
Initial turning time [-]	1.41	1.32	1.50	1.45

Table 8.2: Zig-zag results

KVLCC2 fulfils the IMO criteria of initial turning/course-changing and yaw-checking abili-

ties in both SIMAN and VeSim. Graphical results of the rudder and heading angle from the 10°/10°zig-zag tests from SIMAN and VeSim is presented in figure 8.3.

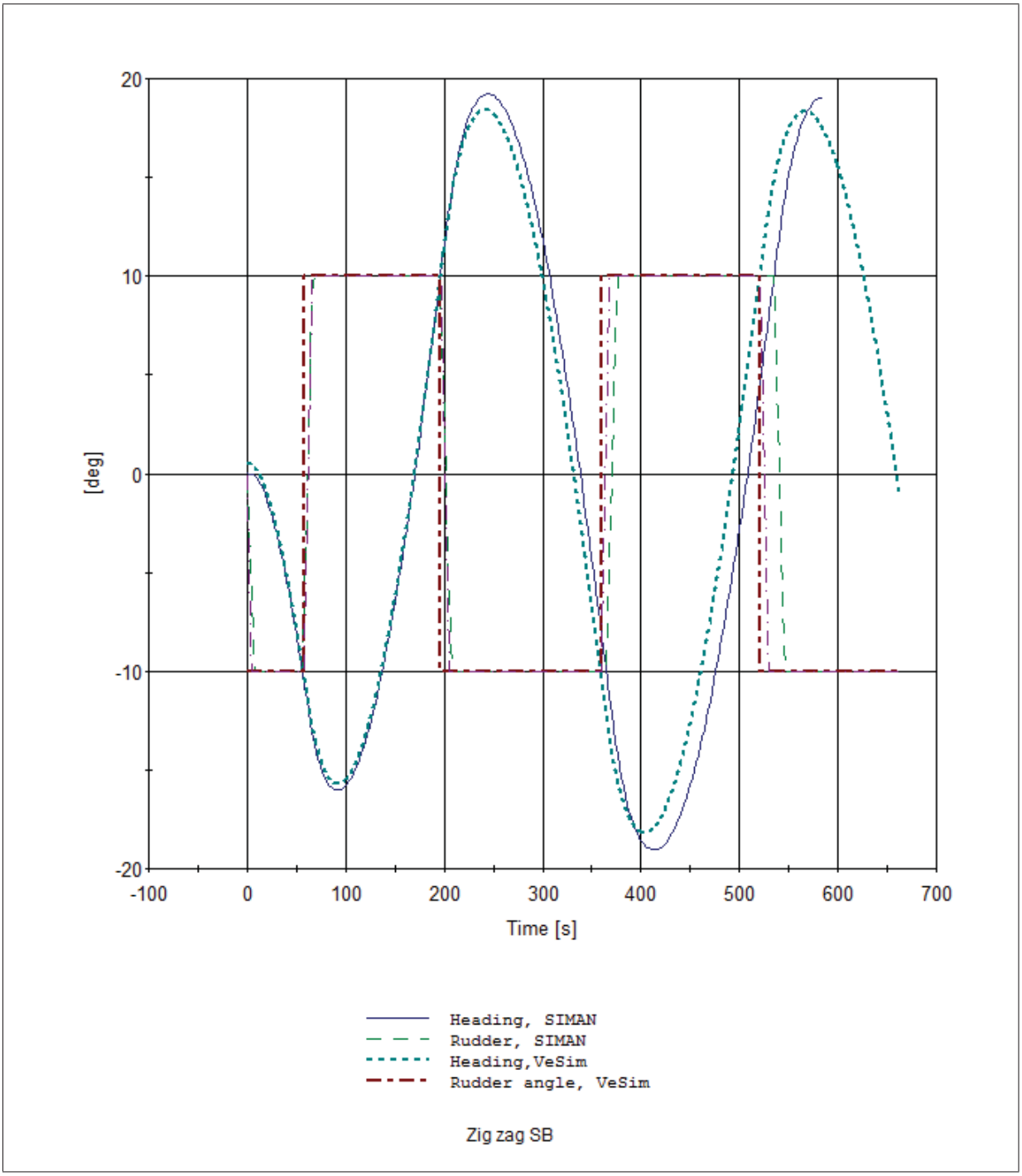

Figure 8.3: Heading and rudder angle plot of Zig-zag 10°/10°for SIMAN and VeSim

Differences are small here as well. Vesim has overall smaller overshoot angles in both 10°/10°and 20°/20°to starboard and port. The initial turning time is varying more in VeSim, being both higher and lower than in SIMAN.

8.1.3 Stopping tests

The stopping test in SIMAN and VeSim is called full astern stopping. The manoeuvre can be simulated by either controlling propeller revolutions or pitch in SIMAN. Required input data is the time to reverse revolutions and max revolutions astern. The only parameter in VeSim is "commanded engine setting astern on main propulsion", which is set to -100%. The manoeuvre is done with zero rudder angle. The results are presented in table 8.3

Stopping test results		
Parameter	**SIMAN**	**VeSim**
Approach speed [kn]	15.5	15.5
Track length [m]	5600	4620
Track length/Lpp [-]	17.5	14.4
Head reach/Lpp [-]	16.99	14.3
Lateral deviation/Lpp [-]	2.74	1.14
Time to stop [s]	1852	1378

Table 8.3: Stopping test results

The stopping test simulation of KVLCC2 does not fulfil the IMO criteria of stopping ability in SIMAN, while it does fulfil it in VeSim. The criteria of the stopping ability is that the track reach should not exceed 15 ship lengths. However, this is strongly dependent of the time to reverse revolutions and max revolutions astern, where the default SIMAN input has been used. The track plot is presented in figure 8.4.

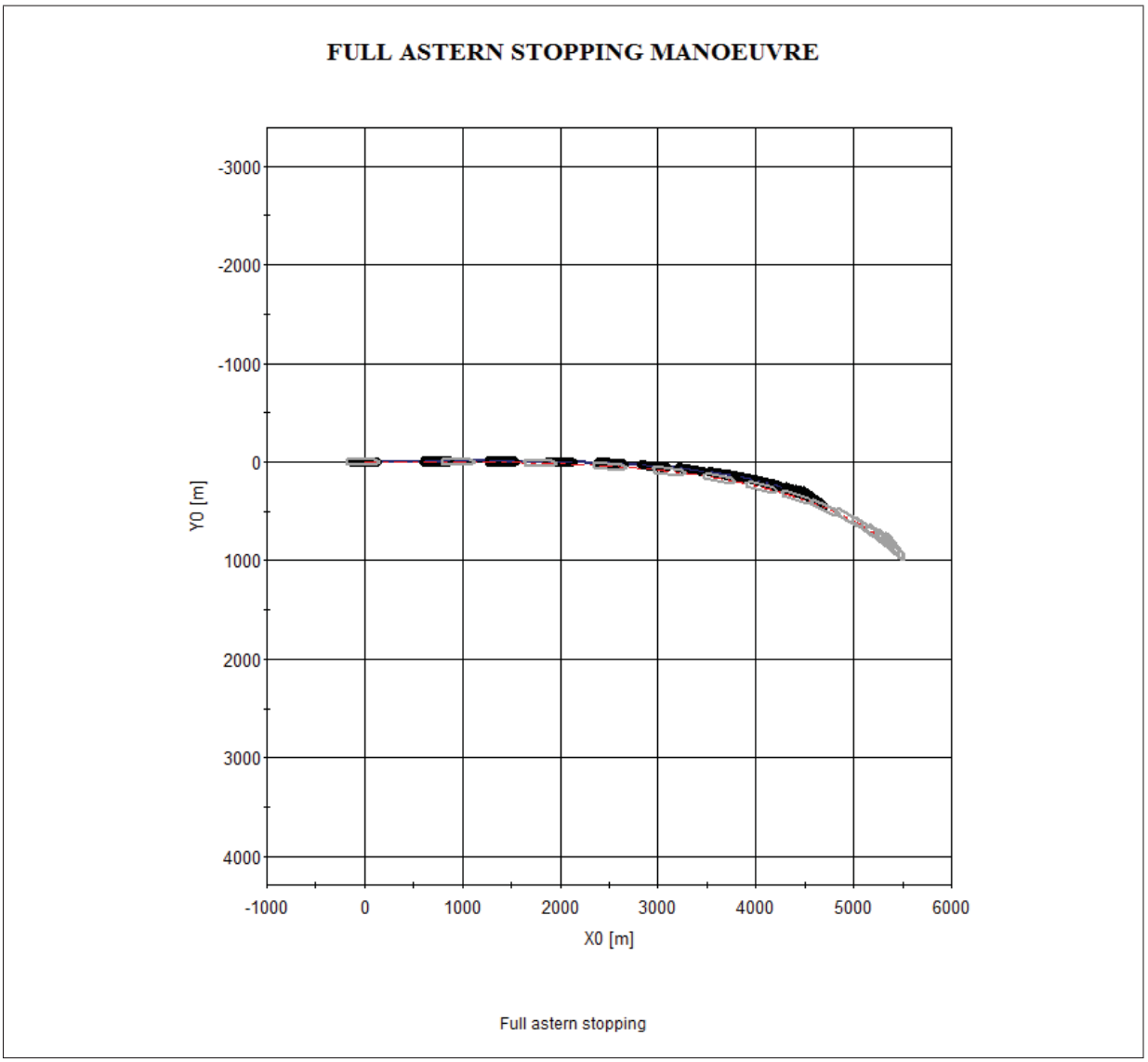

Figure 8.4: Track plot of stopping test, SIMAN (grey) VeSim (black)

8.2 Shallow water and low speed simulations

Shallow water simulations are only conducted in SIMAN as VeSim does not have an option for water depth input.

8.2.1 Turning circle

The turning circle is conducted at shallow water with h/T ratios of 1.2, 1.5 and 1.8 and deep water with an approach speed of 7 knots. The results are given in table 8.4.

Turning circle results				
Parameter	**35°SB**	**35°SB**	**35°SB**	**35°SB**
h/T	1.2	1.5	1.8	Deep water
Approach speed [kn]	7.0	7.0	7.0	7.0
Advance/Lpp [-]	3.05	2.5	2.41	2.32
Transfer/Lpp [-]	1.83	1.38	1.24	1.01
Tactical diameter/Lpp [-]	3.88	3.01	2.8	2.52
Final Turning Radius/Lpp [-]	1.29	0.94	0.8	0.62
Drift Angle at 360°[°]	13.9	17.1	21.7	33.1
Final Speed/Approach Speed [-]	0.31	0.23	0.2	0.16
Final Rate of Turn [-]	0.78	1.07	1.24	1.6

Table 8.4: Turning circle shallow water results

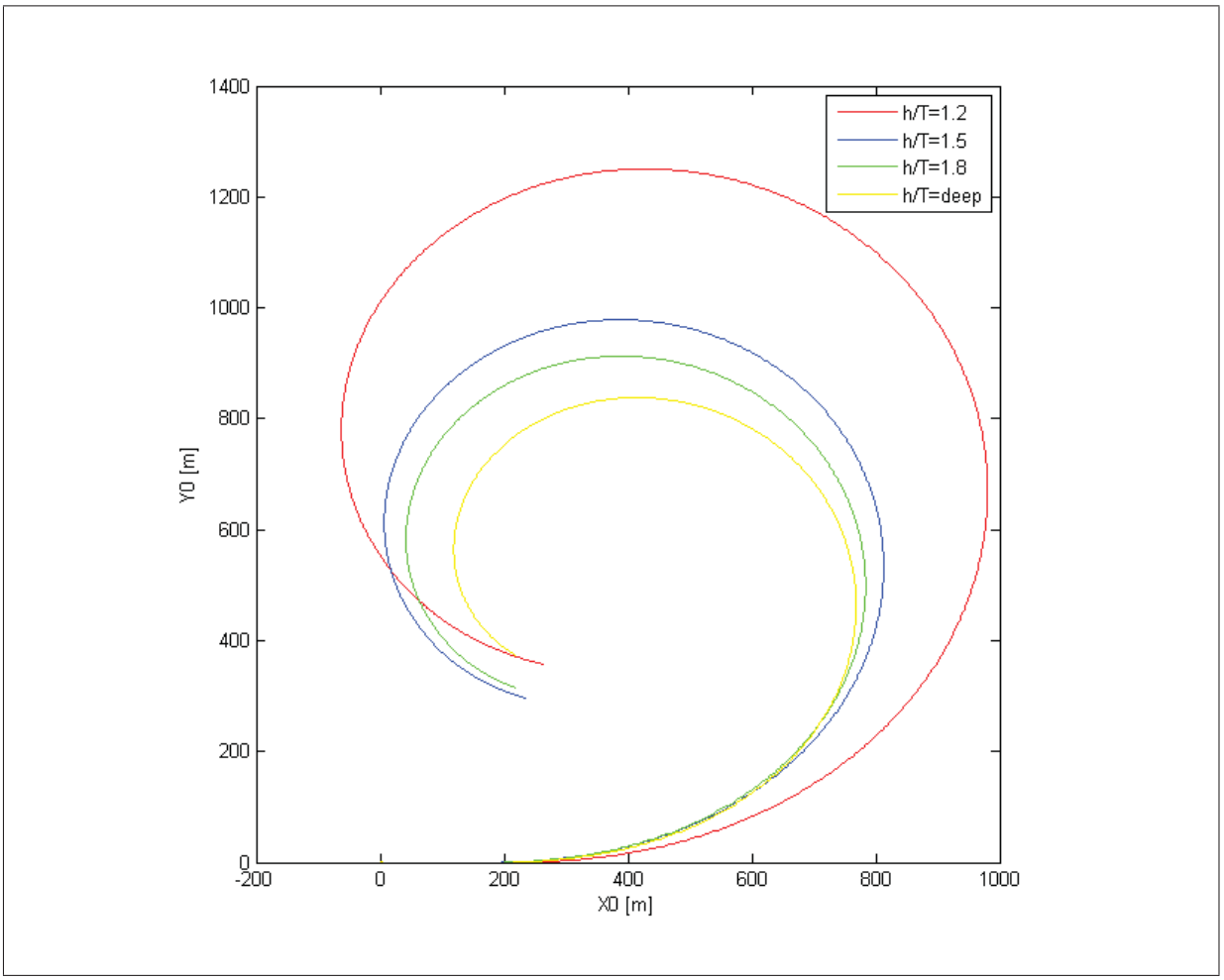

Figure 8.5: Turning circle track at different water depths

The results and figure 8.5 clearly shows the shallow water effects on the turning circle manoeuvre. The trends of turning circle for the Type-U (unstable) ship which KVLCC2 is are correlating with the literature.

8.2.2 Zig-zag tests

The zig-zag tests are conducted with an approach speed of 7.0 knots. The 10°/2.5°zig-zag manoeuvre is performed with a heading change of 3°because of limitations in zig-zag Manoeuvre input in SIMAN.

Zig-zag results, approach speed 7.0 knots				
h/T	Manoeuvre	1st OS [deg]	2nd OS [deg]	Initial TT [-]
1.2	10°/3°SB	2.3	3.9	0.87
1.5	10°/3°SB	2.2	3.9	0.73
1.8	10°/3°SB	2.3	4.0	0.71
Deep	10°/3°SB	2.3	4.0	0.69
1.2	20°/5°SB	4.3	6.3	0.83
1.5	20°/5°SB	4.4	6.5	0.69
1.8	20°/5°SB	4.5	6.8	0.67
Deep	20°/5°SB	4.7	7.2	0.65

Table 8.5: Zig-zag shallow water results

The 10°/3°overshoot angles does not change appreciably with water depth. The initial turning increases going to shallower water, from h/T<1.5 it increases significantly. The overshoot angles in the 20°/5°test decreases when going to shallower water. The trend of the initial turning times is the same as 10°/3°.

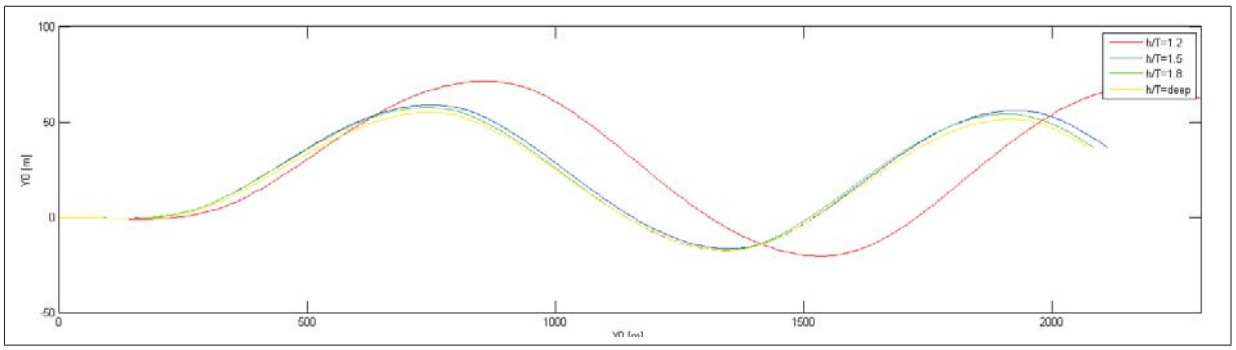

Figure 8.6: Zig-zag track at different water depths

8.2.3 Complete spiral tests

Complete spiral tests have also been conducted in SIMAN at various water depths. It is observed troubleshooting with ShipX when simulating this manoeuvre. New manoeuvring runs had to be made for each water depth. It seems like SIMAN has problems calculating the points in the hysteresis loop, which gave jagged and not continuous points as seen for water depths ratios h/T=1.5 and h/T=1.8 in figure 8.7.

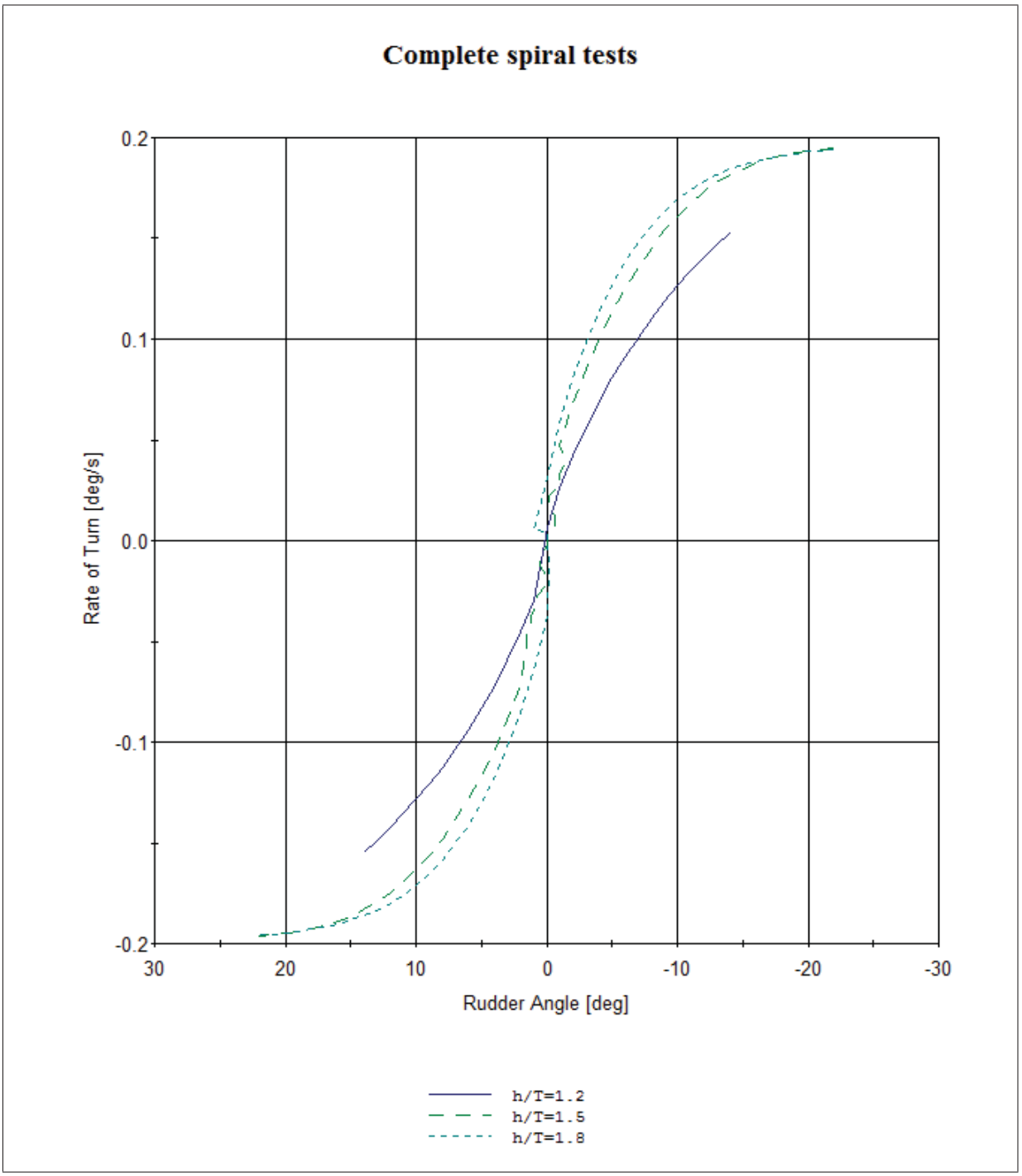

Figure 8.7: Complete spiral tests at different water depths

8.2.4 Zig-zag test at low speed

The previously suggested zig-zag test at low speed to determine the minimum speed at which the ship does not respond to the helm has been attempted to be done in SIMAN's "Real Time Simulation". The "Real Time Simulation" has a tendency to crash as well. So the minimum speed where the helm does not have any effect has not been reached completely. However the rudder lift and drag forces are converging towards zero after 3144 seconds, where the speed is 1.55 knots.

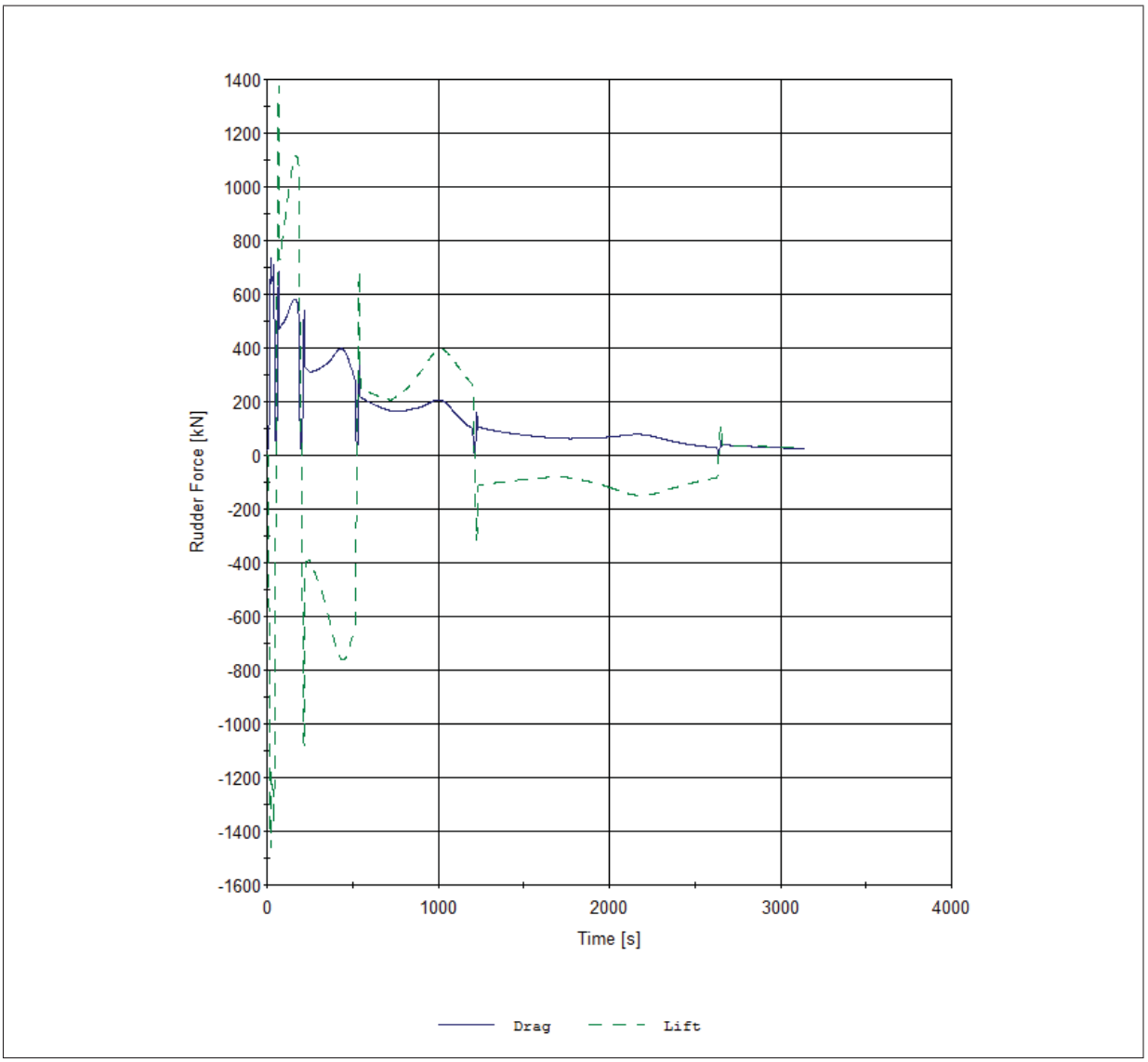

Figure 8.8: Zig-zag test at low speed rudder force plot

Chapter 9

Simulation comparisons

9.1 Comparisons to SIMMAN 2008

The purpose of the SIMMAN 2008 workshop was to benchmark the prediction capabilities of different ship manoeuvring simulation methods. This was done through comparisons and validation against experimental data. All submissions were blind (the model test data was not available before the workshop). 21 submissions for KVLCC2 were received at the workshop. The methods included empirical/semi-empirical methods, methods based on RANS or DES (CFD), methods based on PMM test and CMT test, as well as free sailing model tests. Scatter was large for the different methods as discussed in the project thesis, which proved the need for new validation studies. Reasons for the significant variation in the results can be due to different mathematical models, different number of degrees of freedom, whether model or ship self-propulsion point was used, or whether constant RPM or torque strategy was utilized. In experiences from SIMMAN 2008 it was concluded that empirical methods should be applied with caution. They are able to give good predictions only when restricted to the ship type for which they were developed. Due to similar models and results in SIMAN and VeSim, only SIMAN's results will be compared with the benchmark data and MARINTEK's contribution using SIMAN in 2008.

The advance from the turning circle is the shortest of all the 21 predicted turning circles in SIMMAN 2008. The tactical diameter is at the lower length part of the results as well. Results are not coinciding well with the other predicted turning circles. Especially the advance which is the lowest of all the contributions. The turning circle results scatter as seen in figure 9.1.

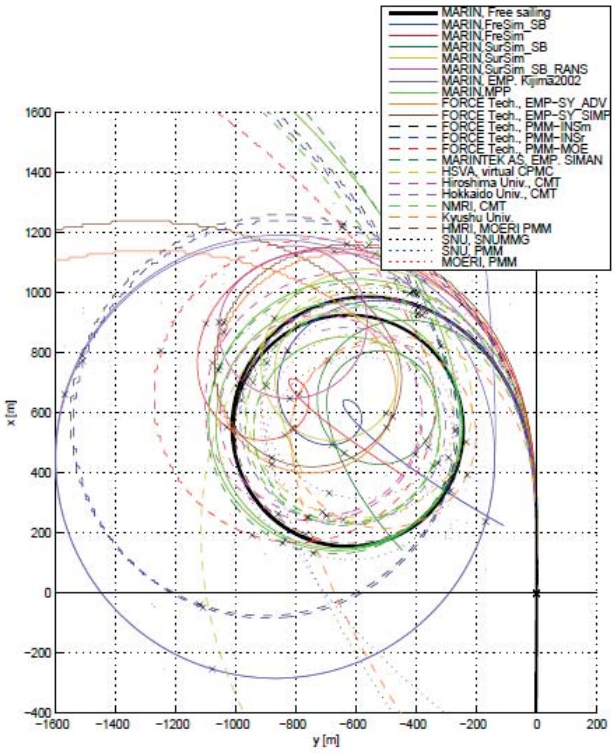

Figure 9.1: Turning circle results SIMMAN 2008 [2]

The overshoot angles looks more coinciding with the results from SIMMAN 2008. Compared to the other predictions it seems the results are around the mean of the other contributions. The scatter between the various overshoot angles are large and not coinciding well.

The 26th ITTC Manoeuvring Committee suggested average benchmark data (table 9.1) from the free sailing tests of KVLCC2 performed by CTO, MARIN and HSVA.

Benchmark	Port	Starboard
10/10 ZZ 1st OS (deg)	7.8	8.5
10/10 ZZ 2nd OS (deg)	15.7	17.6
20/20 ZZ 1st OS (deg)	12.8	13.0
20/20 ZZ 2nd OS (deg)	12.9	14.6
35 TC advance (Lpp)	2.73	3.04
35 TC TD (Lpp)	3.20	3.19

Table 9.1: Average benchmark value of applicable free model test results [9]

It is observed large scatter between the benchmark data and the simulated manoeuvres in SIMAN in table 9.2. The most coinciding measures are the 1st and 2nd overshoot angles in 20°/20°zig-zag tests to both starboard and port. Generally SIMAN underestimates all the other

	Simulated manoeuvres	Avg. benchmark	Sim/Avg. Bench
STARBOARD			
35 TC advance (Lpp)	2.45	3.04	0.806
35 TC TD (Lpp)	2.55	3.19	0.799
1st OS 1010 (deg)	6	8.5	0.706
2nd OS 1010 (deg)	9.2	17.6	0.523
1st OS 2020 (deg)	12	13	0.923
2nd OS 2020 (deg)	14	14.6	0.959
PORT			
35 TC advance (Lpp)	2.44	2.73	0.894
35 TC TD (Lpp)	2.54	3.20	0.794
1st OS 1010 (deg)	6.2	7.8	0.795
2nd OS 1010 (deg)	8.9	15.7	0.567
1st OS 2020 (deg)	12.2	12.8	0.953
2nd OS 2020 (deg)	13.8	12.9	1.070

Table 9.2: Benchmark comparison

manoeuvring indices. The 2nd overshoot angle in 10°/10°zig-zag test is underestimated 47%. While the turning circle advance and tactical diameter are averagely underestimated about 20%. The results are not coinciding well. Hence, the simulation model in SIMAN (and VeSim as well) are not validated based on the benchmark data. The difference between starboard and port are more noticeable in the benchmark data (e.g. the advance is 11.4% higher for turning circle to starboard than port). This could be because of the existence of neutral rudder angle which is necessary for keeping the ship course straight, due to a right-handed propeller.

9.2 Comparisons to MARINTEK

Another (maybe) equally interesting comparison is a comparison with MARINTEK's contribution using SIMAN in the SIMMAN 2008 workshop (denoted as MARINTEK from now). The same geometry file is used, as well as equal input parameters for rudder and propulsion description. The ratios between the various measures of the manoeuvres are presented in table 9.3.

	Simulated manoeuvres	MARINTEK	Sim/MARINTEK
Turning circle, 35°SB			
Advance/Lpp [-]	2.45	3.14	0.785
Transfer/Lpp [-]	1.03	1.35	0.763
Tactical diameter/Lpp [-]	2.55	3.34	0.763
Final Turning Radius/Lpp [-]	0.64	1.27	0.504
Drift angle at 360°[°]	32.5	23.8	1.365
Final Speed/Approach Speed [-]	0.16	0.36	0.444
Final Rate of Turn [-]	1.56	0.79	1.975
Zig-zag, 10°/10°SB			
1st overshoot angle [deg]	6	6.6	0.909
2nd overshoot angle [deg]	9.2	10.3	0.893
Initial turning time [-]	1.39	1.71	0.813
Zig-zag, 20°/20°SB			
1st overshoot angle [deg]	12	10	1.200
2nd overshoot angle [deg]	14	10.8	1.296
Initial turning time [-]	1.48	1.86	0.796

Table 9.3: MARINTEK comparison

It is observed large scatter between the simulated manoeuvres and MARINTEK's simulated manoeuvres in 2008. The deviations are substantial in all of the measures from the manoeuvres (only 1st overshoot angle in 10°/10°zig-zag test is within 10% range). Both transfer and advance is 23.7% less in SIMAN. The final turning radius is 50% less. Drift angle at 360°and final rate of turn is higher whilst the final speed is lower in SIMAN. The 10°/10°zig-zag test underestimates the overshoot angles and initial turning time compared to MARINTEK. The overshoot angles in 20°/20°zig-zag test are higher in SIMAN. The different results are not because of the input parameters, as these are identical to the ones used in 2008. The different results are because there has been done many changes in the plug-in since 2008. However, the documentation of the mathematical model and the estimation of the hydrodynamic forces is not updated since 2008. Therefore, an assessment of why the results deviates is hard to conduct.

	Sim/Benchmark	MARINTEK/Benchmark
Turning circle, 35°SB		
Advance/Lpp [-]	0.806	1.026
Tactical diameter/Lpp [-]	0.799	1.047
Zig-zag, 10°/10°SB		
1st overshoot angle [deg]	0.706	0.776
2nd overshoot angle [deg]	0.523	0.585
Zig-zag, 20°/20°SB		
1st overshoot angle [deg]	0.923	0.769
2nd overshoot angle [deg]	0.959	0.740

Table 9.4: Comparison between SIMAN/MARINTEK against benchmark data

As seen in table 9.4 MARINTEK's contribution using SIMAN in 2008 was more consistent compared to the benchmark data. The turning circle measures were very close to the benchmark data. The overshoot angles for 10°/10°zig-zag test are closer as well. In simulations using the updated version of SIMAN, the overshoot angles in 20°/20°zig-zag test are closer than in 2008. Overall, it looks like SIMAN in 2008 estimated closer values to the benchmark data than SIMAN today. This indicates that the changes made in the plug-in does not give better results for KVLCC2. SIMAN is tuned for offshore vessels, it may be that this has influenced the results.

9.3 Shallow water comparisons

Due to the lack of shallow water free model tests for KVLCC2, the shallow water effects from simulations will be compared with full-scale trial data from Esso Osaka. Only superficial results and trends will be investigated as Esso Osaka has a relative old hull form, as well as uncertainties in measurement data. The tactical diameter increased by 70% with 20% under keel clearance, while drift angle and related speed loss reduce relative to turning in deep water. With 50% bottom clearance the changes from deep water turning were much less. The turning circle track of Esso Osaka full-scale trials is presented in figure 9.2.

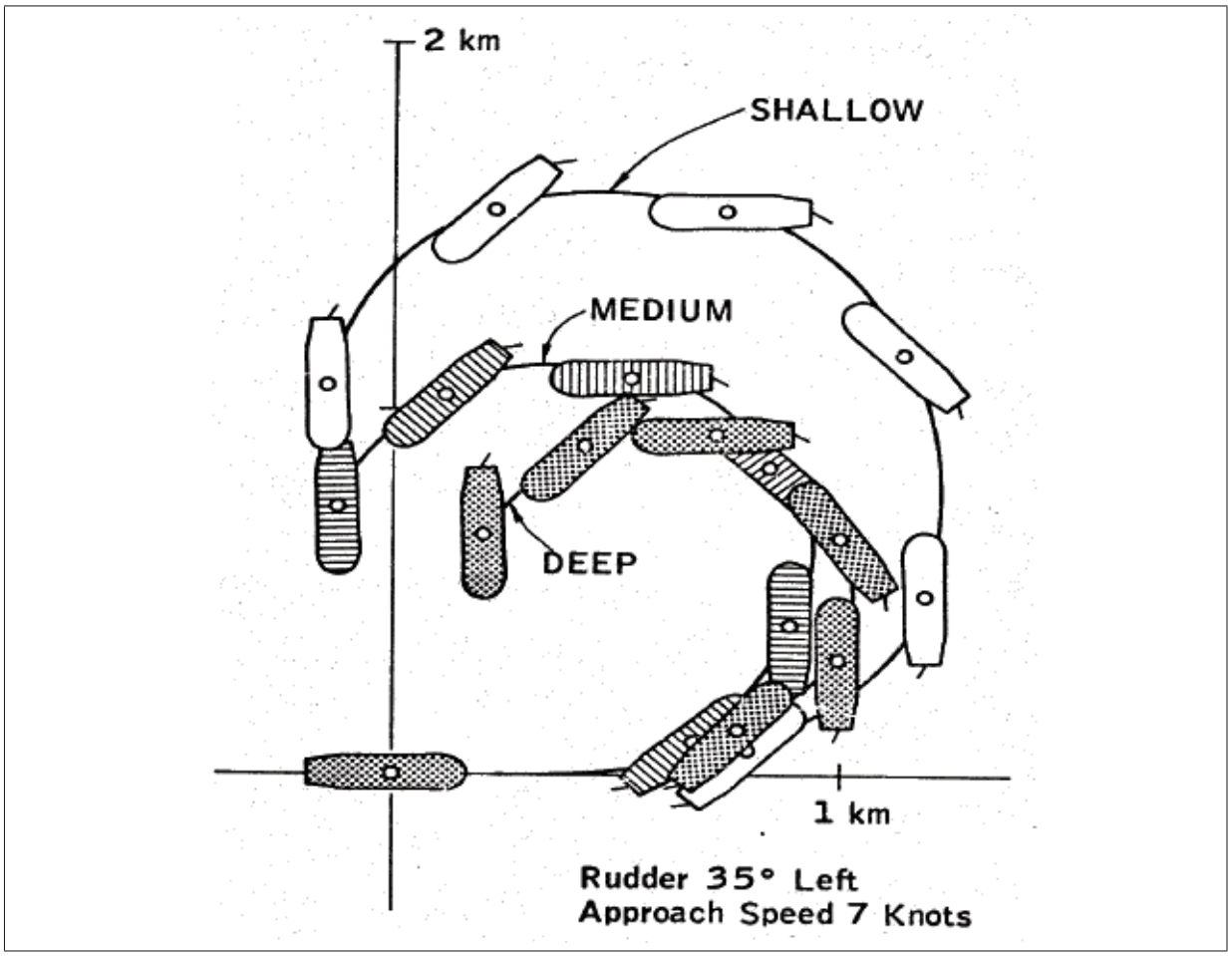

Figure 9.2: Water depth effect on turning circle track (Exxon (1979))

The deep water tactical diameter for KVLCC2 increases by 54% from deep water to 20% under

keel clearance. The drift angle and related speed loss reduce relative to turning in deep water as well. With 50% under keel clearance the changes are not as much. The same trends are observed in the simulation in shallow water as Esso Osaka. A trend which is not observed is that when h/T=1.50 it does not have a shorter advance than in deep water.

The checking and counter turning ability of Esso Osaka reduces as water depth decreases from deep water to 50% under keel clearance. From 50% UKC this ability increases and is better than in deep water as seen in figure 9.3.

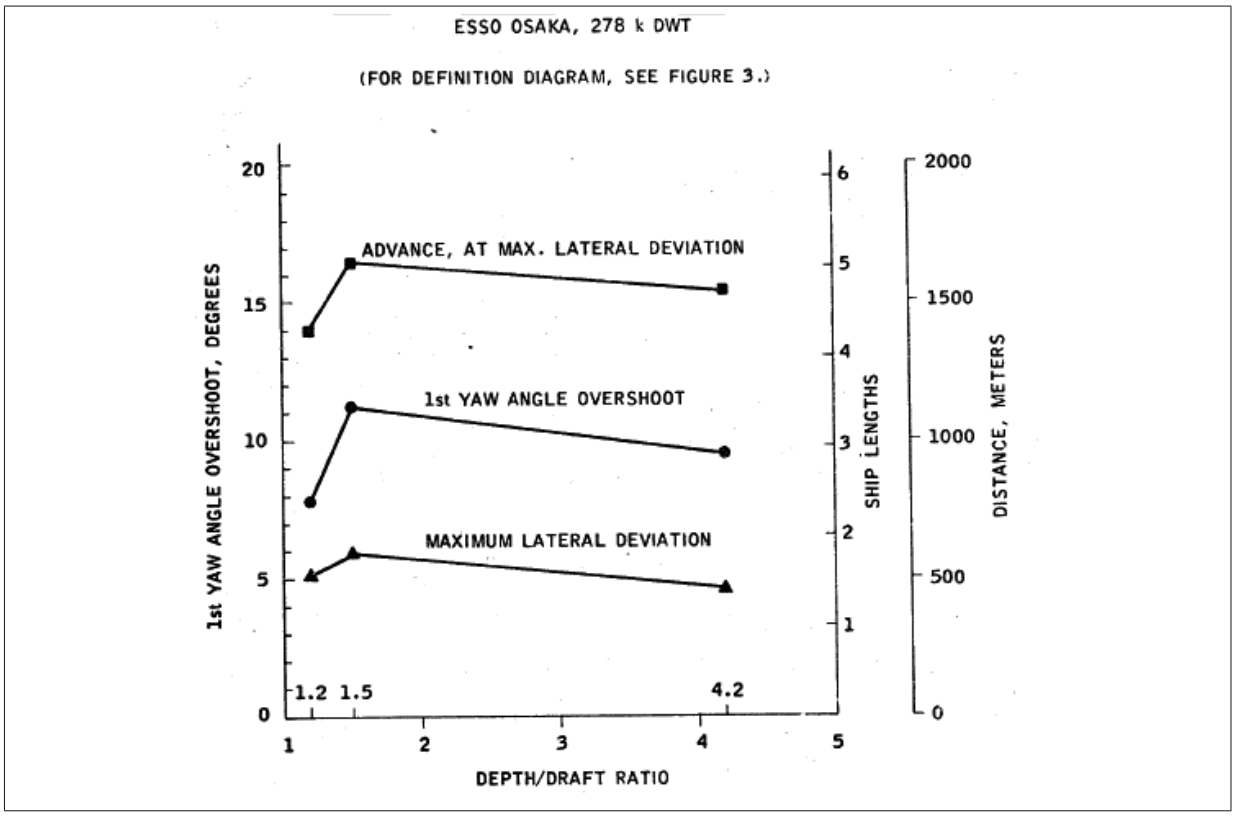

Figure 9.3: 20°/20°zig-zag manoeuvre response vs. water depth (Exxon (1979))

Due to the zig-zag tests of full-scale trials for Esso Osaka in figure 3.6 are not conducted with the same heading changes as the simulated manoeuvres in SIMAN, a quick simulation of 20°/20°zig zag test is performed for trend comparison with figure 9.3. The results are in table 9.5.

Zig-zag results, approach speed 7.0 knots				
h/T	Manoeuvre	1st OS [deg]	2nd OS [deg]	Initial TT [-]
1.2	20°/20°SB	6.6	7.2	1.85
1.5	20°/20°SB	7.3	8.2	1.53
1.8	20°/20°SB	7.8	9.0	1.47
4.2	20°/20°SB	8.7	9.6	1.41

Table 9.5: 20°/20° Zig-zag shallow water results

The same trend for the checking and counter turning ability of KVLCC2 are not found as for

Esso Osaka. The ability increases from deep h/T=4.2 to h/T=1.2 for each depth/draft ratio. The initial turning time increases as water depth decreases.

It is seen from reverse spiral tests of Esso Osaka that as the water depth decreases, the tanker becomes less course stable. In the case of h/T=1.50 the hysteresis loop indicating instability on course. If the water depth is reduced more, the course stability improves. This trend corresponds well in both model and full-scale trials. The complete spiral tests in SIMAN gave jagged points in the hysteresis loop in water depths where KVLCC2 is dynamically unstable. So these are not comparable. Looking at the linear dynamic stability for KVLCC in figure 9.4, it is observed that the stability does not decrease appreciably when going into shallower water ($2.0 < h/T$). The stability increases significantly from $h/T < 1.5$, and becomes positive at around h/T=1.25 .

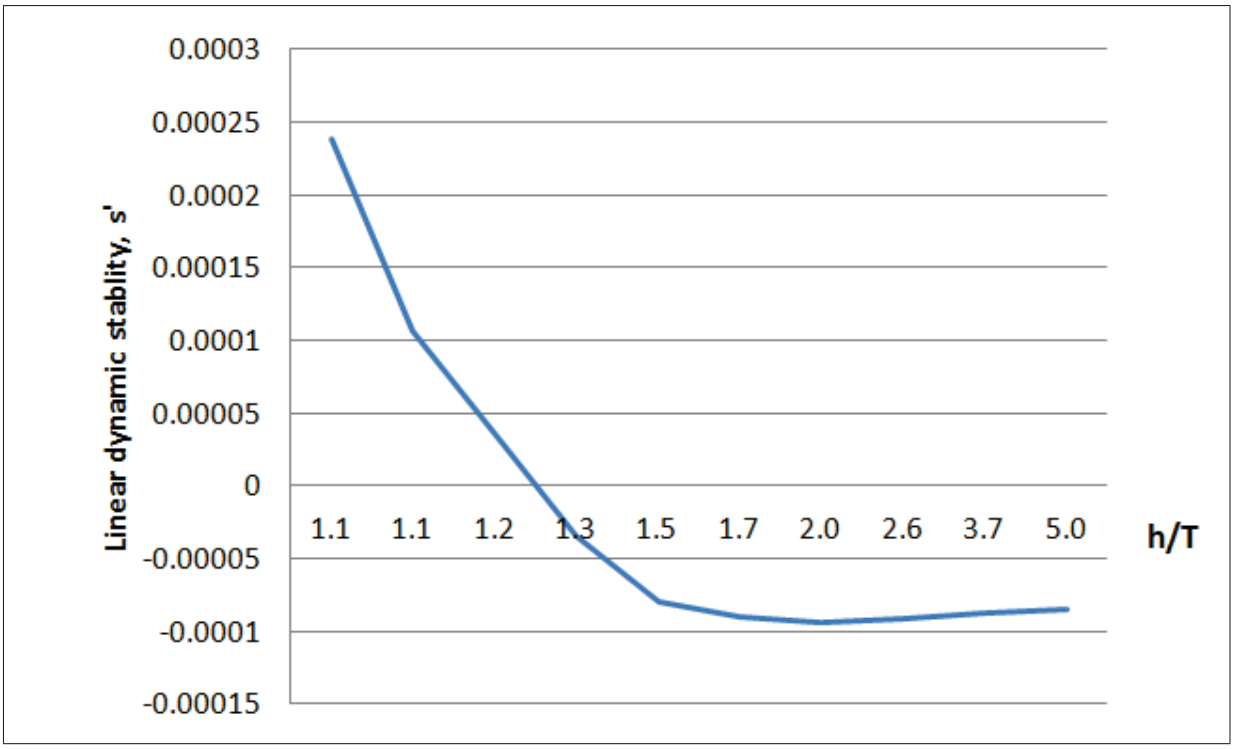

Figure 9.4: Linear dynamic stability for KVLCC2

9.4 Sensitivity analysis

Due to big deviations from MARINTEK's contribution in SIMMAN 2008 a sensitivity analysis is performed. The same procedure is done as in [36] for KVLCC2. The original value of a coefficient is increased and decreased by 20% and used in to simulate same manoeuvres. Each coefficient are changed separately while the evaluation of its sensitivity is measured from the simulator manoeuvre. The simulated manoeuvres performed in the sensitivity analysis are turning circles (35°rudder angle to starboard) and 10/10 and 20/20 zig-zag manoeuvres with first turn to starboard. Other input parameters such as the distance between the rudder and propeller, wake fraction and thrust deduction are also assessed. Abbreviations used in figure 9.5 are: TD is tactical diameter, ADV is advance, OS is overshoot angle and TT is turning time.

Parameter		TD [-]	ADV [-]	Drift angle [°]	Final speed [-]	10/10 1st OS [°]	10/10 2nd OS [°]	10/10 Initial TT [-]	20/20 1st OS [°]
Standard	-0.02096	2.55	2.45	32.5	0.16	6	9.2	1.39	12.1
Yv(+20%)	-0.02515	2.57	2.44	30.7	0.16	5.7	8.4	1.4	11.6
Yv(-20%)	-0.01677	2.58	2.45	33.9	0.16	6.4	10.3	1.38	12.7
Yr(+20%)	0.00596	2.57	2.45	31.5	0.16	5.7	8.6	1.4	11.7
Yr(-20%)	0.00398	2.55	2.45	33.4	0.16	6.3	9.9	1.38	12.5
Nv(+20%)	-0.01336	2.38	2.33	31.4	0.16	7.6	13	1.34	14.6
Nv(-20%)	-0.0089	2.81	2.6	33.2	0.16	4.8	6.5	1.45	9.9
Nr(+20%)	-0.00331	2.68	2.56	32.9	0.16	5.2	7.7	1.45	10.7
Nr(-20%)	-0.00221	2.44	2.34	31.9	0.16	7.1	11.3	1.34	13.9
Yvd(+20%)	-0.02015	2.58	2.46	32.7	0.16	5.8	8.9	1.41	11.9
Yvd(-20%)	-0.01343	2.52	2.43	32.4	0.16	6.2	9.5	1.37	12.4
Yrd(+20%)	-0.00047	2.55	2.44	32.5	0.16	6.1	9.2	1.39	12.1
Yrd(-20%)	-0.00031	2.55	2.45	32.5	0.16	6.1	9.2	1.4	12.1
Nvd(+20%)	-0.00047	2.55	2.44	32.5	0.16	6	9.2	1.39	12.1
Nvd(-20%)	-0.00031	2.55	2.45	32.5	0.16	6	9.2	1.4	12.1
Nrd(+20%)	-0.00132	2.54	2.48	32.6	0.16	6.3	9.8	1.43	12.5
Nrd(-20%)	-0.00088	2.56	2.41	32.5	0.16	5.8	8.7	1.35	11.6
Xrr(+20%)	0.00047	2.55	2.45	32.3	0.16	6	9.2	1.39	12.1
Xrr(-20%)	0.00031	2.55	2.45	32.8	0.16	6	9.2	1.39	12.1
Xud(+20%)	-0.00167	2.56	2.45	32.1	0.16	6	9.1	1.4	12
Xud(-20%)	-0.00111	2.54	2.44	33	0.16	6.2	9.4	1.39	12.2
Xvr(+20%)	0.00347	2.54	2.44	33.2	0.15	6	9.2	1.39	12.1
Xvr(-20%)	0.00231	2.56	2.45	31.9	0.17	6	9.2	1.39	12.1
Xvv(+20%)	-0.00155	2.55	2.45	32.7	0.16	6	9.2	1.39	12.1
Xvv(-20%)	-0.00103	2.55	2.45	32.4	0.16	6	9.2	1.39	12.1
Xvvvv(+20%)	0.05414	2.55	2.45	31.8	0.17	6	9.2	1.39	12.1
Xvvvv(-20%)	0.0361	2.54	2.44	33.4	0.15	6	9.2	1.39	12.1
Rudder/propeller(+20%)	8.64	2.55	2.45	32.7	0.16	6.1	9.3	1.4	12.2
Rudder/propeller (-20%)	5.76	2.55	2.46	33.7	0.15	6	9.3	1.4	12.1
Wake fraction(+20%)	0.18	2.6	2.5	31.9	0.16	6	9.3	1.43	12
Wake fraction(-20%)	0.12	2.5	2.39	33.1	0.16	6	9.1	1.36	12.2
Trust deduction (+20)	0.264	2.51	2.41	33.9	0.15	6	9	1.37	12.1
Trust deduction (-20)	0.176	2.59	2.49	31.1	0.17	6.1	9.3	1.42	12.1

Figure 9.5: Sensitivity analysis, conditionally formatted

From the conditional formatting in figure 9.5 it is clear that the manoeuvres are most sensitive to the linear velocity derivatives. Especially N_v and N_r seems to affect both turning circle and zig-zag tests. Increasing/decreasing Y_v and Y_r seems to have most effect on the drift angle at 360 degrees and the overshoot angles. The linear acceleration derivatives does not have much impact on the simulated manoeuvres. Only the linear coefficient for hydrodynamic mass moment of inertia in yaw due to yaw acceleration, $N_{\dot{r}}$ has small impact on the overshoot angles and initial turning time. The wake fraction and thrust deduction are of some significance as well. A higher wake fraction gives increases the indices of the turning circles, while thrust deduction increases the indices it is lower, both yielding more coinciding results with the benchmark data.

Old coefficients (new Rt)		3	2.75	35.2	0.13	4.6	6.6	1.5	9.4
Old coefficients (old Rt)		2.91	2.68	35.8	0.13	4.6	6.5	1.46	9.5
MARINTEK2008		3.34	3.14	23.8	0.36	6.6	10.3	1.71	10

Figure 9.6: Sensitivity analysis, including MARINTEK's coefficients

The hydrodynamic derivatives and the resistance polynomial from MARINTEK's contribution in SIMMAN 2008 have been obtained. These have been utilized in SIMAN to simulated the same manoeuvres. Looking at the two bottom rows in figure 9.6 which are:

- 1st row: Using old hydrodynamic coefficients with the new resistance polynomial calculated in HullVisc.
- 2nd row: Using old hydrodynamic coefficients with the old resistance polynomial calculated in 2008.

- 3rd row: The results of MARINTEK's contribution in 2008

It is possible to see the influence of the resistance polynomial, as well as the differences of using the old coefficients. When using the old coefficients as well as the old resistance polynomial (row 2) in SIMAN today, the difference between MARINTEK (row 3) is:

- Advance is 13% less
- Tactical diameter is 15% less
- Drift angle is 50% higher
- The final speed is 64% less
- The 1st overshoot angle in 10°/10°zig-zag is 30% less
- The 2nd overshoot angle in 10°/10°zig-zag is 37% less
- The initial turning time in 10°/10°zig-zag is 15% less
- The 1st overshoot angle in 20°/20°zig-zag is 5% less

These deviations have to be due to changes done in SIMAN during the last six years, because all the input data which is possible to input for the user are identical. The differences are not because of hydrodynamic coefficients, resistance polynomial, wake fraction or any other input parameters in SIMAN and HullVisc. Again, due to lack of updated documentation it is hard to assess this remaining difference. The differences above are most likely because of changes in either non-linear cross-flow drag coefficients, rudder module or propeller module (or all). It has been several changes to various subroutines in the model, which has not been updated in the documentation. The last full description of the hydrodynamic forces is from 2008, six years ago.

9.5 Velocity derivatives

Due to sensitiveness of the linear velocity derivatives these are calculated with the empirical methods which have been assessed earlier in the thesis. The calculation results are given in table 9.7.

	Y'_v	Y'_r	N'_v	N'_r
Jones	-0.01327	0.006637	-0.00664	-0.00332
Wagner Smitt	-0.02110	0.004247	-0.00823	-0.00279
Clarke	-0.02526	0.004305	-0.00871	-0.00341
Norrbin	-0.02319	0.008199	-0.00811	-0.00452
Inoue	-0.02641	0.006524	-0.00831	-0.00342
Lee	-0.02238	0.006413	-0.00787	-0.00299
Kijima	-0.03702	0.01441	-0.01353	-0.00445
ShipX	-0.02096	0.00497	-0.01113	-0.00276
MARINTEK 2008	-0.01947	0.00319	-0.01013	-0.00376

Table 9.6: Velocity derivatives calculated for KVLCC2

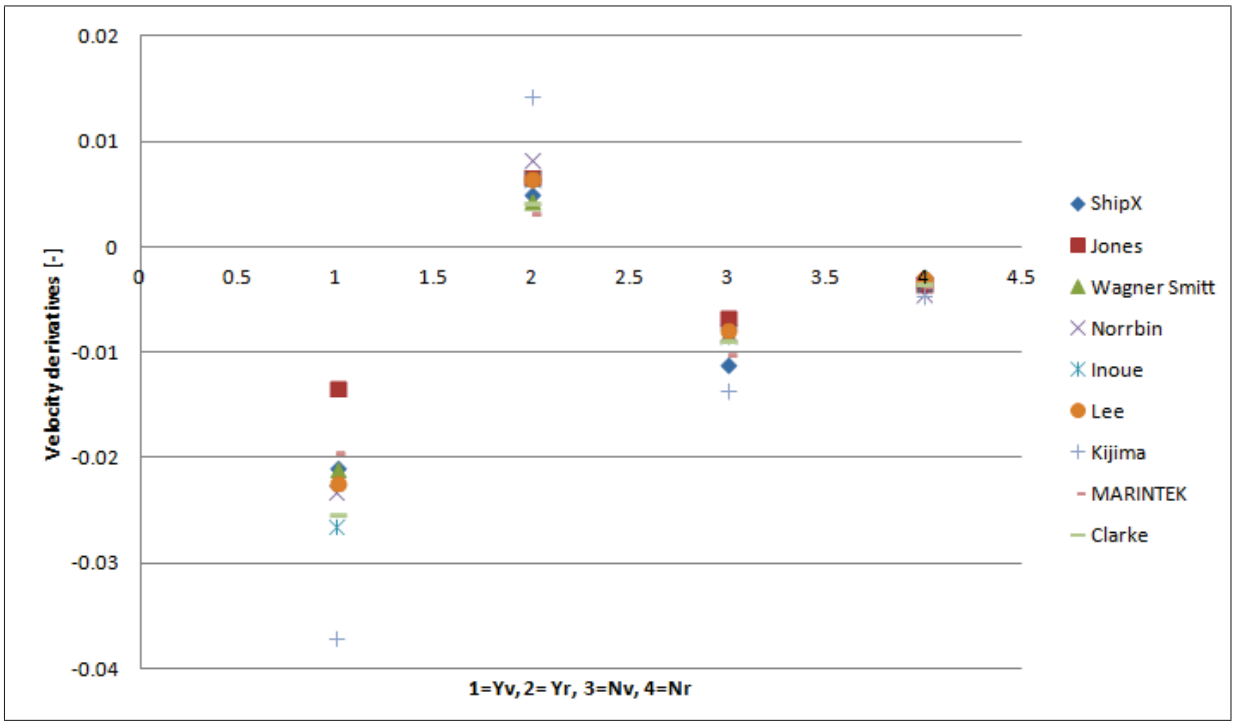

Figure 9.7: Linear velocity derivatives calculated for KVLCC2

Method of Kijima deviates from most of the velocity derivatives, atleast Y_v and Y_r. The water plane area coefficient and prismatic coefficient of the aft hull between APP and ship station five were tried to be estimated, but more reliable values were used from "The prediction of the manoeuvrability of KVLCC1 and KVLCC2", by Kijima et al. (2008) [3]. The values used were:

- $C_{pa} = 0.7350$
- $C_{wa} = 0.8901$

Y_v and Y_r deviates from the predicted hydrodynamic derivatives in the same paper as well. It might be some incorrect calculation of the normalized m'_x or other reasons. Jones flat plate theory underestimates Y_r. ShipX estimates the second largest N_v, which from the sensitivity

analysis affect the turning circle results greatly. It overestimates compared to the other methods, which shortens the tactical diameter and advance. ShipX estimates the lowest N_r. This also shortens the turning circle indices.

The hydrodynamic derivatives from PMM tests are obtained from various papers in [3].

	Y'_v	Y'_r	N'_v	N'_r
FORCE (INSEAN)	-0.01947	0.00626	-0.00927	-0.00437
FORCE (MOERI)	-0.01947	0.00653	-0.00821	-0.00373
MOERI	-0.01619	0.00472	-0.00875	-0.00312

Table 9.7: Linear velocity derivatives from PMM tests

The PMM tests from FORCE with both the INSEAN(1:45.714) and MOERI(1:58.000) model agrees well for Y_v and Y_r. The results from MOERI using the same model as FORCE (MOERI) deviates, even though the use of the same model as FORCE. The different results could be that the tests were conducted at different facilities with different equipment and procedures. Compared to the all the methods and PMM tests it looks like ShipX overestimates N_v and underestimates N_r. It is hard to say something specific about Y_r when FORCE's derivatives are larger while MOERI's are smaller. Y_v coincides well compared to the PMM test conducted by FORCE, while the empirical methods seems to overestimate this derivative. The linear damping coefficients are not validated against the PMM test results since these results differ as well. Y_r could be validated against MOERI's PMM results and Y_v could be validated against FORCE's PMM results. N_v and N_r can not be validated against neither. If the estimated contributions of Kijima's and Jones method (which deviates most from the others) are excluded, the average and the standard deviations of the linear velocity derivatives becomes:

	Y'_v	Y'_r	N'_v	N'_r
Average	-0.02139	0.005533	-0.0089	-0.0035
Standard deviation	0.003032	0.001490	0.00103	0.00061

Table 9.8: Statistics of the linear velocity coefficients

From the standard deviation it is clear that most uncertain (most variation in data) is Y_v, and the most consistent is N_r. However, the simulated manoeuvres are more sensitive to the N_r. When using the averages of the linear velocity derivatives in ShipX the advance increases 13.5%, the transfer increases 19.4% and the tactical diameter increases 18.4%. It gives smaller overshoot angles, and longer initial turning times. It is many uncertainties in the hydrodynamic derivatives. SIMAN and VeSim is tuned for offshore vessels, so it might be something in this tuning which give the underestimation of N_r and overestimation of N_v. Both which yields to smaller turning circle parameters. A correction for the integration of added mass distribution is based on empirical data for the linear derivatives from 25 ship models, this correction might be wrong if it is mostly based on offshore vessels. The different methods linear stability is calculated in figure 9.8, in which ShipX gives the lowest value, in other words the most unstable ship.

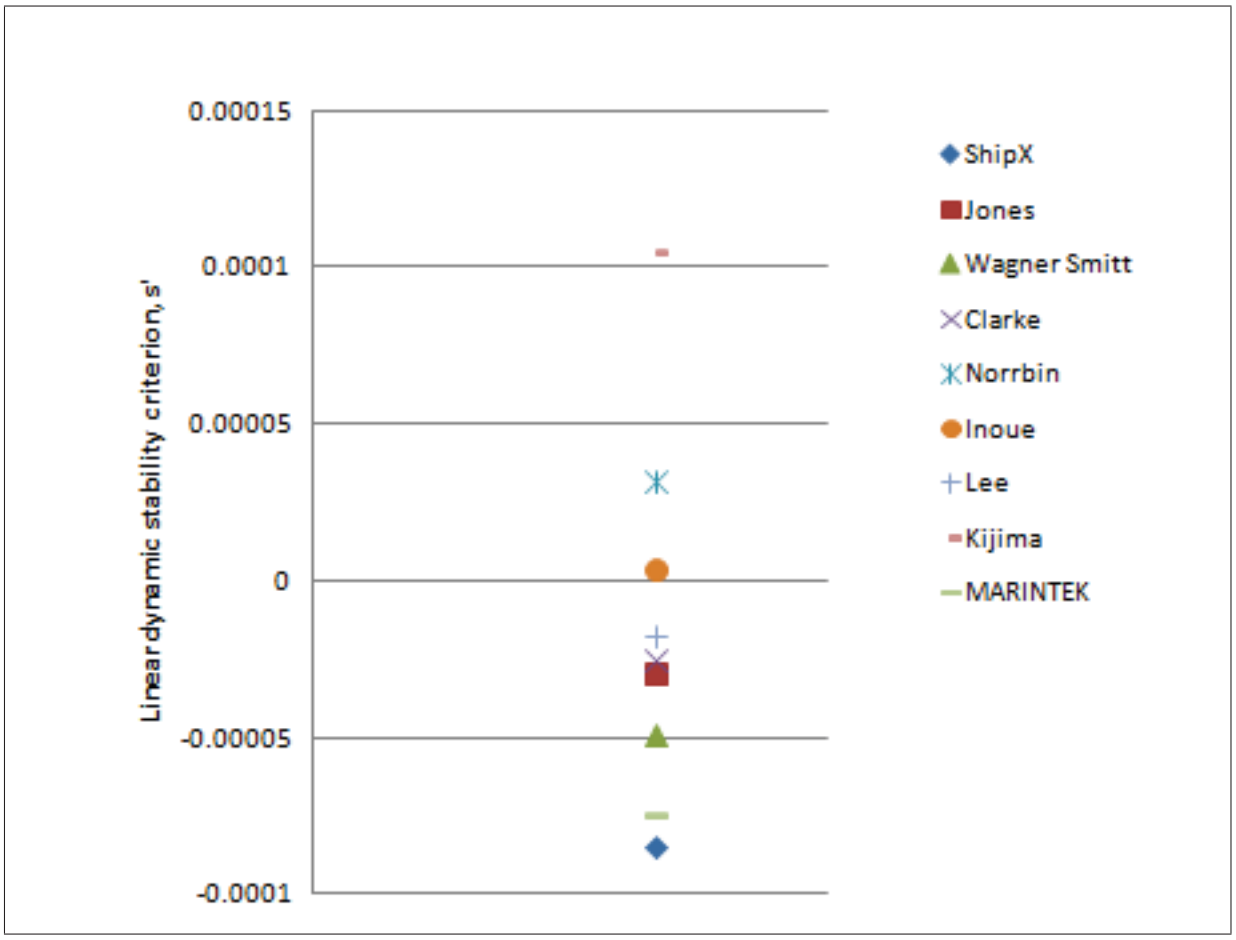

Figure 9.8: Linear dynamic stability criterion comparison

Comparing the hydrodynamic derivatives with the ones which were calculated by HullVisc in MARINTEK's contribution to SIMMAN 2008, most derivatives are within 10% of the previous as seen in table 9.9. The ones which differ substantially are Y_r and N_r, the linear yaw damping derivative and the sway damping coupling derivative. The changes that have been made to the calculation of these are not known to the author. An increase of N_r will result in higher tactical diameter and advance according to the sensitivity analysis, which are more coinciding with benchmark data. It will also result in smaller overshoot angles, which are not more coinciding with the benchmark data. A decrease of Y_r will results in higher overshoot angles. Using the old coefficients gives more coinciding turning circle results but not zig-zag results. Turning circle is a non-linear manoeuvre because of large drift angles so the non-linear parameters are of importance. The zig-zag manoeuvre is more linear so the linear parameters are of importance.

	ShipX	MARINTEK	ShipX/MARINTEK
Y'_v	-0.02096	-0.01947	1.077
Y'_r	0.00497	0.00319	1.558
N'_v	-0.01113	-0.01013	1.099
N'_r	-0.00276	-0.00376	0.734
$Y'_{\dot{v}}$	-0.01679	-0.01669	1.006
$Y'_{\dot{r}}$	-0.00039	-0.00036	1.083
$N'_{\dot{v}}$	-0.00039	-0.00036	1.083
$N'_{\dot{r}}$	-0.0011	-0.00108	1.019
X'_{rr}	0.00039	0.00036	1.083
$X'\dot{u}$	-0.00139	-0.00139	1.000
X'_{vr}	0.00289	0.00288	1.003
X'_{vv}	-0.00129	-0.00129	1.000
X'_{vvvv}	0.04512	0.04512	1.000
Linear stability index	-0.0000851	-0.0000747	1.139

Table 9.9: Comparison hydrodynamic coefficients

9.5.1 Shallow water ratios

The shallow water ratios for the linear velocity derivatives are calculated according to theory in Chapter 4. Methods of Clarke, Aukudinov and Kijima are used to obtain these. Clarkes formulae are not valid for $h/T < 1.20$. Kijimas ratio for Y_r are not given explicitly, but inclusive non dimensional mass and surge acceleration derivative so this is not included in the ratios.

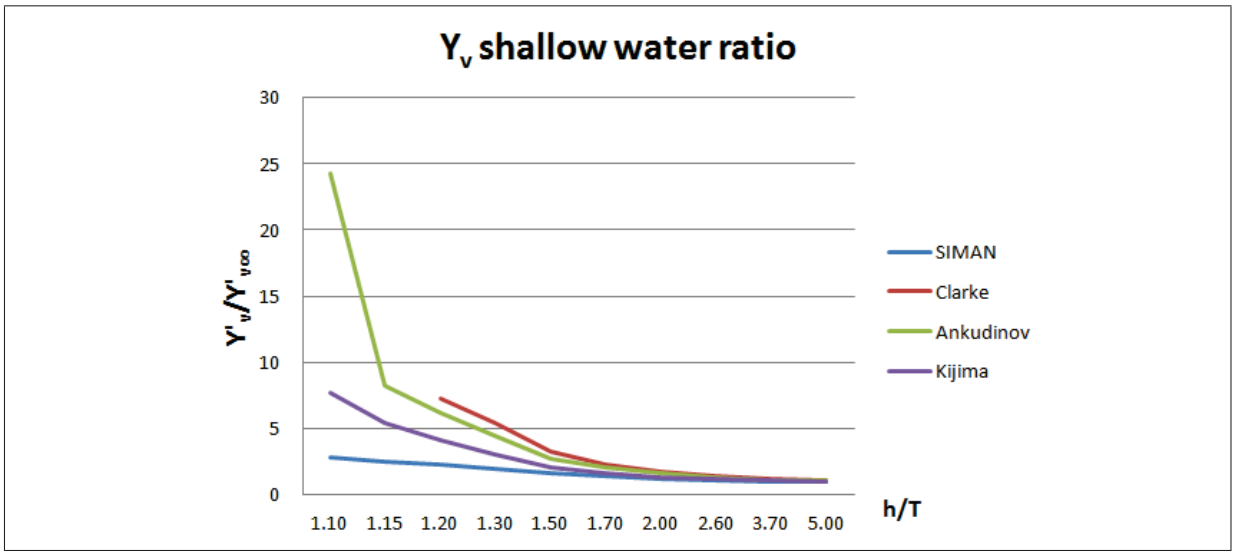

Figure 9.9: Shallow water ratio Yv

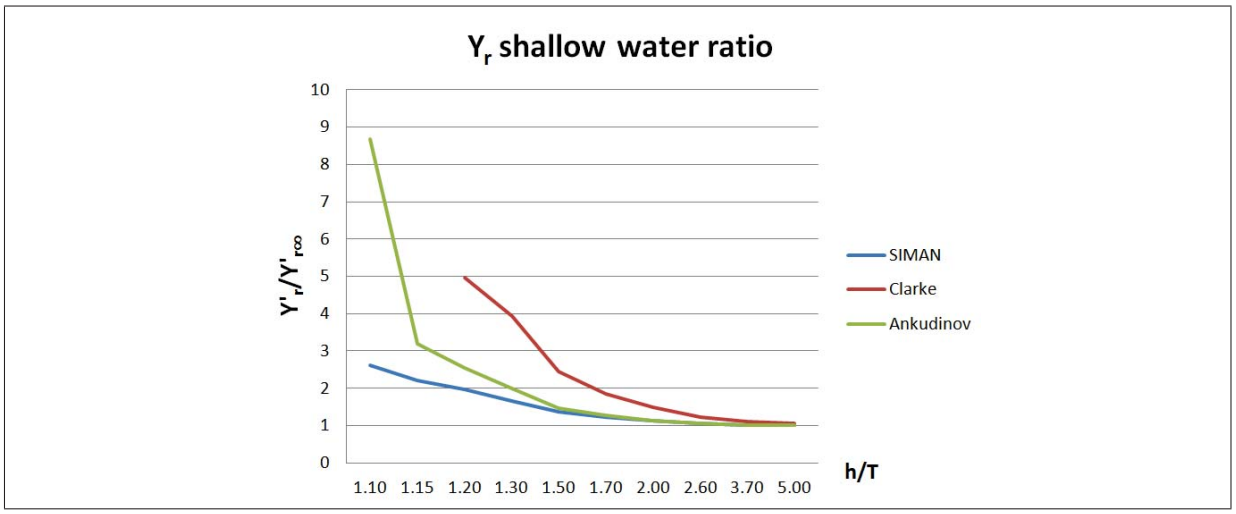

Figure 9.10: Shallow water ratio Yr

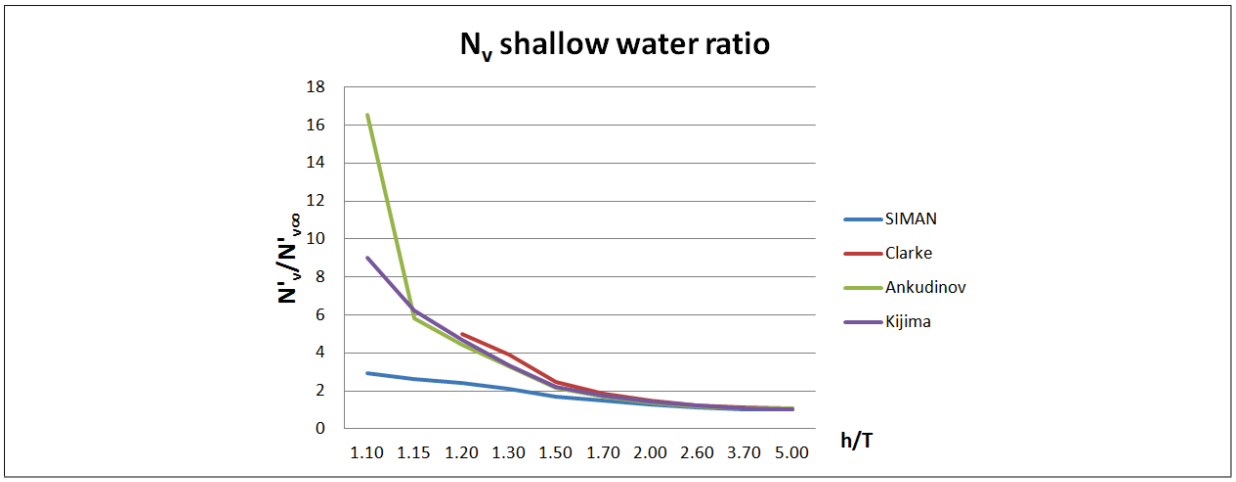

Figure 9.11: Shallow water ratio Nv

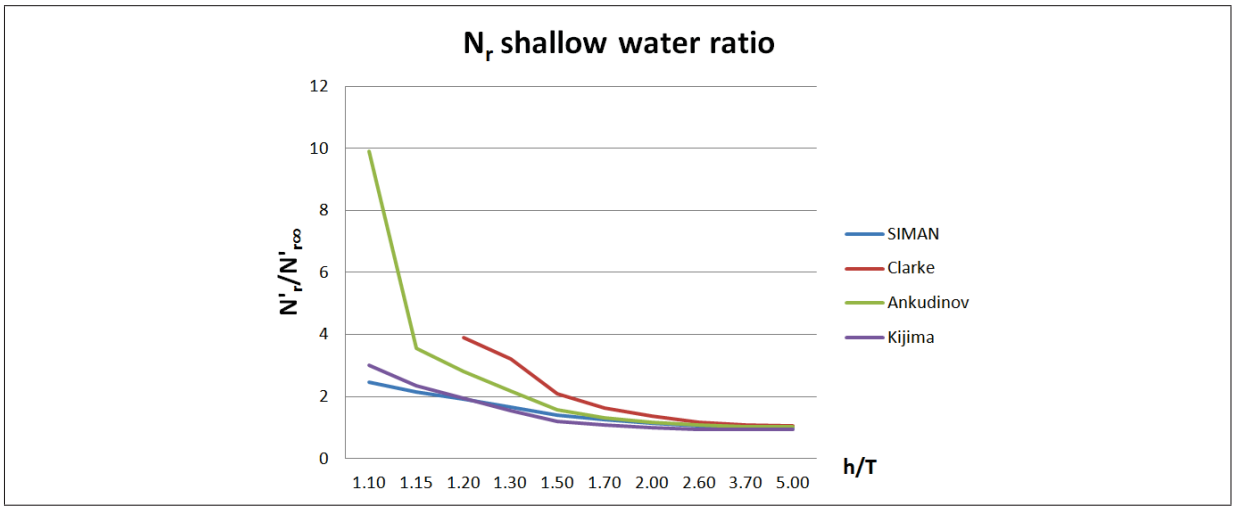

Figure 9.12: Shallow water ratio Nr

SIMANs shallow water ratios are lower than the other formulae for Y_v, Y_r, N_v. N_r has higher

ratios than Kijima for $h/T > 1.20$. The proposed ratio equations are not necessary any more correct than in SIMAN, but it could be that SIMAN underestimates the ratios. The author has not been able to obtain the literature that the shallow water ratio calculations are based on in SIMAN. It is partly based on "Fartøys manøveregenskaper paa grunt vann" by S. Falch (1982). In the 23rd ITTC manoeuvring committee's review of the empirical shallow water correction methods they concluded that the various methods differ considerably when going towards shallow water, which we can see from the results of KVLCC2 as well. Especially Ankudinovs formula increases considerably when going to very shallow water. The conclusion also included that it should be noticed that Kijima's formulae generally tend to underestimate the linear velocity coefficients, while the non-linear coefficient ratios are overestimated. This statement are based on the shallow water ratios obtained from experiments of a model of Esso Osaka and a container carrier model. If the shallow water formulae of Kijima underestimates, then SIMAN's shallow water formulae underestimates the linear velocity coefficients as well. However, it is advisable to look at the shallow water derivatives obtained from the captive model test after the SIMMAN 2014 workshop is completed.

9.6 Resistance

From figure 9.6 it is clear that the sensitivity of the resistance polynomial is also of some importance of the simulated manoeuvres. Figure 9.13 shows the resistance polynomial from 2008(blue line) and 2014(red line).

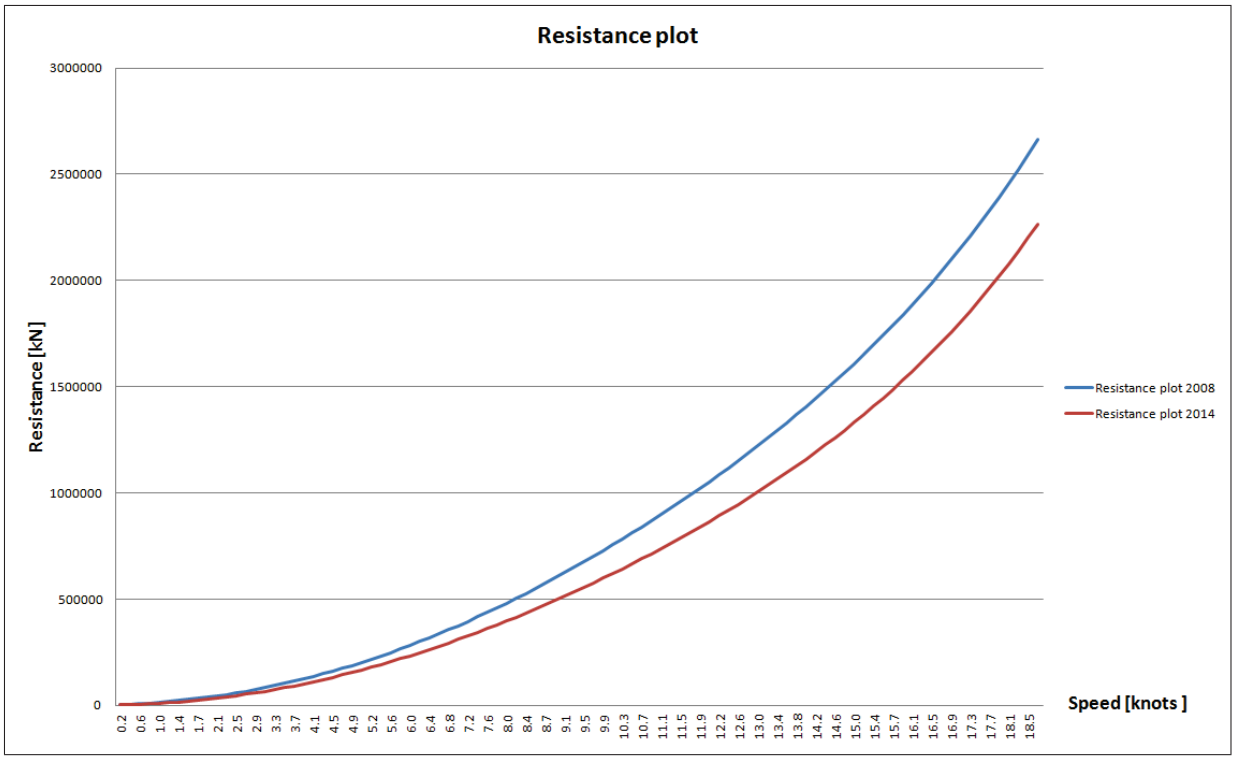

Figure 9.13: Resistance plot comparison

If the resistance polynomial was calculated by the empirical method in 2008 changes has been made here as well. These changes (purely based on higher turning circle indices) are good compared to the benchmark data. The overshoot angles seems unaffected.

9.7 Drag coefficients

The drag sectional drag coefficients are presented in figure 9.14. There is a large value at the foremost section. The sectional drag coefficients are found as a function of breath-to-draft ratio B/T. The breath at section 20 is 0.002 meter (probably because of the ship plate thickness which is set to 0.002 meter) and the draft is 18.39, which results in a B/T ratio of 0.0019. This results in an unnatural high drag coefficient in the foremost section.

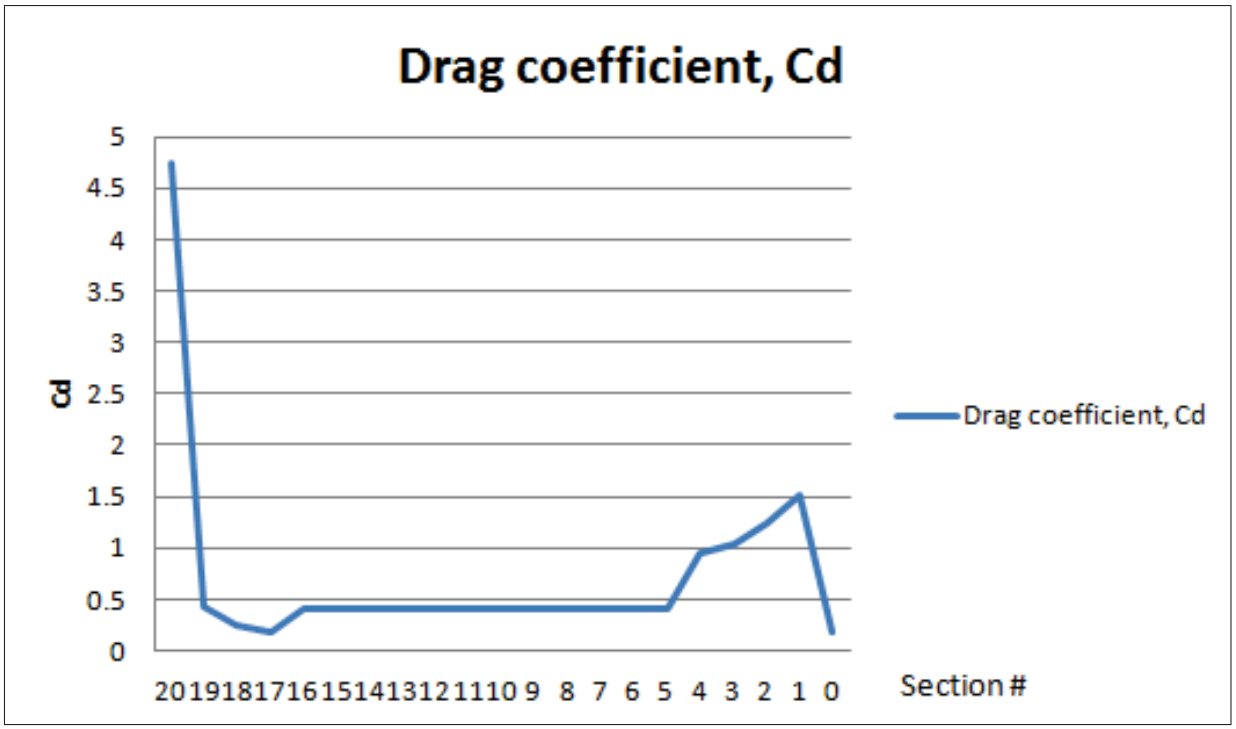

Figure 9.14: Sectional drag coefficients (# 0-Aft, # 20-Bow)

SIMAN defines a cross section where flow separation occurs abaft of. As the drift angle increases, this cross section moves forward. When the drift or yaw angle is 90°the complete hull is subjected to cross-flow force. So the large drag coefficient in the foremost section will only influence in this case. It does not not give any difference in the IMO standard manoeuvres but is pointed out as a possible error in the calculation of drag coefficients.

9.8 Wake fraction and thrust deduction

The previously used wake fraction in SIMMAN 2008 was 0.150 [-]. Due to the sensitivity of the wake fraction this value has been checked against literature. Wake fraction can be obtained from empirical formulae or model tests. IMO MEPC. Res 232(65) recommends wake fraction values as in table 9.10. According to table 9.10 the wake fraction for a ship with a block coefficient of 0.8 or more and one propeller (KVLCC2) should be around 0.35 [-]. By changing the wake fraction to this value it increases the advance by 18%, transfer by 25% and tactical diameter by 17%. Empirical methods for estimation of the wake fraction and thrust deduction factor for preliminary design purposes are looked into. These are mainly for models and its results are not strictly correct due to scale effects. The model boundary layer when scaled is thicker than the ship boundary layer. Hence, the wake fraction tends to be smaller for the

Block coefficient	One propeller	Two propellers
0.5	0.14	0.15
0.6	0.23	0.17
0.7	0.29	0.19
0.8 and above	0.35	0.23

Table 9.10: Recommended values for wake fraction w (2013)

ship, although extra ship roughness compensates to a certain extent [11]. ITTC adopted a formula for wake fraction scale effects in 1978, but detailed full-scale measurements of wake are sparse. Empirical expressions derived from regression of databases for wake fraction and thrust deduction are calculated for a single screw ship using methods of Taylor, Van Manen, BSRA and Holtrop (Harvald is only valid for block coefficients between 0.525 and 0.75) in table 9.11 from [11]. Looking into the SIMMAN 2008 proceedings [3] other wake fractions and

Method	Wake fraction	Trust deduction
Taylor (w) / Van Manen (t)	0.3549	0.2484
BSRA	0.4634	0.2417
Holtrop	-	0.3084

Table 9.11: Empirical values for w and t

thrust deduction factors are found. It was not clear which wake fractions which were listed. The wake fraction to input in HullVisc is the wake fraction of the hull. In "Manoeuvring Motions of KVLCC2 and KVLCC2 using MMG model" by SANO and YASUKAWA, the values used were:

- Thrust deduction factor=0.21
- Wake fraction ("the wake fraction coefficient w_P")=0.451

In "ANALYSIS OF STEADY HYDRODYNAMIC FORCE COMPONENTS AND PREDICTION OF MANOEUVRING SHIP MOTION WITH KVLCC1, KVLCC2 AND KCS" by Yoshimura et al., the values used were:

- Thrust deduction factor=0.238
- Wake fraction("self propulsion factor, w_P")=0.463

The thrust deduction factor coincides well with the value calculated in SIMAN. The wake fraction is much higher, but it is not clear if these are the same are the wake fraction which is input in HullVisc. But due to the high values in the literature and possibly from SIMMAN 2008 it is recommended to take a closer look at the wake fraction to be used for SIMMAN 2014.

Chapter 10

Conclusion

10.1 Conclusion

Simulation models of KVLCC2 based on simulation tools developed by MARINTEK (SIMAN and VeSim) have been used to calculate manoeuvring forces/moments in deep and shallow water. The models have been utilized to simulate the IMO standard manoeuvres in deep water. These have been compared with the manoeuvring characteristics specified in IMO MSC Res. 137(76). The simulation model of KVLCC2 fulfils the IMO criteria of turning, initial turning/course-changing, yaw-checking abilities in both VeSim and SIMAN. The model in VeSim fulfil the IMO criteria of stopping ability, while the model in SIMAN does not. Generally there are small differences in the results from VeSim and SIMAN. The reasons for this could be because of roll damping or small deviation of the calculation of the linear velocity derivatives which VeSim calculates independently.

Comparisons have also been made with average benchmark data based on the free models tests from SIMMAN 2008. They do not correspond well. The most coinciding measures are the 1st and 2nd overshoot angles in 20°/20°zig-zag tests to both starboard and port. Generally SIMAN underestimates all the other manoeuvring indices. The 2nd overshoot angle in 10°/10°zig-zag test is underestimated 47%. While the turning circle advance and tactical diameter are averagely underestimated about 20%. The results are not coinciding well. Hence, the simulation model in SIMAN (and VeSim as well) are not validated based on the benchmark data. It is possible to tune parameters but this is not the purpose of this thesis.

MARINTEK's contribution using SIMAN in 2008 was more consistent compared to the benchmark data. The turning circle measures were very close to the benchmark data. The overshoot angles for 10°/10°zig-zag test were closer as well. In simulations using the updated version of SIMAN the overshoot angles in 20°/20°zig-zag test are closer than in 2008. Overall, it looks like SIMAN in 2008 estimated closer values to the benchmark data than SIMAN today. This indicates that the changes made in the plug-in does not give better results for KVLCC2. SIMAN is tuned for offshore vessels, it may be that this has influenced the results. Using same input parameters as well as the same hydrodynamic coefficients and resistance polynomial as MARINTEK in 2008 does not give same simulation results as back then. The deviations are quite significant:

- Advance is 13% less

- Tactical diameter is 15% less
- Drift angle is 50% higher
- The final speed is 64% less
- The 1st overshoot angle in 10°/10°zig-zag is 30% less
- The 2nd overshoot angle in 10°/10°zig-zag is 37% less
- The initial turning time in 10°/10°zig-zag is 15% less
- The 1st overshoot angle in 20°/20°zig-zag is 5% less

These differences are not because of hydrodynamic coefficients, resistance polynomial, wake fraction or any other input parameters in SIMAN and HullVisc inputs. The differences above are most likely because of changes in either non-linear cross-flow drag coefficients, rudder module or propeller module (or all). It has been several changes to various subroutines in the model, which has not been updated in the documentation. The last full description of the hydrodynamic forces is from 2008, six years ago. Generally it seems like the models from 2008 was better considering the average benchmark data from the free model test. These model test deviates as well, even though same model was used. The difference of these could be due to that the tests have been conducted at different facilities with different equipment. The results could be analysed by different methods. Hopefully, the model test for SIMMAN 2014 will give more coinciding results.

A sensitivity analysis is performed. The linear damping coefficients proved to be of high importance, especially N_r and N_v. Wake fraction and thrust deduction are also of some importance. The linear damping coefficients are calculated using empirical methods for comparison. ShipX estimates the second largest N_v, the lowest N_r and the second lowest Y_v. The coefficients calculated by HullVisc in 2008 and coefficients obtained from PMM tests are also used for comparison. Compared to the PMM tests ShipX tends to overestimate N_v and underestimate N_r. The PMM test results vary as well, this could be because the tests were conducted at different facilities with different equipment and procedures. The linear damping coefficients are not validated against the PMM test results since these differ as well. Y_r could be validated against MOERI's PMM results and Y_v could be validated against FORCE's PMM results. N_v and N_r can not be validated against neither. Eleven of the hydrodynamic coefficients calculated in HullVisc today are within 10% of the ones calculated in HullVisc in 2008. The ones that deviates more than 10% are the coefficient for yaw damping and the coefficient for sway damping due to yaw velocity, N_r and Y_r. The changes are not known to the author. N_r is of high importance according to the sensitivity analysis. N_r calculated in 2008 contributes to a higher turning circle indices, but lower overshoot angles. Which conflicts the benchmark data by giving more similar results for turning circle, but not for the zig-zag manoeuvre. Y_r calculated in 2008 will results in higher overshoot angles. It is possible to tune the hydrodynamic derivatives to improve the model, but this will not improve the physical models. Changes have been made in the resistance polynomial as well, there changes (purely based on higher turning circle indices) are good compared to the benchmark data. An input value of 0.150 [-] for the wake fraction of the hull has been observed to be too low compared to literature and other wake fractions used in SIMMAN 2008.

The same trends are seen in the turning circle simulation in shallow water with KVLCC2 as for Esso Osaka. KVLCC2 does not have shorter advance in h/T=1.50 than deep water. The same trend for the checking and counter turning ability of KVLCC2 are not found as for Esso Osaka. The ability increases from deep h/T=4.2 to h/T=1.2 for each depth/draft ratio. The initial turning time increases as water depth decreases. Calculation of deep to shallow water ratio has been conducted using the methods by Clarke, Ankudinov and Kijima. From this as well as the 23rd ITTC committee review of shallow water ratios it seems like SIMAN's shallow water formulae underestimates the linear velocity coefficients.

Case specific low speed manoeuvres has been defined as the shallow water manoeuvres at low speeds that will be published after SIMMAN 2014, which should be used for shallow water model validation.

10.1.1 Suggestions for further work

Due to the lack of documentation an improvement of the physical models is hard to evaluate. It is strongly suggested to update the documentation for SIMAN, as well as some parts of VeSim where the manoeuvring forces differs. Which is relevant for the linear velocity derivatives. Changes that have been observed are especially in calculation of Y_r, N_r and the resistance polynomial. Unknown changes have been noticed in other modules which are impossible for the author to assess; cross-flow drag module, rudder or propeller module.

It is advisable to look closer at the calculation methods for N_r and N_v. These are the parameters which are the most sensitive according to the sensitivity analysis. Also, it is observed deviations with the empirical methods as well as the PMM tests results.

When the free model tests are released after SIMMAN 2014 it it advisable to use this as shallow water model validation. This assessed also low speed manoeuvres. The shallow water ratios should be looked into after SIMMAN 2014 as well. PMM tests will be conducted. From the documentation of the physical models in SIMAN for shallow water it is accounted for added mass terms, linear damping terms as well as rudder and propeller forces. Ratios for $X\dot{u}$, X_{vv}, X_{vr} and X_{rr} could also be included as proposed by Ankudinov et al. For assessment of low speed manoeuvres there is a need for a comparison such as SIMMAN 2008 with a series of typical low speed manoeuvres which are selected and standardized to be used for model validation. The 27th ITTC will look into possible criteria for manoeuvring at low speed.

Bibliography

[1] 16th ITTC Manoeuvring Committee. Proceedings of 16th ITTC. 1981.

[2] SIMMAN 2008. Part G: Comparison of Results for Free Manoeuvre Simulations - Systems and CFD Based Methods. 2008.

[3] SIMMAN 2008. Preprints of Workshop Proceedings. *Volume 1*, 2008.

[4] SIMMAN 2008. MOERI Tanker KVLCC2. `http://www.simman2008.dk/KVLCC/KVLCC2/tanker2.html`, Accessed 30 October 2013.

[5] 22nd ITTC Manoeuvring Committee. Proceedings of 22nd ITTC. 1999.

[6] 23rd ITTC Manoeuvring Committee. Proceedings of 23rd ITTC. 2002.

[7] 24th ITTC Manoeuvring Committee. Proceedings of 24th ITTC. 2005.

[8] 25th ITTC Manoeuvring Committee. Proceedings of the 25th ITTC. 2008.

[9] 26th ITTC Manoeuvring Committee. Proceedings of 26th ITTC. 2011.

[10] 26th ITTC Manoeuvring Committee. Validation of Manoeuvring Simulation Models. 2011.

[11] S. R. Turnock A. F. Molland and D. A. Hudson. *Ship Resistance and Propulsion*. Cambridge University Press, first edition, 2011.

[12] M.A. Abkowitz. *Lectures on Ship Hydrodynamics: Steering and Maneuvrability*. Hydrodynamisk og aerodynamisk Laboratorium; report; series Hy. Danish Technical Press i komm, 1964.

[13] T. E. Berg. Lecture notes, TMR4220 Naval Hydrodynamics, Ship Manoeuvring. *Department of Marine Technology, NTNU*, 2014.

[14] T. E. Berg. State of the art document on validation of simulation models for ship manoeuvring. 2014.

[15] T. E. Berg and E. Ringen. Validation of shiphandling simulation models. 2011.

[16] Simon Burnlay and Vladimir Ankudinov. The prediction of hydrodynamic forces acting on the hull of a manoeuvring ship based upon a database of prediction methods. *Proc. of MARSIM03*, 2003.

[17] R. E. Shannon C. D. Pegden and R. P. Sadowski. *Intruduction to simulation using SIMAN*. McGraw.Hill, Hightstown, NJ, second edition, 1995.

[18] D. Clarke. A Two-Dimensional Strip Method for Surface Ship Hull Derivatives: Comparison of Theory with Experiments on a Segmented Tanker Model. *Journal of Mechanical Engineering Science, Vol. 14, No. 7, Supplementary Issue*, 1972.

[19] SIMMAN 2014 Committee. System based methods, intructions for submitting of manoeuvring predictions.

[20] G. Hine D. Clarke, P. Gedling. The application of manoeuvring criteria in hull design using linear theory. *The Naval Architect*, 1983.

[21] Ian Dand. Low speed manoeuvring criteria: Some considerations. *BMT Sea Tech Limited, United Kingdom*, 2003.

[22] Katrien Eloot. Selection, Experimental Determination and Evaluation of a Mathematical Model for Ship Manoeuvring in Shallow Water. *Doctoral thesis, Gent university*, 2006.

[23] Katrien Eloot and Marc Vantorre. Ship behaviour in Shallow and Confined Water: an Overview of Hydrodynamic Effects through EFD. *Flanders Hydraulics Research, Maritime Technology Division*.

[24] Hwang W et al. An exploratory study to characterize ship maneuvering performance at slow speed. *International Conference on Marine Simulation and Ship Manoeuvrability, MARSIM'03, Volume III*, 2003.

[25] T.-I. Lee et al. On an empirical prediction of hydrodynamic coefficients for modern ship hulls. *Proc. of MARSIM03*, 2003.

[26] Dariusz Fathi. Vesim documentation. 2013.

[27] Yasukawa H. and Kobayashi E. Shallow water model experiments on ship turning performance.

[28] J. Holtrop. *A statistical re-analysis of resistance and propulsion data*. Vol. 31, No. 363, 1984.

[29] R.T. Jones. Properties of Low Aspect Ratio Pointed Wings of Speeds Below and Above the Speed of Sound. *NACA Rep.No.835*, 1946.

[30] J.M.J. Journee and J.A. Pinkster. *SHIP HYDROMECHANICS - Part I: Introduction*. Delft University of Technology, 2001.

[31] K. Kijima and Y. Nakiri. On the practical prediction method for ship manoeuvring characteristics. *Proc. of MARSIM03*, 2003.

[32] E. Kobayashi and S. Asai. A simulation study on ship manoeuvrability at low speeds. *International Conference on Ship Manoeuvrability. Prediction and achievement, Vol.1, Paper 10, London*, 1987.

[33] J. M. Kvale. Simulation model for a Very Large Crude Carrier (VLCC). 2013.

[34] E. V. Lewis. *Principles of Naval Architecture, Second Revision, Motions in Waves and Controllability*. The Society of Naval Architects and Marine Engineers, 1989.

[35] K. Martinussen and E. Ringen. SIMULATION OF KVLCC1 AND KVLCC2 MANOEUVRING MOTIONS.

[36] K. Martinussen and E. Ringen. Manoeuvring Prediction During Design Stage. 2000.

[37] N.H. Norrbin and SWEDISH STATE SHIPBUILDING EXPERIMENTAL TANK GOTEBORG. *Theory and Observations on the Use of a Mathematical Model for Ship Manoeuvring in Deep and Confined Waters*. Meddelanden fran Statens skeppsprovningsanstalt. Statens Skeppsprovningsanstalt, 1971.

[38] The Specialist Committee on Esso Osaka. Final Report and Recommendations to the 23rd ITTC.

[39] International Maritime Organization. EXPLANATORY NOTES TO THE STANDARDS FOR SHIP MANOEUVRABILITY. 2002.

[40] Quadvlieg and Coevorden. Manoeuvring Criteria More than IMO A751 Requirements Alone. *MARSIM 2003, Kanazawa, Japan*, 2003.

[41] E. Ringen. ShipX Manoeuvring Plug-In. 2011.

[42] E. Ringen. MARINTEK, FACT SHEET, ShipX - Manoeuvring. `http://www.sintef.no/upload/MARINTEK/PDF-filer/Sofware/ShipX_Manoeuvring.pdf`, Accessed 30 October 2013.

[43] R. G. Sargent. VERIFICATION AND VALIDATION OF SIMULATION MODELS. 2010.

[44] R. G. Sargent. VERIFICATION AND VALIDATION OF SIMULATION MODELS. *Proceedings of the 2011 Winter Simulation Conference*, 2011.

[45] Sissel Tjøswold. Verifying and Validation of a Manoeuvring Model for NTNUs Research Vessel R/V Gunnerus. *Department of Marine Technology, NTNU*, 2012.

[46] B.K. Jakobsen VK. Ankudinov, E.R Miller and L.L Daggett. Manoeuvring perforcemance of tug/barge assemblies in restricted waterways. *Proceedings MARSIM and ICMS 90, Tokyo, Japan*, 1990.

[47] Zou Zaojian. Lecture notes on ship manoeuvring and seakeeping. *Shanghai Jiao Tong University*, 2006.

Appendix A

Appendix

A.1 ShipX - Principal hull data KVLCC2

PRINCIPAL HULL DATA	ENCL. 1)
	REPORT
	DATE 2014-05-04
	REF

SHIP: **KVLCC.mgf (imported)**
Loading condition: Not given - SIMAN Test Condition
Draught AP/FP: 20.800 / 20.800 [m]

	Symbol	Unit	
Length overall	L_{OA}	[m]	333.500
Length on designed waterline	L_{WL}	[m]	325.500
Length betw. perp.	L_{PP}	[m]	320.000
Breadth moulded	B	[m]	58.002
Breadth waterline	B_{WL}	[m]	58.000
Depth to 1st deck	D	[m]	28.014
Draught at $L_{PP}/2$	T	[m]	20.800
Draught at FP	T_{FP}	[m]	20.800
Draught at AP	T_{AP}	[m]	20.800
Trim (pos. aft)	t	[m]	0.000
Rake of keel		[m]	0.000
Rise of floor		[m]	0.000
Bilge radius		[m]	0.000
Sea water density	ρ_s	[kg/m^3]	1025.00
Shell plating thickness		[mm]	2
Shell plating in % of displ.		[%]	0.40
Volume displacement	∇	[m^3]	312748.0
Displacement	Δ	[t]	321848.9
Prismatic coefficient*	C_P	[-]	0.8117
Block coefficient*	C_B	[-]	0.8101
Midship section coefficient	C_M	[-]	0.9981
Longitudinal C.B. from $L_{PP}/2$	LCB	[m]	11.176
Longitudinal C.B. from $L_{PP}/2$*	LCB	[% L_{PP}]	3.493
Longitudinal C.B. from AP	LCB	[m]	171.176
Wetted surface	S	[m^2]	27821.21
Wetted surface of transom stern	A_T	[m^2]	17.23

Remarks: *Refers to L_{PP}
Hydrostatic corrections not included

ShipX (RepGen version 2.0.21) 04-May-2014 12:51:56 - Licensed to: JMK (NTNU)

A.2 ShipX - Hydrostatics KVLCC2

HYDROSTATICS	ENCL. 1)
	REPORT
	DATE 2014-05-04
	REF

SHIP: **KVLCC.mgf (imported)**
Loading condition: Not given - SIMAN Test Condition
Draught AP/FP: 20.800 / 20.800 [m]

	Symbol	Unit	
Length overall	L_{OA}	[m]	333.500
Length betw. perp.	L_{PP}	[m]	320.000
Breadth moulded	B	[m]	58.002
Depth to 1st deck	D	[m]	28.014
Draught at $L_{PP}/2$	T	[m]	20.800
Draught at FP	T_{FP}	[m]	20.800
Draught at AP	T_{AP}	[m]	20.800
Trim (pos. aft)	t	[m]	0.000
Rake of keel		[m]	0.000
Rise of floor		[m]	0.000
Bilge radius		[m]	0.000
Sea water density	ρ_s	[kg/m^3]	1025.00
Shell plating thickness		[mm]	2
Shell plating in % of displ.		[%]	0.40
Length on waterline	L_{WL}	[m]	325.500
Breadth waterline	B_{WL}	[m]	58.000
Volume displacement	∇	[m^3]	312748.0
Displacement	Δ	[t]	321848.9
Prismatic coefficient*	C_P	[-]	0.8117
Block coefficient*	C_B	[-]	0.8101
Midship section coefficient	C_M	[-]	0.9981
Longitudinal C.B. from $L_{PP}/2$	LCB	[m]	11.176
Longitudinal C.B. from $L_{PP}/2$*	LCB	[% L_{PP}]	3.493
Longitudinal C.B. from AP	LCB	[m]	171.176
Vertical C.B.	VCB	[m]	10.872
Wetted surface	S	[m^2]	27821.21
Wetted surface of transom stern	A_T	[m^2]	17.23
Waterplane area	A_W	[m^2]	16734.38
Waterplane area coefficient	$C_W(L_{WL})$	[-]	0.865
Longitudinal C.F. from $L_{PP}/2$	LCF	[m]	-0.002
Longitudinal C.F. from AP	LCF	[m]	159.998
Immersion	DP_1	[t/cm]	171.527
Trim moment	MT_1	[t·m/cm]	3880.884
Transverse metacenter above keel	KM_T	[m]	24.306
Longitudinal metacenter above keel	KM_L	[m]	387.402

Remarks: *Refers to L_{PP}
Hydrostatic corrections not included

ShipX (RepGen version 2.0.21) 04-May-2014 13:02:20 - Licensed to: JMK (NTNU)

A.3 Effects on water depth on manoeuvring coefficients for Esso Osaka

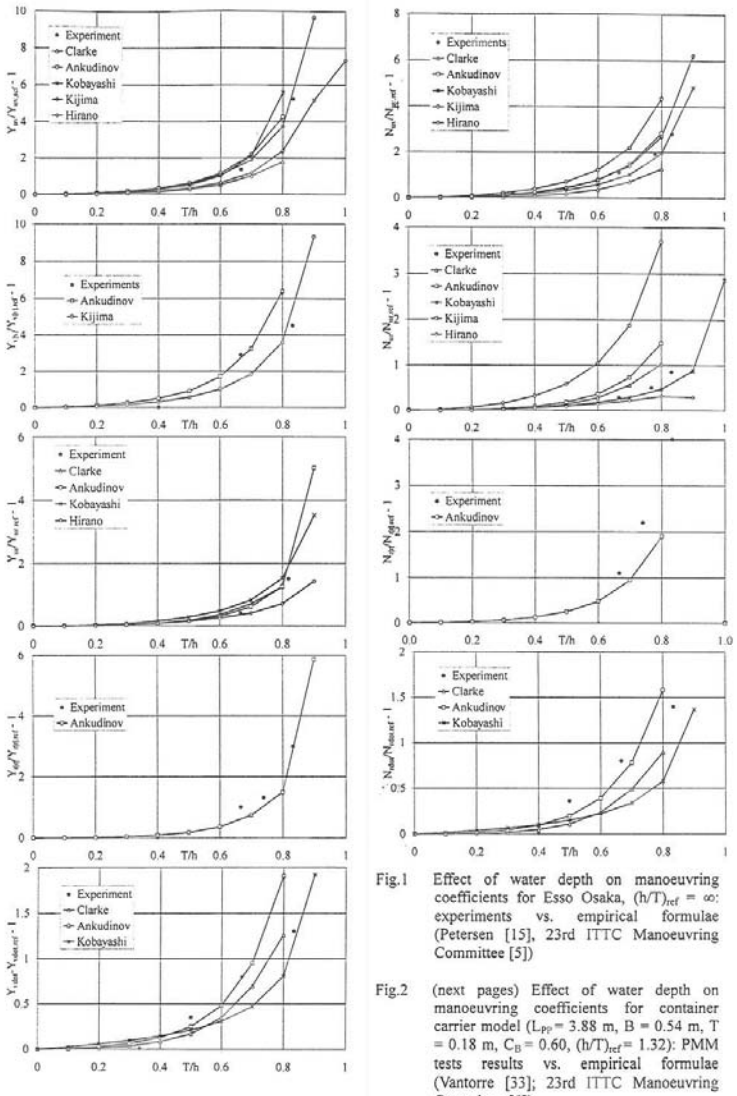

Fig.1 Effect of water depth on manoeuvring coefficients for Esso Osaka, $(h/T)_{ref} = \infty$: experiments vs. empirical formulae (Petersen [15], 23rd ITTC Manoeuvring Committee [5])

Fig.2 (next pages) Effect of water depth on manoeuvring coefficients for container carrier model (L_{PP} = 3.88 m, B = 0.54 m, T = 0.18 m, C_B = 0.60, $(h/T)_{ref}$ = 1.32): PMM tests results vs. empirical formulae (Vantorre [33]; 23rd ITTC Manoeuvring Committee [5])

A.4 VeSim - Propulsor Input

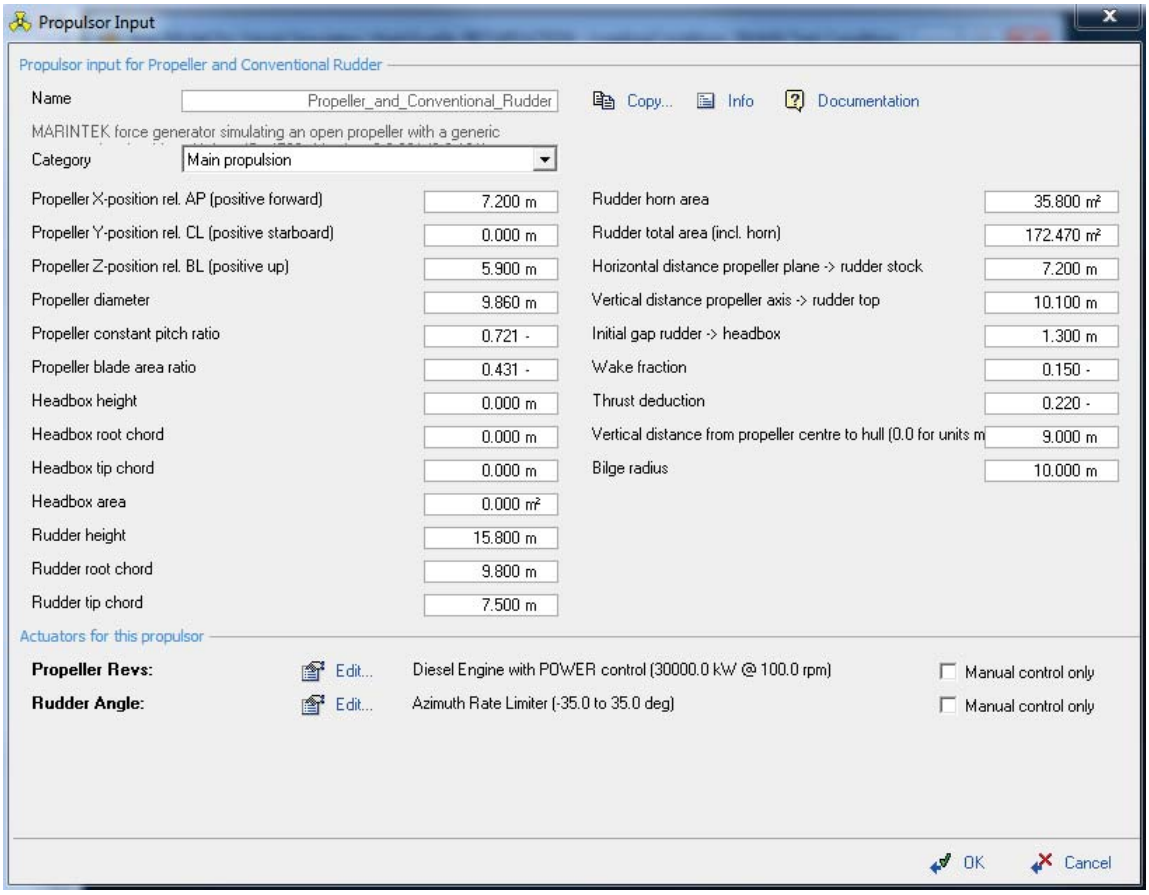

A.5 VeSim - Engine Input